# THE CHARACTER AND SETTING OF GOLD MINERALIZATION ASSOCIATED WITH THE BETTS COVE COMPLEX



TOM A. AL

# THE CHARACTER AND SETTING OF GOLD MINERALIZATION ASSOCIATED WITH THE BETTS COVE COMPLEX

BY

Tom A. Al

A thesis submitted to the School of Graduate Studies in partial fulfillment of the requirements for the degree of Master of Science

Department of Earth Sciences
Memorial University of Newfoundland

January, 1990

St. John's, Newfoundland

ISBN 0-315-59233-8

# ABSTRACT

The Ordovician Betts Cove ophiolite is located in northeast Newfoundland on the southeast side of the Baie Verte peninsula, between the communities of Tilt Cove and Nippers Harbour. Ultramafic rocks occur at the base of the ophiolite in fault contact with the upper ophiolite stratigraphy (mainly pillow lava) to the south. North of the ophiolite, intermediate and felsic volcanic and sedimentary rocks of the Silurian Cape St. John Group, and the Cape Brule Quartz-Feldspar Porphyry are in fault contact with the ultramafic rocks. Locally the Cape St. John Group unconformably overlies the ophiolite.

Fresh, cumulate ultramafic rocks are altered to carbonate-bearing assemblages. The onset of carbonate alteration is marked by a serpentine-magnesite assemblage which appears where fresh ultramafic rocks are cross cut by shear zones. Serpentine-magnesite reacts to form talc-magnesite with progressive shearing. Talc-magnesite is the most abundant ultramafic rock type present in the area. Localized quartz-hematite-dolomite alteration assemblages with minor fuchsite are present.

Two types of gold mineralization are described. The first type occurs in a talc-magnesite host and consists of a simple quartz, magnesite, Cu-sulphide mineralogy. The

second type is hosted by the quartz-hematite-dolomite altered ultramafic rocks and shear zones within the Silurian Cape St. John Group. These Au-mineralized veins consist of quartz, ankerite, fuchsite, and specularite plus or minus magnetite and Cu-Fe sulphides.

Gold enrichment in the ultramafic rocks is associated with regional scale carbonate alteration. This link is important for defining exploration targets. Rare earth element and Sr isotope evidence implicate an ultramafic source rock and a fluid derived from hydrated ultramafic rocks (Ordovician seawater).

Mineralization probably occurred as a result of metamorphic dehydration of serpentinized ultramafic rocks during Acadian Orogenesis. Faults on the margin of a caldera complex to the north, and older structures related to obduction of ophiolitic rocks during the Middle Ordovician, probably acted as fluid conduits.

# ACKNOWLEDGMENTS

I received much assistance from my supervisors Dr. B.J. Fryer and Dr. G.A. Jenner. Financial assistance was provided in the form of a Memorial University Graduate Student Fellowship and Bursary. All analytical costs were paid for by operating grants to Drs. B.J. Fryer. and G.A. Jenner. Dr. H. Longrich of Memorial University is thanked for the time he saved me by introducing me to computer applications pertinent to this study. P. King, P. Clarke, B. Gosse, D. Healey and S. Jackson were very helpful in teaching me all there is to know about analytical geochemistry. J. Tuach helped by critically reading the first draft and by providing me time at work to carry out the "final corrections".

Dr. J.W. Lydon, through the Geological Survey of Canada, provided field support and many hours of conversation about the problems at hand. Capable and enjoyable field assistance was provided by Jamie Lavigne, also through the G.S.C.

Consolidated Rambler Mines Ltd., Inco Exploration, R. Gingrich, Esso Minerals, V. French and Ionex Ltd. are thanked for allowing access to their respective properties in the area.

# TABLE OF CONTENTS

Table of Contents cont...

# LIST OF FIGURES

LIST OF FIGURES cont...

LIST OF FIGURES cont...

# LIST OF PLATES

LIST OF PLATES cont...

LIST OF PLATES cont...

List of Plates cont...

# LIST OF TABLES

# CHAPTER 1

# INTRODUCTION

## 1.1 General:

A surge in gold exploration has occurred in Newfoundland over the last 4 to 5 years. Consequently, many geologic environments are becoming recognized as important exploration targets on the basis of analogies with established world mining camps such as the California Mother Lode district and those in Archean Greenstone Belts of PreCambrian shields world wide. The Mother Lode-type deposits are well documented by Knopf, (1929) Bohlke and Kistler (1986) Landefield (1986) and Weir et. al. (1987). The Archean greenstone hosted lode gold deposits are described by Hodgson and MacGeehan (1982) and Colvine et. al. (1984).

One setting that has been given particular emphasis in Newfoundland is the major structure, ultramafic-related environment. The main constituents are: major structural zones containing dismembered ophiolite lithologies - particularly ultramafic rocks, structurally controlled carbonatization and silicification and the common occurrence of granitic plutonic rocks. The Baie Verte - Brompton Line (Williams and St. Julien, 1982) and the Gander River Ultrabasic Belt (GRUB-line) (Blackwood, 1982)

are the two most prominent examples of this setting in Newfoundland, with strike lengths of 70 and 110 Km respectively. The rapidly growing number of reported gold occurrences in the province (Tuach et. al., 1988) show a striking spatial relationship to major structures (Figure 1.1).

Gold exploration work in the study area during 1984 and 1985 outlined extensive areas of anomalous gold in overburden. The anomalous concentrations occurred over strong carbonate alteration in a fault-bounded sliver of ultramafic rocks and over the adjacent Cape St. John Group and Betts Cove Ophiolite. Several small showings were found within the ultramafic rocks at that time. This study was initiated in 1986 to document known occurrences of mineralization, determine geochemical signatures that may be associated with such mineralization and develop a genetic model to explain the occurrence of the mineralization.

## 1.2 LOCATION:

The study area is located on the southeast side of the Baie Verte Peninsula between the nearly deserted mining town of Tilt Cove and the outport community of Nippers Harbour. The Baie Verte Peninsula is situated on the north

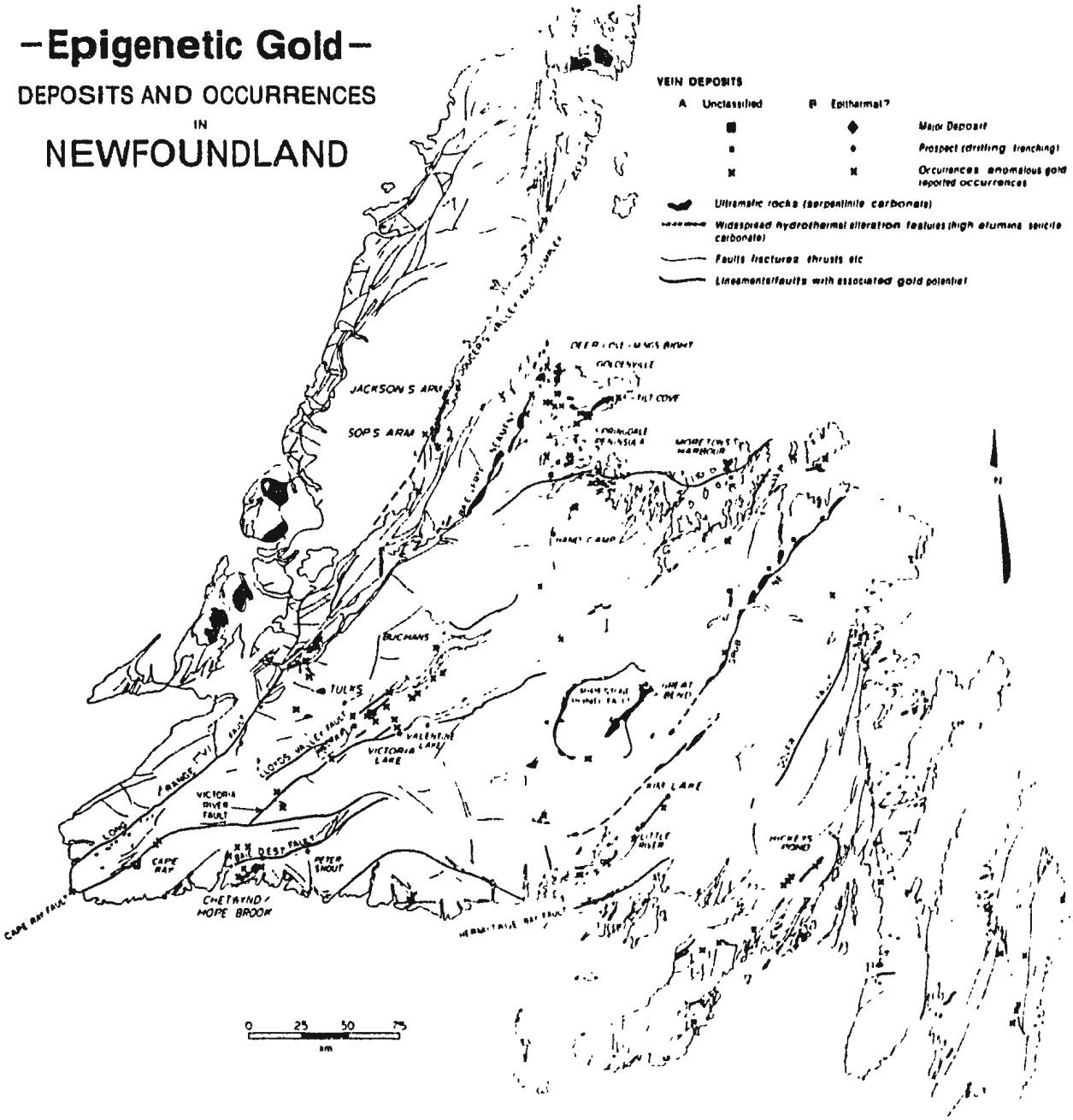


Figure 1.1. Gold occurrences of Newfoundland (after Tuach et. al., 1988)

central coast of Newfoundland, immediately southeast of the Great Northern Peninsula (see Figure 1.2).

By road, Tilt Cove is approximately 500 Km from Port aux Basques in the southwest and 650 Km from St. John's in the southeast. All communities on the peninsula are served by paved or gravel all season roads.

## 1.3 Geologic Setting:

In the scheme of tectono-stratigraphic divisions proposed for the Newfoundland Appalachians by Williams et. al. (1987), the Baie Verte Peninsula is located at the boundary between the Dunnage and Humber zones (Figures 1.3 and 1.4). The Humber Zone represents shelf and shelf-margin deposits within the Cambrian to early Ordovician Iapetus Ocean, on the ancient continental margin of North America. The Dunnage Zone is considered to be remnants of an ocean floor in existence prior to the closure of Iapetus and an island-arc regime formed during the ocean closure. Figure 1.4 illustrates the geology of the Baie Verte Peninsula with the Humber and Dunnage boundaries included. Table 1.1 summarizes the geology of the Baie Verte Peninsula.

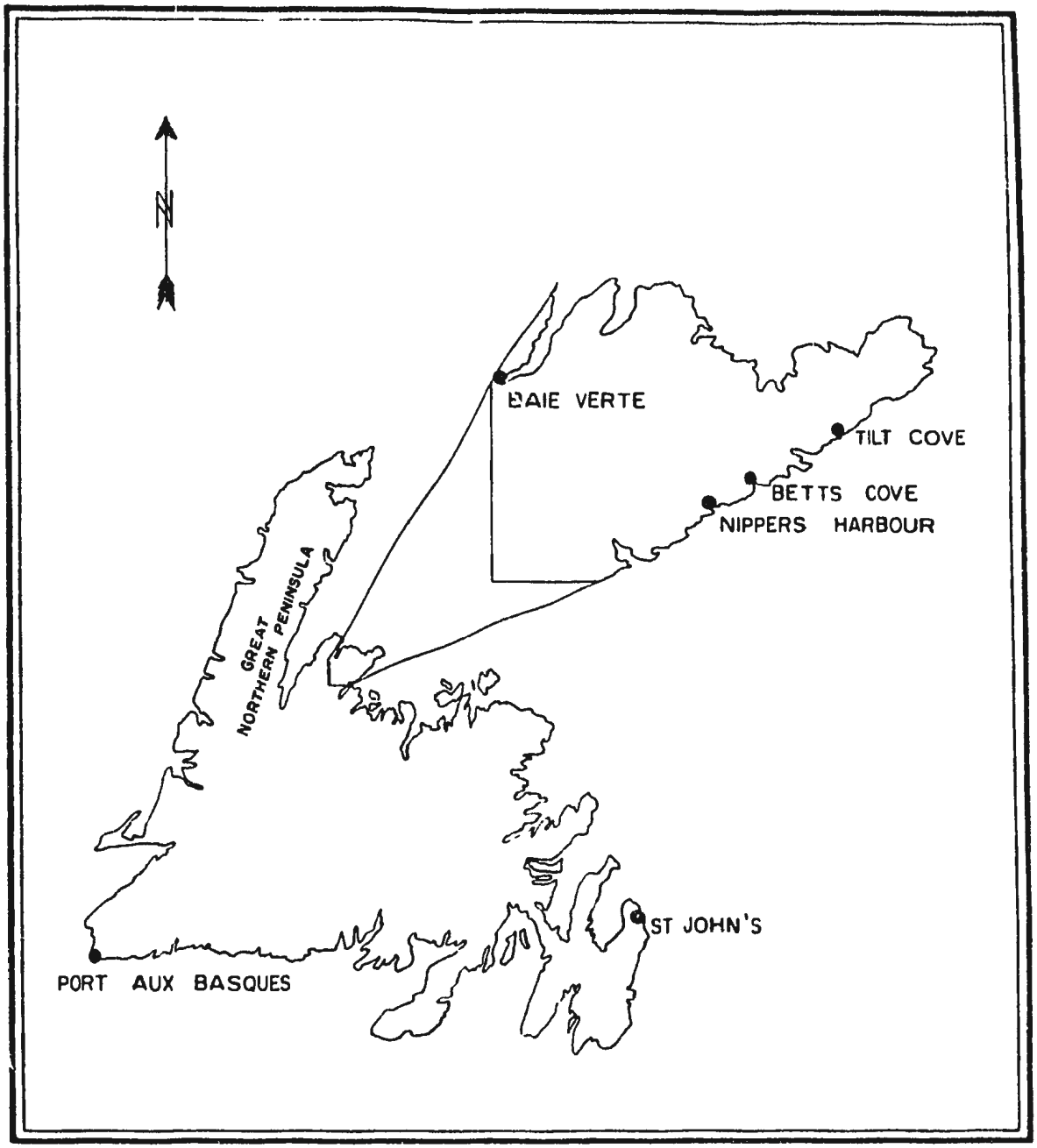


FIGURE 1.2 LOCATION MAP

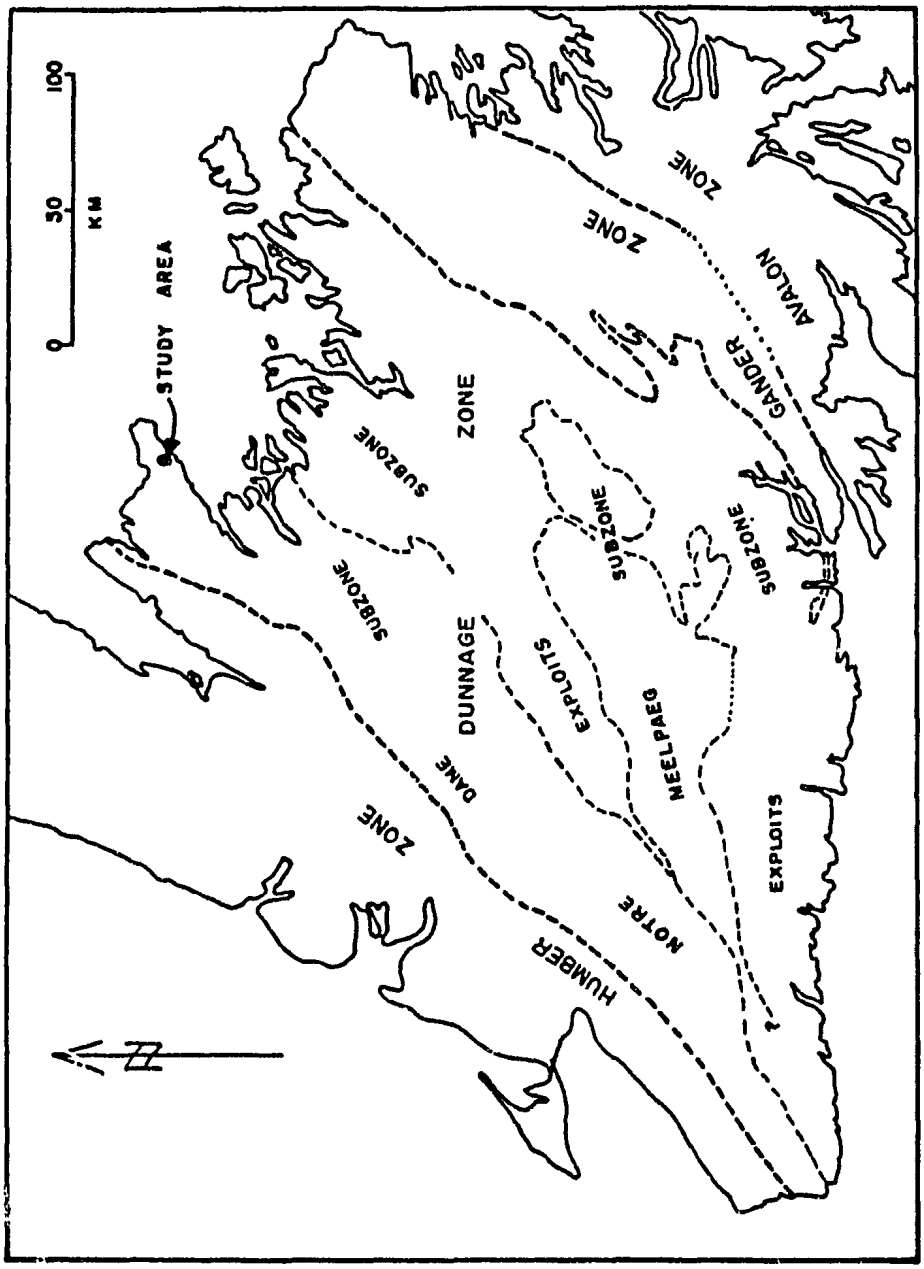


Figure 1.3 Tectono-stratigraphic subdivisions of the Newfoundland Appalachians (after Williams et. al., 1987)

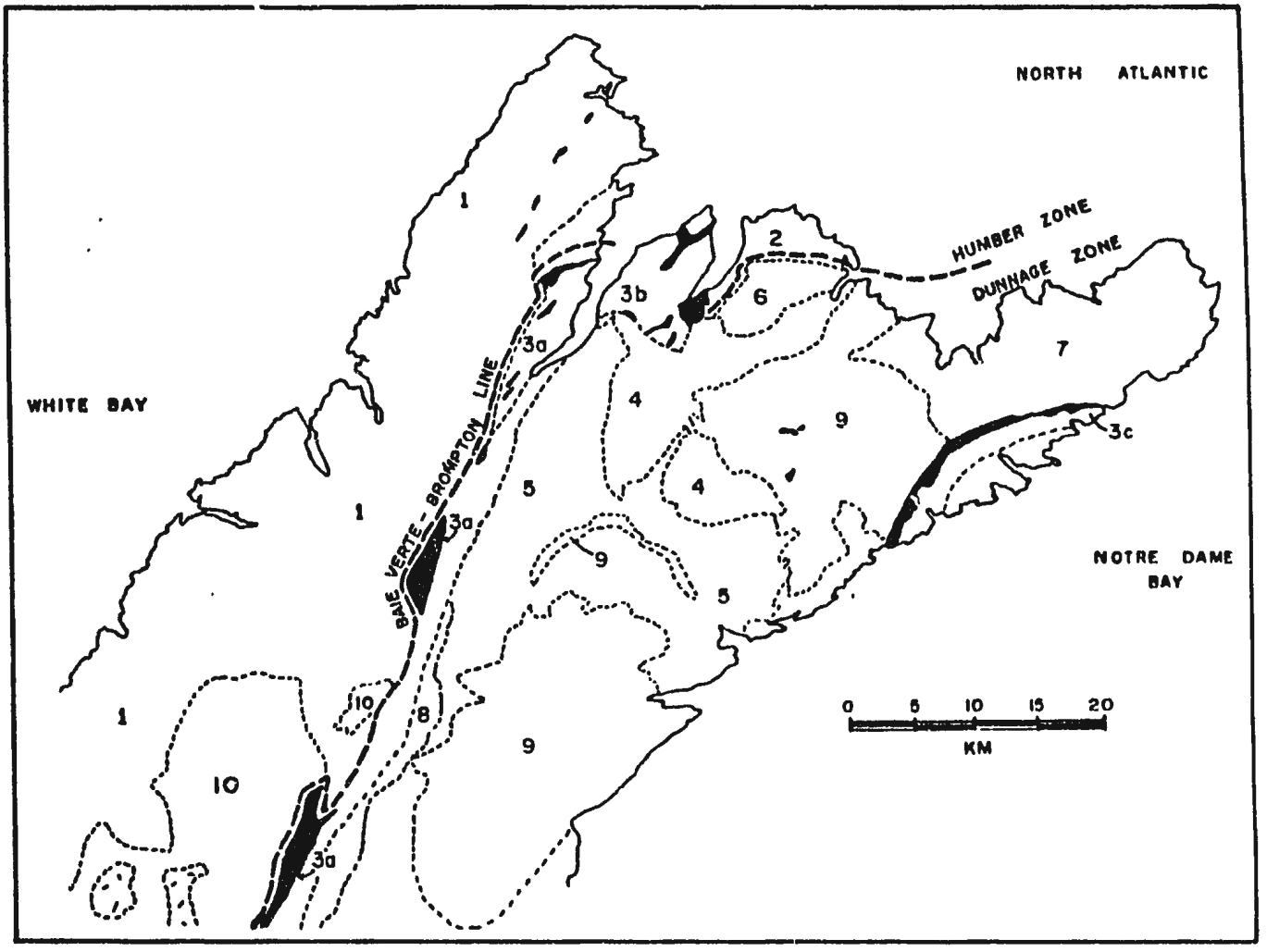


DEVONIAN

10 WILD COVE POND IGNEOUS SUITE

9 CAPE BRULE PORPHYRY

ULTRAMAFIC ROCKS

SILURIAN

8 MICMAC LAKE GROUP

7 CAPE ST. JOHN GROUP

ORDOVICIAN

6 DILLAMAGON GRANITE

5 BURLINGTON GRANODIORITE

4 PACQUET HARBOUR GROUP

3 OPHIOLITE: a) ADVOCATE b) POINT ROUSSE

c) BETTS COVE

PRECAMBRIAN - CAMBRIAN

2 MINGS BIGHT GROUP

1 FLEUR DE LYS SUPERGROUP

FIGURE 1.4. GEOLOGY OF THE BAIE VERTE PENINSULA

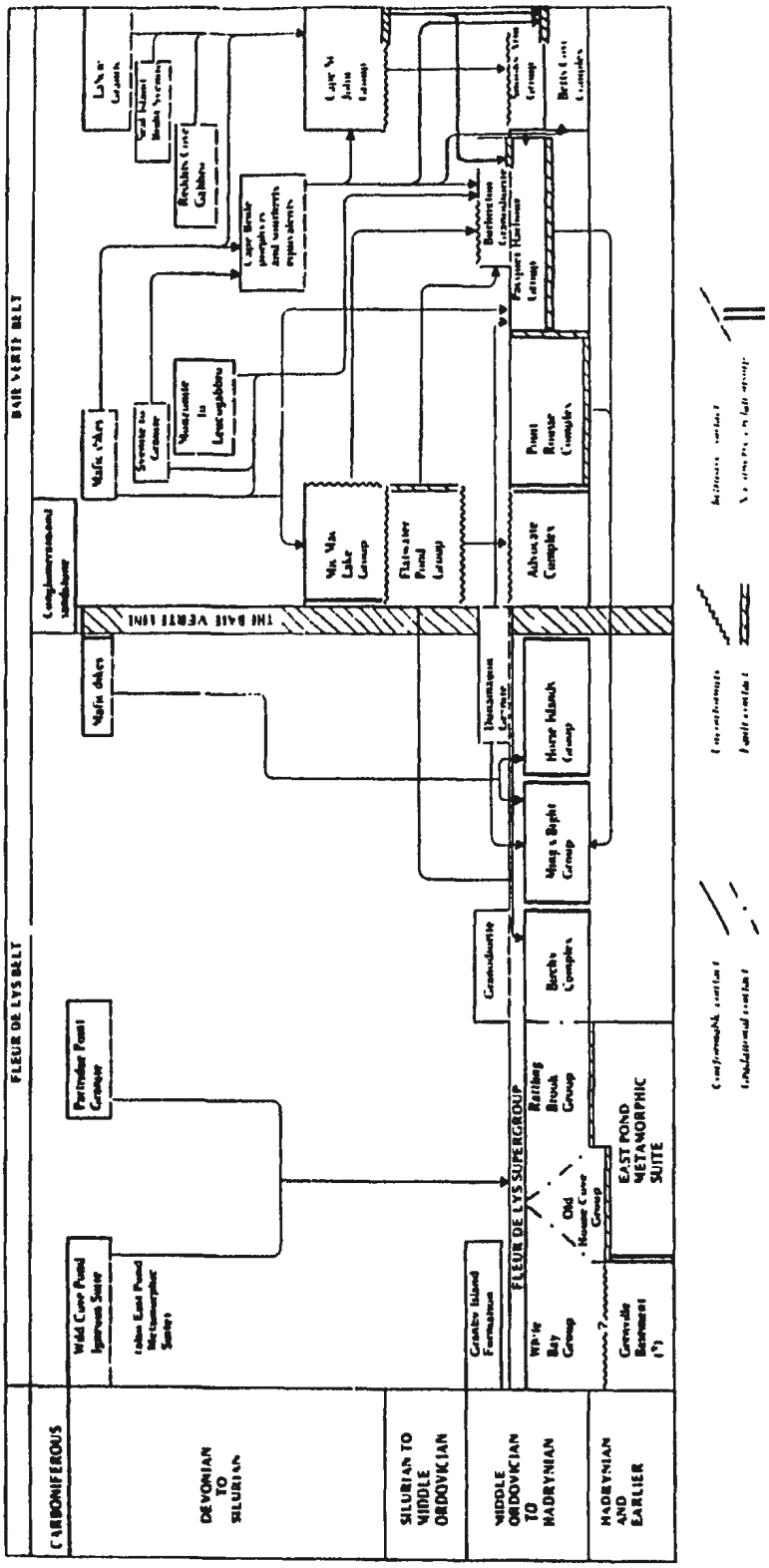


Table 1.1. Relationships between lithologies of the Baie Verte Peninsula. (modified after Hibbard, 1983)

### 1.3.1 Humber Zone:

The Humber Zone represents the ancient continental margin of North America where a passive margin sedimentary sequence accumulated during the Late Cambrian to Early Ordovician growth of Iapetus (Williams et. al., 1987). The Humber zone is underlain by Grenvillian basement gneiss and Cambro-Ordovician shelf-margin sediments. During the Taconic Orogeny, ophiolitic and sedimentary allochthons were emplaced over the shelf margin. On the Baie Verte Peninsula, the Humber Zone consists of a Group of polydeformed and metamorphosed psammites and semipelites termed the Fleur de Lys Supergroup by Church (1969) and redefined by Hibbard (1983).

The main deformation and metamorphism in the Humber Zone are considered to be of early Ordovician age (Bursnal and De Wit, 1975; Hibbard, 1983) and related to the westward obduction of ophiolites during the Taconian event. The eastern margins of the Humber Zone are most affected by Acadian deformation but Taconic allochthons in the western Humber Zone show evidence of post Taconic deformation (Cawood and Williams, 1988). Carboniferous deformation in the Humber Zone is evident at Sops Arm and Deer Lake where faulting juxtaposes Ordovician, Silurian and Carboniferous rocks (O'Laughlin, 1981; Williams, 1982).

Metamorphism in the Humber Zone spans a wide range from virtually unmetamorphosed shelf carbonates to granulite facies Grenville gneiss. On the Baie Verte Peninsula, the Fleur de Lys Supergroup is comprised of upper greenschist to middle amphibolite facies schists and gneisses (Hibbard, 1983).

### 1.3.2 Dunnage Zone:

East of the Humber Zone are rocks of ocean floor and island-arc affinity comprising the Dunnage Zone. These rocks record the formation of oceanic crust and island-arc assemblages prior to and during the early stages of the Taconic orogeny. Oceanic crust is present on the Baie Verte Peninsula in the Advocate, Point Rousse and Betts Cove ophiolites. The Pacquet Harbour Group is a dominantly mafic island-arc volcanic rock unit. Several granitic to granodioritic plutons such as the large Burlington Granodiorite on the Baie Verte Peninsula intrude the ophiolitic and island-arc sequences of the Dunnage, and are considered to be products of melting subducted crust (Dean, 1977).

The Dunnage Zone is deformed by the middle Ordovician Taconian, and the Devonian Acadian orogenies. Taconian effects are strongest in the west and Acadian effects strongest in the east, although Acadian re-activation of

presumed Taconic structures often masks the earlier event and causes difficulty distinguishing the two. The extent of Carboniferous deformation in the Dunnage Zone is uncertain. Movement along major faults has occurred intermittently into the Carboniferous.

Metamorphic grades in the Dunnage Zone range from lower greenschist to lower amphibolite facies, the higher grade rocks occur toward the southeast.

### 1.3.3 Humber-Dunnage Boundary:

The Baie Verte - Brompton Line, a major northeast-southwest trending structural lineament that transects the peninsula, forms the boundary between the Humber and the Dunnage Zones. This lineament is traceable into the eastern townships of Quebec and represents the roots of ophiolites obducted onto the North American continent during the early Ordovician (Williams and St. Julien, 1982). Dismembered ophiolite lithologies are preserved along the lineament on the Baie Verte Peninsula (Hibbard, 1983). At the town of Baie Verte, the Baie Verte - Brompton Line swings sharply into an east-west orientation in what Hibbard (1983) calls the Baie Verte Flexure. North of the flexure, the Fleur de Lys Supergroup is represented by deformed psammites and pelites of the Mings Bight Group. Figure 1.5 is a compilation of major

structural features on the peninsula, the Baie Verte Line being the most prominent.

### 1.3.4 Geological Features which Transgress the Humber/Dunnage Boundary:

A final phase of volcanic activity recognized in Newfoundland occurs within the Dunnage and eastern Humber Zone. This volcanism is subaerial, it is Silurian to lower Devonian in age (Coyle and Strong, 1986; Chandler et. al., 1986) and is a bimodal (matic-felsic) assemblage with intermixed volcanogenic sedimentary rock. Coyle and Strong (1986) interpret many of these volcanic terranes as calderas. These volcanic rocks, represented on the Baie Verte Peninsula by the Micmac and Cape St. John Groups, unconformably overly the Ordovician volcanic and edimentary sequences. They are related to melting of lower crust as a result of Taconic crustal thickening (Coyle and Strong, 1986).

Plutons of dominantly granitic composition occur in association with the Silurian volcanic sequences. The Cape Brule Quartz Feldspar Porphyry is an example of these intrusives on the Baie Verte Peninsula. These Siluro-Devonian rocks are virtually unmetamorphosed except where they are affected by Acadian deformation.

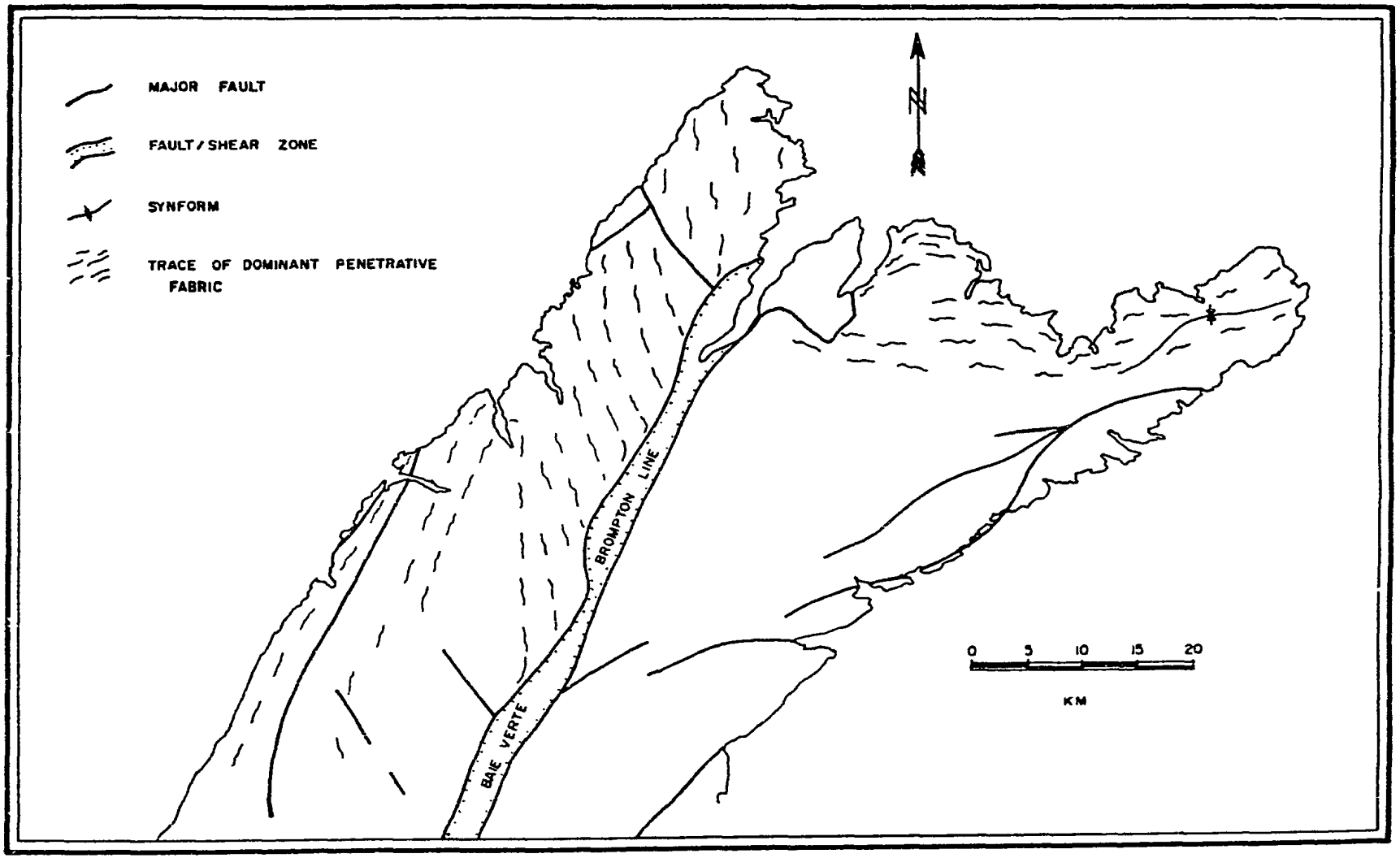


FIGURE 15 PROMINENT STRUCTURAL ELEMENTS OF THE BAIE VERTE PENINSULA.

Carboniferous clastic sedimentary rocks unconformably overly rocks of Grenville to Devonian age in the Humber and Dunnage Zones. Carboniferous sedimentary rocks occur in a small area on the southern Baie Verte Peninsula (Hibbard, 1983).

### 1.3.5 The Study Area:

The study area for this thesis occurs within the western margin of the Dunnage Zone. The area encompasses rocks of the Lower Ordovician Betts Cove Complex and conformably overlying, Middle Ordovician Snooks Arm Group, as well as the Silurian Cape St. John Group (see Figure 1.4). The Ordovician and Silurian units are juxtaposed along a fault zone marked by ultramafic rocks related to the ophiolite, except in the eastern section of the study area where the ophiolite and Snooks Arm Group are unconformably overlain by the younger Cape St. John Group.

## 1.4 Physiography:

The coast line between Tilt Cove and Nipper's Harbour is rugged with steep cliffs rising abruptly from the ocean to elevations of 100 to 200 hundred metres. These cliffs are inundated by ice carved coves and inlets. Inland from the coast, the land levels off but relief is still in the range of 25 to 50 metres. The relief is characterized by

steep, sharp ridges and cliffs trending east-west to northeast-southwest. The northern portion of the study area is especially rugged, where the more resistant Silurian Cape St. John Group felsic volcanic rocks, and the Cape Brule Quartz-Feldspar Porphyry outcrop. The contact between the ophiolite and the felsic rocks to the north is a fault zone which is eroded to form a long arcuate valley.

The extent of vegetative cover is largely controlled by the underlying geology. The less resistant mafic rocks to the south support a variable forest cover which consists mainly of black spruce and balsam fir. The more rugged terrain to the north has little vegetation except in flat areas that have been able to accumulate a soil horizon. Most low lying areas are occupied by peat bog due to poor drainage development.

The outcrop exposure is good and ranges from 5-10% in the heavily wooded areas to almost 70% in the rugged, unvegetated areas in the north and west. Unfortunately, even with the large amounts of outcrop exposure, textures are often difficult to discern because of heavy growth of lichen on the outcrop surface.

## 1.5 Previous Work:

The Baie Verte Peninsula has been the focus of mining and exploration activity since the mid 1800's when the Tilt Cove copper deposits were discovered. The majority of exploration focussed on ophiolite-type base metal deposits and very little effort was expended in exploring for or developing gold mining potential.

The past lack of interest in gold as a separate commodity is perhaps reflected in the large number of significant showings that have turned up since 1980, when exploration efforts for gold intensified (see Figure 1.1). Prior to 1980, only about half a dozen showings with significant gold values were known on the peninsula (Snelgrove, 1935; Fitzpatrick, 1981; Hibbard, 1983; Martin, 1983). Of these showings only one, the Goldenville near Mings Bight, ever produced any gold. At present there are 40 gold occurrences reported on the Baie Verte peninsula (Tuach, 1988).

The discovery of many new gold showings in the Baie Verte area makes it an appropriate location for studying the genesis and mode of occurrence of gold mineralization. Limited research has been carried out in the past on the old Mings Bight occurrences (Howley, 1918; Snelgrove, 1935; Watson, 1947; Frew, 1971; Fitzpatrick, 1981) but much work

is needed to understand the controls on mineralization.

## 1.6 Scope of Thesis:

This thesis has three objectives. First, to document recently discovered gold occurrences in the study area to add to a growing list throughout Newfoundland. Factors taken into consideration are:

1/ the ore/gangue mineralogy of the occurrences, as well as host rock and alteration mineralogy,

2/ the setting of the mineralization, be it structurally controlled, lithologically controlled or other,

3/ timing of the mineralizing event with respect to major geological processes such as plutonism and orogenesis.

Factors 1 and 2 are mostly descriptive issues and are considered on the basis of field and laboratory observations. Factor 3 also involves a large input from observational data but has been supplemented by geochemical studies.

The second objective was to determine the geochemical characteristics of the gold mineralization and alteration. Particular care was taken in attempting to find effective lithogeochemical pathfinders such as As, Sb, and Te.

The last objective was to generate a genetic model for the gold mineralization, the model being the culmination of all research in the area. The geologic setting, geochemistry, petrography and age relationships are all combined to define the most suitable sequence of events which gave rise to the gold mineralization.

# CHAPTER 2

## Detailed Geology

### 2.1 General Geology:

Rock units of contrasting origins and compositions are present in the area and may be described in terms of the pre-Carboniferous tectonic and volcanic evolution of the Newfoundland Appalachians (Williams, 1969; Colman Sadd, 1982; Hibbard, 1983; Stockmal et. al., 1987). Early work in the area by Neale et. al. (1957), Upadhyay (1973), Neale et. al. (1975), DeGrace et. al. (1976) and Jenner and Fryer (1980) has contributed greatly to the present level of geologic understanding.

The oldest rocks present are the mafic-ultramafic volcanic and plutonic rocks comprising the Betts Cove Complex (U/Pb zircon geochronology, 489 $^{+}3.1/^{-}1.8$ ma; Dunning and Krogh, 1985). The ophiolite outcrops in the southeastern portion of the study area. Ultramafic rocks mark the base of the ophiolite and occur in a northeasterly trending belt from Burtons Pond in the southwest, to Beaver Cove Pond in the northeast, a distance of approximately 16 km. In Betts Cove, a complete section of ophiolite stratigraphy is exposed (Riccio, 1972) younging to the southeast. To the northeast, the gabbro and sheeted dyke

members are present only locally and ultramafic rocks are in fault contact with the pillow lavas. Within the study area, ophiolite stratigraphy is vertical to steeply north-dipping and overturned.

Conformably overlying the ophiolite, south of the study area, is the Snooks Arm Group of basalt and mafic pyroclastic rocks. The group is comprised of a basal pyroclastic and sedimentary formation overlain by a pillow lava unit. This sequence is repeated once in the overlying rocks. The group has been dated as Arenig (Middle Ordovician) by fossil graptolites in shales within the upper pyroclastic formation (Snelgrove, 1931; Dean, 1978; pers. comm., Williams, 1988).

The Snooks Arm Group was interpreted by Strong (1977) to be of island-arc origin but later work by Jenner and Fryer (1980) refutes this theory on the basis of geochemistry. They suggest an origin within an oceanic island setting or as part of a back-arc, marginal basin. The ophiolite and the Snooks Arm Group are thought to have formed in a suprasubduction zone environment prior to obduction onto the North American continental margin during Taconic orogenesis (Coish, 1979).

The Cape St. John Group is the youngest volcanic package in the area and unconformably overlies the Snooks

Arm Group at Beaver Cove, 2 Km northeast of Tilt Cove (Neale et. al., 1975). The Cape St. John Group also overlies the ophiolite at Tilt Cove (Strong, 1984a), between the Snooks Arm road and Long Pond (Kusmirski and Norman, 1982; and this report) and southwest of Nippers Harbour (DeGrace et. al., 1976). In contrast to the Betts Cove Complex and the Snooks Arm Group which are submarine, dominantly mafic volcanic assemblages, the Cape St. John Group is comprised of subaerial volcanic and volcanogenic sedimentary assemblages. The group is deformed, presumably by the Acadian orogenic event. Coyle and Strong (1987) correlate the Cape St. John Group with the Springdale Group to the southwest for which there is an U/Pb zircon date of 429 ma (Chandler et. al., 1986). The Cape St. John Group has been dated at approximately 427 ma (Coyle, pers. comm., 1988) by U/Pb zircon geochronolgy.

The Cape Brule quartz-feldspar porphyry occurs in the northwest portion of the map area. It intrudes the Cape St. John Group north of the study area and the ophiolite in the southwest, near Nippers Harbour (DeGrace et. al., 1976). A small apophisis of the porphyry intrudes the Snooks Arm Group at Tilt Cove. The age of the pluton is not well established but the intrusion is thought to relate to Siluro-Devonian plutons throughout central Newfoundland such as the Topsails Igneous Suite, the Gull Lake Granite and the Wild Cove Pond Igneous Suite (Coyle and Strong,

1987). The relationship between the porphyry and the Cape St. John Group is not clearly defined but the porphyry was considered by Hibbard (1983) to be cogenetic with the volcanic rocks of the Cape St. John Group. Accepting this interpretation, the 427 ma date for the Cape St. John Group should apply to the porphyry as well. The Cape Brule Porphyry is deformed and shows a well developed foliation, especially in the north.

## 2.2 Detailed Geology:

The zone of greatest potential for economic gold mineralization was assumed to be centered on the ultramafic rocks where they are in fault contact with the upper ophiolite, the Cape St. John Group and the quartz-feldspar porphyry. Following this model, mapping was restricted to a narrow band encompassing the fault zone. For a detailed account of the regional geology, the reader should refer to references cited in the above section. Map 87-01, included at the back, portrays pertinent geologic information such as distributions of alteration and known mineralization.

### 2.2.1 Ultramafic Rocks:

Ultramafic rocks (unit 1) outcrop in a narrow linear belt in the center of the map area. The belt extends for approximately 16 Km in a northeasterly direction. It is

disrupted by a fault in one location only, from the Snooks Arm road to Long Pond, a distance of 1.2 Km. The maximum thickness of the unit within the map area is 500 meters at the northeast end of Red Cliff Pond. The minimum thickness is 10 meters at the east end of Long Pond.

It is likely that the altered ultramafic rocks present within the study area originated as cumulate harzburgites like those present further southwest at Betts Cove. The ultramafic rocks at Betts Cove have been described by Riccio (1972) and Upadhyay (1973). The most complete description is provided by Riccio (1972) from which the following section has been extracted.

> The ultramafic rocks commonly show well developed gravitational layering, the distribution and overall structure of which are shown in map 1. The best developed sections of ultramafic rocks occur north-northeast of Kitty Pond and on the ridge southwest of Big Duck Pond. At Kitty Pond the section is 120 m. thick and at Big Duck Pond approximately 200 m. thick. These sections are considered to be typical of the ultramafic zone.
>
> The layering consists of parallel layers containing varying amounts of pyroxene crystals. Pyroxene-rich layers such as clinopyroxenite, orthopyroxenite and websterite are dark grey and more resistant to erosion as compared to pyroxene-poor layers which are reddish or yellowish and more easily eroded (Plate 1). On the weathered surfaces of olivine-clinopyroxenite and wehrlite layers, greenish clinopyroxenes stand out in relief. Some poikilitic wehrlite layers are deep green in colour and have weathered surfaces spotted with white subspherical pyroxene crystals (Plate 2). In the field it is not easy to distinguish between different types of pyroxenite. Dunite has a characteristically smooth weathered surface which may be red, yellowish or brown, whereas harzburgite layers have rough weathered surfaces and are brick-red in colour.

The thickness of individual layers ranges from a few mm. to several meters but commonly the layers are between 2 and 10 cm. thick. Thicker layers appear to be concentrated toward the top of the ultramafic zone. The upper and lower contacts of layers are usually sharp.

The layers are repeated in sequences or cycles (Jackson, 1961). Dunite-harzburgite (orthopyroxenite) sequences constitute the lower part of the ultramafic zone. The middle part of the ultramafic section is made up predominantly of dunite (harzburgite)-orthopyroxenite-websterite sequences (Plate 3 and 4). At the top of the ultramafic zone the layers are composed of dunite, wehrlite, olivine-clinopyroxenite, and clinopyroxenite. However some olivine-clinopyroxene bearing sequences do occur below dunite-orthopyroxenite-websterite sequences. Rock types displaying poikilitic textures are found at any stratigraphic level within the ultramafic zone but they are more abundant near the contact with the mafic zone.

The uppermost part of the ultramafic zone is characterized by the common occurrence of normal and reverse clinopyroxene size-graded layers varying in composition between olivine clinopyroxenite and wehrlite (Plate 5). The upper contact of the size-graded layers is transitional into a finely laminated zone consisting of alternating layers of contrasting grain size, whereas the basal contact is sharp (Plate 5).

Layers may usually be traced to the limits of the outcrop (Plate 6). In the lower part of the Kitty Pond section however some of the layers are laterally discontinuous and sometimes boudinaged.

There are no fresh ultramafic rocks in the study area. A progressive increase in shearing and related hydration and carbonatization may be traced northeastward from the cumulate rocks near Betts Cove, into the heavily sheared and altered ultramafic rocks within the study area. Altered ultramafic assemblages consist of combinations of serpentinite, serpentine-magnesite, talc-magnesite and hematite-rich, quartz-dolomite.

Serpentinite is rare within the study area. Small outcrops occur in the extreme southwest, (see Map 87-01) just northeast of Betts Big Pond. These rocks are fine grained, heavily fractured, dark green to pale green-brown on weathered surfaces. Minor chrysotile occurs locally in fractures. In thin section, serpentine pseudomorphs of olivine may be discerned but these are most often overprinted by foliated serpentine.

Serpentine-magnesite assemblages occur sporadically throughout the entire belt of ultramafic rocks, usually where the intensity of shearing has been low. These rocks vary from massive to fractured. The magnesite occurs as fine to medium grained euhedral crystals overprinting a serpentine matrix. Maximum carbonate content is around 10%. Weathered surfaces produce a rusty brown mottled texture of magnesite on a pale green to light brown serpentine background.

Talc-magnesite is the most common alteration assemblage. From the southwest of the map area to the Snooks Arm road, the ultramafic belt consists exclusively of talc-magnesite except for the minor serpentinite mentioned above and some serpentine-magnesite along the shores of Red Cliff Pond. Talc-magnesite is also the dominant ultramafic rock between the east end of Long Pond and Beaver Cove Pond.

The principle mineralogy of the talc-magnesite rocks is simply talc and magnesite with rare quartz, chlorite and opaque minerals. Talc forms an irregular bluish-green matrix to orange-brown 0.5-5mm clusters of interlocking carbonate grains. The ratio of talc to magnesite varies but is in the range of 0.75:1. Opaque minerals consist of specular hematite, magnetite and chromite in grains less than 1mm disseminated throughout. Specular hematite as subhedral and euhedral crystals is most abundant.

The talc-magnesite rocks are cross cut locally by late quartz veins which transect schistosity and often occur as conjugate sets. Two main localities display these veins best. One is immediately west of the northwest shore of West Pond, the second is at Arrowhead Pond (Figure 2.1). These veins are often of a coarsely crystalline or massive nature and some commonly have disseminated or banded magnesite parallel to the vein walls (Plate 2.1). These veins are mostly barren except for two at Arrowhead Pond that contain chalcocite and gold. They are rarely more than 0.2 meters thick and tend to pinch out over a strike length of 10 meters or less.

Ultramafic rocks consisting of quartz, dolomite and hematite are the most unusual and striking in appearance. This rock type occurs only at Dump Pond and between the west and east ends of Long Pond. Exposures are rarely

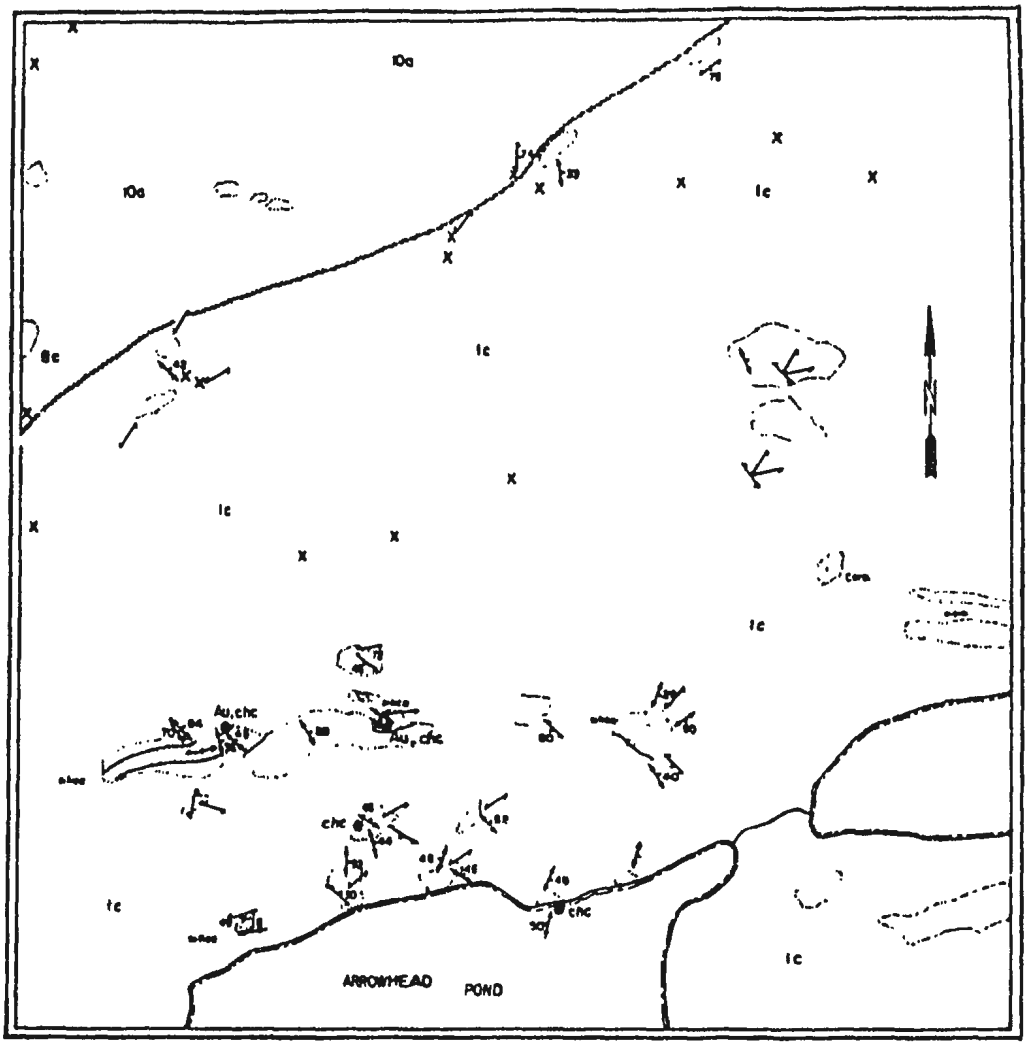


ARROWHEAD POND SHOWING

MAP NO. 87-01-A

SCALE

0 meters 90

LEGEND

- Mineral Showing
- Sample Location
- Schistosity (inclination unknown / orientation as shown)
- Fracture Cleavage
- Quartz Vein
- Fault
- Outcrop
- Alteration Zone (carbonate)

10a Amygdaloidal Basalt
8c Quartz-Eye Tuff
Cape St. John Group

1c Ultramafic — Talc Carbonate
Betts Cove Complex

MINERAL ABBREVIATIONS

Au - Gold
Chc - Chalcocite
Silica - Silicification
Carb. - Carbonatization

DETAILED LEGEND ON MAP 87-01 ALONE WITH LOCATION OUTLINE

Figure 2.1. Detailed map of Arrowhead Pond Showing area (listwaenite-type).

Plate 2.1. Thin quartz veins typical of those commonly found cross cutting the talc-magnesite schist in several localities; northwest of West Pond.

more than 25 meters wide. The rock is red to rusty-brown-weathering massive dolomite, with abundant randomly oriented quartz veins 0.5-15 cm wide (Plate 2.2) that anneal fractures. Cavities lined with euhedral quartz crystals are common (Plate 2.3). Quartz veining increases in intensity toward the contact with the Cape St. John Group to the north.

### 2.2.1a Contact Relationships:

Contacts between the ultramafic rocks and other lithologies are usually fault controlled. The southern fault contact with the ophiolite pillow lava is best exposed at the northwest end of Red Cliff Pond. The northern bounding fault separates the ultramafic rocks from various lithologies of the Cape St. John Group and the Cape Brule Porphyry. In the area around Tilt Cove, clastic rocks of the Cape St. John Group unconformably overlie pillow lavas of the ophiolite, which are in fault contact with the ultramafic rocks (Plate 2.4). The amount of deformation evident at the Cape St. John Group - ultramafic contact is variable, ranging from minor fracturing to mylonitization, as at the north shore of Red Cliff Pond; here there is mylonite developed in probable interbedded pyroclastic and clastic sedimentary rocks of the Cape St. John Group. Extensive alteration accompanies the deformation.

Plate 2.2. Quartz-hematite-dolomite alteration. Note the distinctive rusty-brown colour and the prominent-weathering quartz veins.

Plate 2.3. Cavity wall in quartz-dolomite-hematite altered zone lined with euhedral quartz. (1/2 actual size)

Plate 2.4. Fault contact between talc-magnesite altered ultramafic rocks and sheared pillow lava. Unconformity between the pillow lava and the overlying Cape St.John Group is just out of photo at the upper right. (Tilt Cove Road)

A felsic volcanic and sedimentary unit (presumably related to the Cape St. John Group) occurs within ultramafic rocks on the west side of Tilt Cove. Sedimentary rocks at the base of the sequence unconformably overly the talc-magnesite altered ultramafic rocks. Thus, the Cape St. John Group is locally in fault contact with the ophiolite and also unconformably overlies a variety of ophiolite stratigraphy, indicating significant erosion of the ophiolite prior to deposition of the Cape St. John Group.

### 2.2.2 Ophiolite Volcanic Sequence:

The ophiolite volcanic stratigraphy is well documented by Upadhyay (1973) and DeGrace et. al. (1976). Pillow lava (unit 4) and a thin unit of interbedded argillite (unit 5) are the only ophiolite lithologies commonly encountered in the study area except the ultramafic rocks. Gabbro (unit 2) and some sheeted dykes (unit 3) are exposed at Long Pond.

The pillow lava unit is uniform along strike with pillows ranging from 0.5 to 1 meter in maximum dimension. Minor diabase dykes cut the pillow lava and some discontinuous sills are present also. Within the pillow lava, an argillite unit varies in thickness from 10 to 50 meters and marks a hiatus in volcanism. It is interbedded

with pillow lava at the base (see Plate 2.5). The argillite occurs continuously along strike from the east side of the Snooks Arm road to the area south of Betts Big Pond (Upadhyay, 1973). The sediments vary in colour from buff-white, through green to bright maroon-red colour. Some coarser grained turbiditic greywacke sequences are interbedded with the argillite.

All of the ophiolitic rocks have been subjected to greenschist facies metamorphism. Typically, the mafic volcanic rocks consist of primary plagioclase and clinopyroxene as well as the alteration assemblage; albite, amphibole, chlorite, epidote, quartz and calcite (Upadhyay, 1973). The alteration assemblage is representative of submarine, sea water-related hydration processes (Mottl, 1983).

### 2.2.3 Cape St. John Group:

The Cape St. John Group is comprised of a subaerial to shallow marine sequence of interbedded volcanic and sedimentary rocks (DeGrace et. al., 1976). The volcanic rocks range in composition from massive basaltic flows to rhyolites. Pyroclastic rocks are common as ignimbrites, ash flow and lapilli tuffs. Sedimentary rocks are interbedded with the sequence throughout and are generally composed of locally derived volcanogenic detritus.

Plate 2.5. Red and brown, cherty argillite interbedded with ophiolite pillow lava at the base of the inter-ophiolite argillite unit (unit 5). (East Pond)

Within the study area, the main lithologies of the Cape St. John Group are coarsely amygdaloidal, massive basaltic flows, massive crystal-lithic tuffs and sedimentary rocks of variable composition and grain size.

The mafic volcanic rocks (unit 10) occur as discreet flow horizons interbedded with the pyroclastic and sedimentary rocks. These volcanic rocks are easily distinguished from the ophiolitic volcanic rocks in that they are less altered, they are coarsely amygdaloidal and pillowed structures have not been observed. Flow tops may be discerned in some cases on the basis of amygdule concentrations and flow top breccia horizons. Ropy textures are locally preserved.

The crystal-lithic tuffs (unit 8a) have a uniform quartz and feldspar content and may be mistaken for granite in some outcrops. In thin section there are abundant broken feldspar crystals and embayed quartz grains in a fine grained quartz-feldspar to sericitic matrix (DeGrace at. al., 1976). Lithic fragments within this unit consist dominantly of green and red altered ultramafic fragments up to 20 cm across, as well as some red jasperoid, rhyolite and minor fragments of the host rock.

The sedimentary rocks are of two main types; 1/ uniformly bedded shallow marine arkose (unit 9a) and 2/ coarse fluviatile conglomerates (units 9b and 9B). The arkosic sedimentary rocks are restricted to the eastern map area around Tilt Cove and Dump Pond. They are probably a reworked equivalent of the crystal-lithic tuffs described above.

The conglomerates are usually poorly sorted and polymictic. At least two distinct types are recognized. The first type occurs at the unconformity between the Cape St. John Group and the ophiolite, between Red Cliff Pond and Long Pond. This conglomerate contains abundant clasts of mafic volcanic material presumably derived from the ophiolite. This assumption is supported by the common occurrence of red and green finely bedded argillite clasts identical to lithologies that occur within the ophiolitic pillows less than 400 meters to the south.

The second type of conglomerate occurs higher up in the Cape St. John Group stratigraphy and is characterized by the presence of abundant coarse jasperoid clasts and finer grained ultramafic material in the matrix. This conglomerate is often spatially associated with pronounced structural lineaments and shear zones and consequently, may be highly deformed. This association with structures implies an origin along reactivated fault scarps which

also exposed the ultramafic unit.

### 2.2.4 Cape Brule Porphyry:

The Cape Brule Porphyry (unit 11) outcrops in the north-western part of the study area. The porphyry here is complex and rarely resembles the uniform textured, medium grained batholith exposed to the northwest and described by DeGrace et. al. (1976). In this area, the porphyry is fine to medium grained and contains grey quartz grains, less than 1mm in diameter, randomly distributed within a matrix of indistinct feldspar crystals. Hibbard (1983) suggests that some portions of the unit may be subaerial extrusive phases of a high level magma chamber. This concept is supported by outcrops northwest of West Pond where the "porphyry" displays compositional banding, fragmented feldspar phenocrysts and quartz-eye bearing aphanitic rocks more similar to an ash flow tuff than an intrusive. Also, units of poorly sorted and bedded conglomerate grade into these extrusive-looking rocks. The conglomerates contain clasts of dominantly felsic volcanic material although some carbonate altered ultramafic material occurs as well.

## 2.3 Structure:

Structures are considered to be the primary control on

localization of mineralization. Consequently, understanding the structural development of the region is important in attempting to develop a metallogenic model for the mineralization.

The structural geology of the region has been addressed by Neale (1957); Neale and Kennedy (1967); Marten (1971); Upadhyay (1973) and DeGrace et. al., (1976). The ophiolite outcrops in a southeast plunging syncline with overturned, steep north-dipping stratigraphy at the base becoming upright and shallow-dipping toward the south. DeGrace et. al. (1976) established that the Cape St. John Group is deformed into a horizontal, east-west trending syncline. One main penetrative fabric is present throughout and a second overprinting fabric occurs to the north related to late thrusting (DeGrace et. al., 1976).

Structures interpreted to have significance in terms of gold potential have been outlined on Figure 2.2. The main structural feature of the area ,the fault bounded ultramafic unit, forms the junction of two oppositely verging synclines within the ophiolite and the Cape St. John Group. These bounding faults also encompass the carbonate alteration zone occurring within the ultramafic unit.

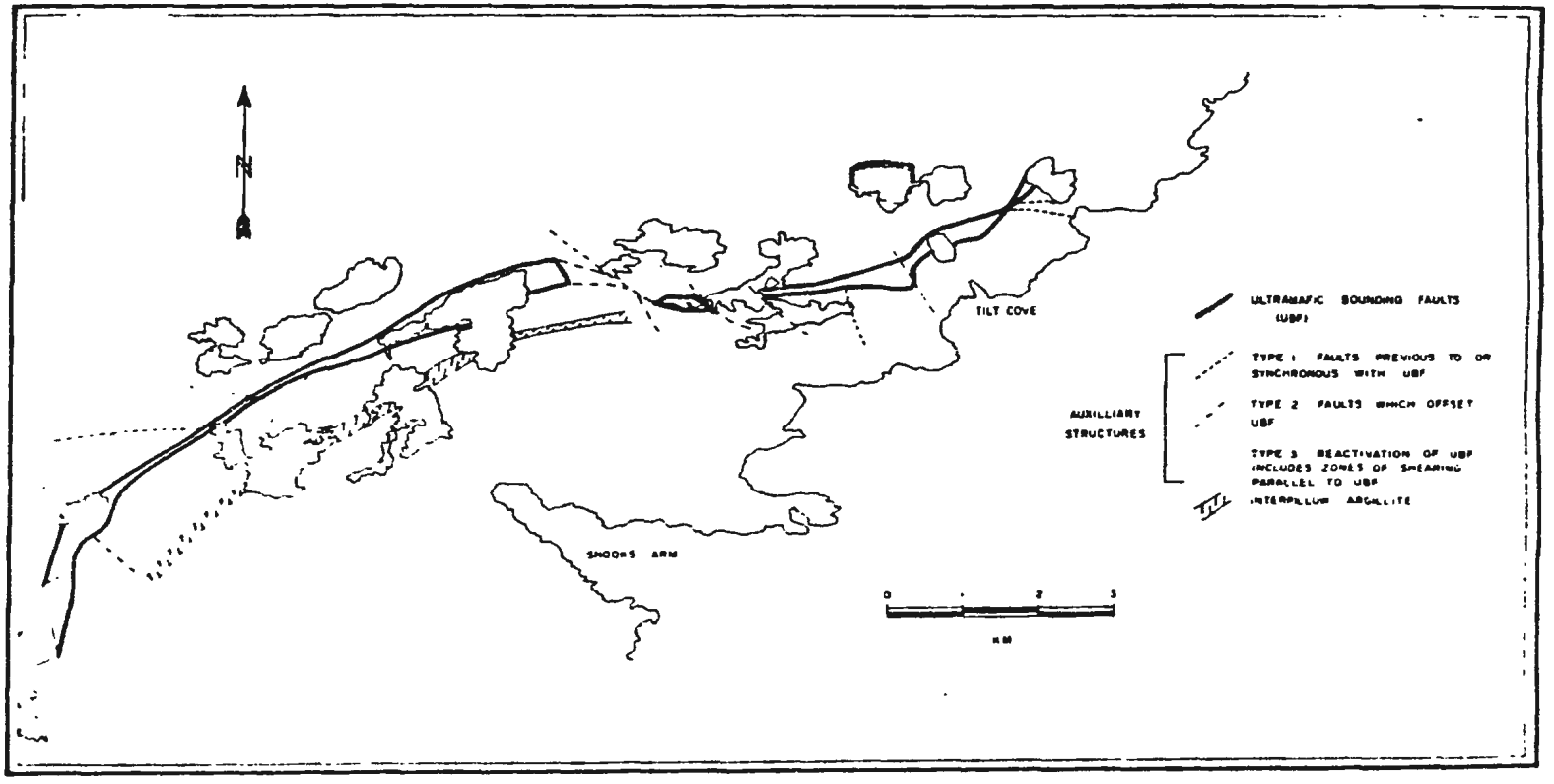


FIGURE 2.2 REPRESENTATION OF MAJOR STRUCTURAL ZONES CONSIDERED TO HAVE SIGNIFICANT POTENTIAL FOR AU MINERALIZATION SCALE DOES NOT PERMIT THE PORTRAYAL OF ALL AUXILLIARY STRUCTURES WITHIN EACH CATEGORY

Structures defined as auxilliary structures on Figure 2.2 are those that appear to be synchronous with or later than the development of the main ultramafic bounding structure. They are subdivided into three main groups: 1/ structures oblique to, and truncated against the main break; these are probably slightly older or coeval with the development of the ultramafic bounding faults, 2/ structures which appear to offset the ultramafic unit and, 3/ late reactivation of the main break structure. The best example of a type 1 auxilliary structure is the east-west trending fault which intersects the main break just north west of West Pond. This structure is interpreted by Kean (1977) as having a strike extension of 24 Km.

The best example of a type 2 auxilliary structure is in the area between Red Cliff Pond and Long Pond where the ultramafic rocks disappear beneath the Cape St. John Group unconformity. A northwest lineament offsets the linear trends of the ultramafic rocks. Movement sense appears to have been dominantly dip-slip as evidenced by pronounced lineations on the sheared surfaces.

Late reactivation of the main break structure is best observed on the northeast shore of Red Cliff Pond where a shear zone is developed within the Cape St. John Group directly against the ultramafic rocks. Sense of movement

was dominantly dip-slip with a minor strike-slip component; the south block moved up and to the west, relative to the north block. The late reactivation along the main break is likely related to movement along the type 2 structure described above. This is evidenced by the spatial proximity to the type 2 structure, similarity in sense of movement and the identical alteration characteristics in both structures. The significance of these structures in terms of gold mineralization becomes evident when Figure 2.2 is compared with Map 87-01 showing alteration features and gold showings.

The ophiolite volcanic sequence, especially the pillow lava unit, would be expected to have a significant competency contrast with the altered ultramafic rocks during deformation. This is verified by an almost complete lack of deformation in the pillow lava. The interpillow argillite on the other hand, represents a layer of anisotropy in the pillows where isoclinal folding and penetrative schistosities have developed. The argillite unit is therefore a zone of structural weakness where dilation could occur (Plate 2.6).

Plate 2.6. Isoclinal folding of bedding-parallel quartz veins in argillite unit at East Pond.

# CHAPTER 3

# ALTERATION AND MINERALIZATION

## 3.1 General:

The ultramafic alteration assemblages in the study area consist of a gradation from peridotite to serpentinite, serpentine-magnesite, talc-magnesite and hematite-rich, quartz-dolomite. Talc-magnesite (plus or minus quartz) rocks have been termed listwaenite by Lobochnikov (1936).

One type of mineralization identified in the study area is confined to the ultramafic unit and bears close resemblance to mineralization and alteration described by Buisson and Leblanc (1985, 1986, 1987) for ophiolite ultramafic assemblages in Morocco and Saudi Arabia. Gold mineralization occurs in quartz-magnesite-sulphide veins within talc-magnesite alteration zones in Morocco and Saudi Arabia and is referred to as listwaenite-type gold mineralization by Buisson and Leblanc (1985). The talc-magnesite hosted mineralization described in this section is thus referred to as listwaenite-type (L-type) mineralization. There are three known occurrences of this mineralization in the study area, two at Arrowhead Pond and a third at West Pond Ridge.

A second type of mineralization is spatially related but not confined to the ultramafic rocks. This mineralization contrasts with the ultramafic hosted showings in that specular hematite is ubiquitous in quartz veins and carbonate is insignificant. This mineralization is refered to as the Long Pond West-type (LPW-type). Most showings of this type occur within the Cape St. John Group; one is found within the ultramafic rocks. The wall rock alteration expression within the Cape St. John Group hosted mineralization contrasts sharply with the alteration observed in the ultramafic rocks.

Mineralogy, style of mineralization and alteration associated with both types are described below. The major distinction between the two types of mineralization is the dominance of sulphide versus oxide metallic mineral phases. It is possible that the two types represent end-member manifestations of one mineralizing system. Detailed maps of areas containing showings (Figure 2.1 and Map 87-01b) have been included to show relationships between gold mineralization, structure and alteration.

## 3.2 Listwaenite-Type Mineralization:

### 3.2.1 Mineralogy:

Listwaenite-type mineralization consists of veins of quartz and ferroan magnesite (Plate 3.1) in variable

Plate 3.1. L-type vein mineralization. Tabular quartz (white) and magnesite (orange-brown) veins within talc-magnesite altered ultramafic rock (blue-grey).

proportions. The magnesite is coarsely crystalline and intergrown, with grain aggregates up to 1 cm across. Coarsely crystalline quartz occurs interstitial to the magnesite in one of the Arrowhead Pond showings and at West Pond Ridge. In the third example the quartz and magnesite display a banded texture parallel to the vein walls (Plate 3.2). Accessory phases within the veins include rutile as interlocking crystals (Plate 3.3) and talc interstitial to the quartz and magnesite.

Metallic minerals within the veins consist of chalcocite and bornite in the Arrowhead Pond showings and pyrite, chalcopyrite and bornite in the West Pond Ridge showing. Microinclusions of galena are common in chalcocite and less common in bornite. The Arrowhead Pond showings also contain minor magnetite and have the highest gold contents (in excess of 10 ppm). The third vein has a gold content of only 800 ppb. Copper-rich phases are replaced by increasingly iron-rich phases as evidenced by grain boundary replacement of chalcocite by bornite and bornite by magnetite (Plates 3.4 and 3.5).

Native gold occurs in the chalcocite-bornite bearing veins (Plates 3.6 and 3.7) usually as grains up to 100 microns but rarely up to 300 microns. Gold is always associated with the copper sulphide minerals. Assays of portions of the veins that are not sulphide bearing have

Plate 3.2. Listwaenite-type vein mineralization displaying banded texture defined by quartz and magnesite.

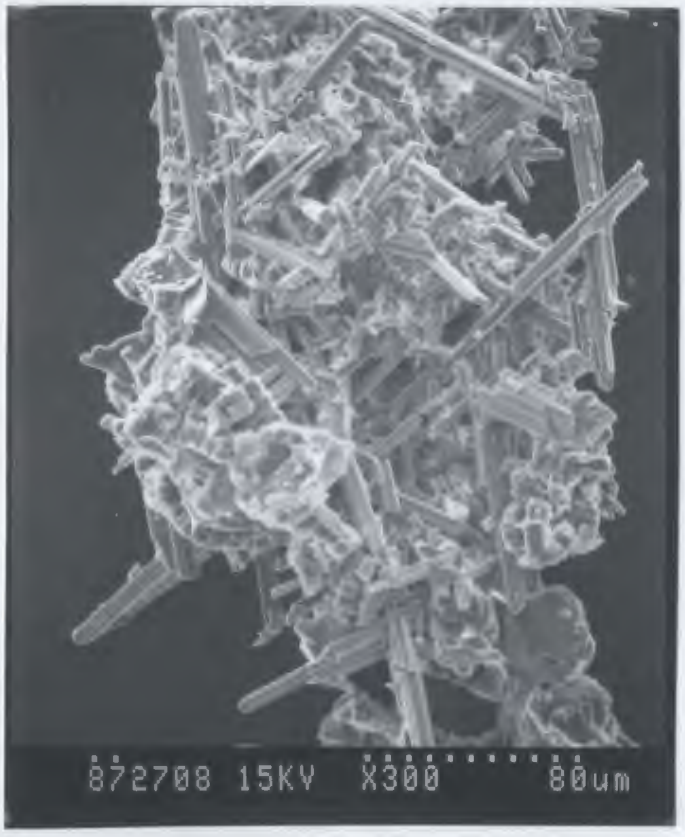


Plate 3.3. Scanning electron micrograph of hydrothermal rutile from L-type vein.

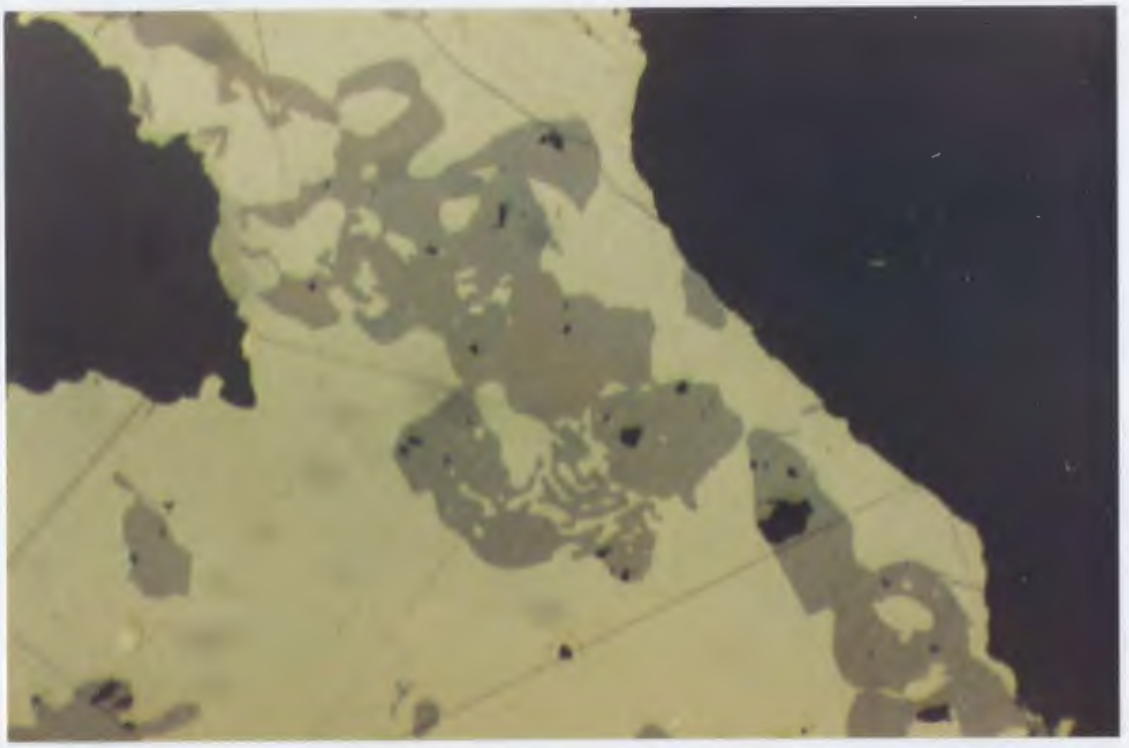

Plate 3.4. Photomicrograph of bornite replacing chalcocite along grain margins in L-type vein. (x40)

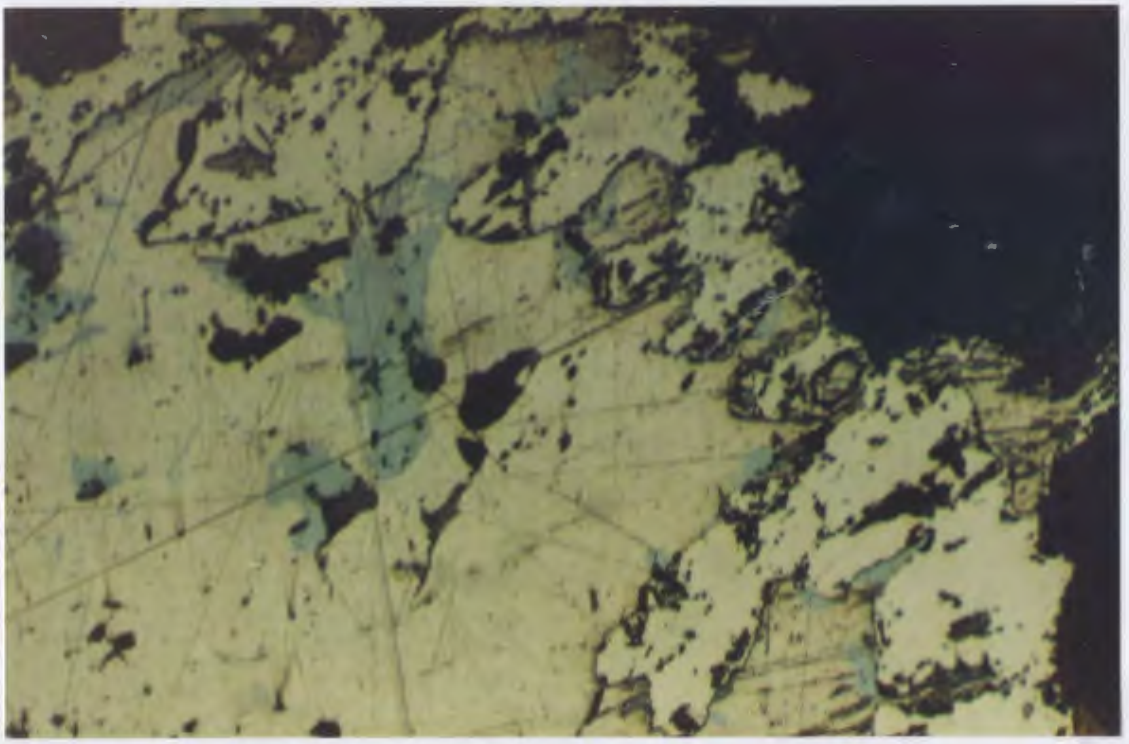

Plate 3.5. Photomicrograph of magnetite replacing chalcocite-bornite precursor assemblage in L-type vein. (x40)

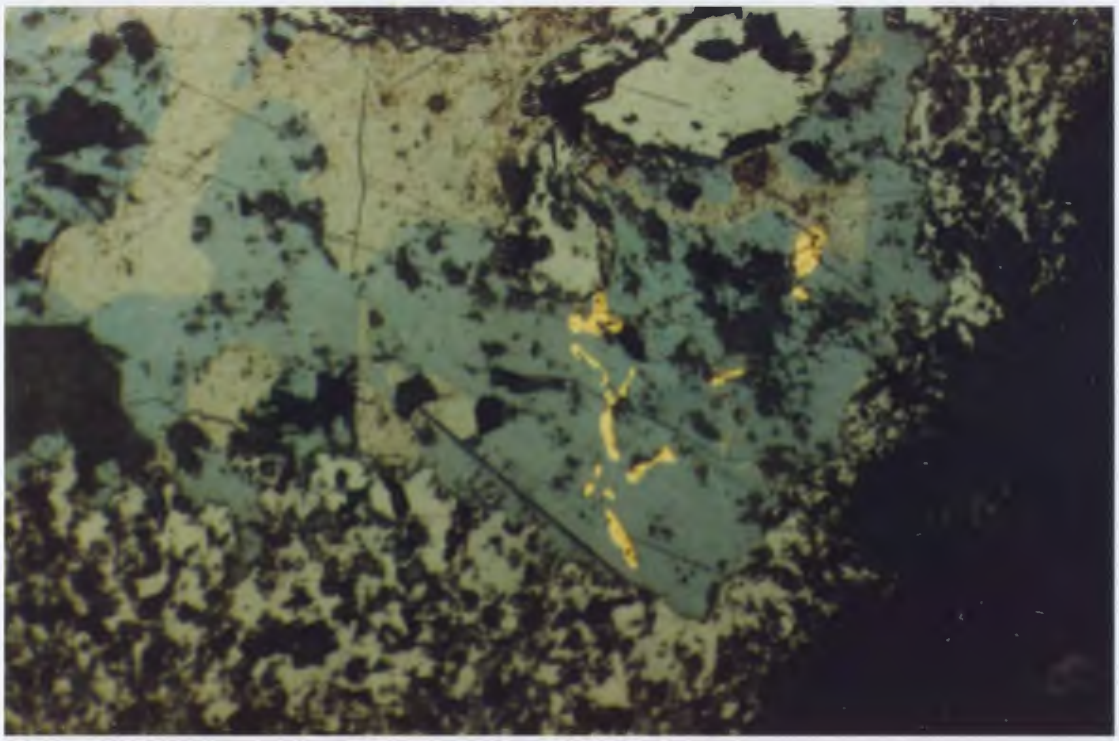

Plate 3.6. Photomicrograph of native gold occurring in bornite (right center) of an L-type vein. (x40)

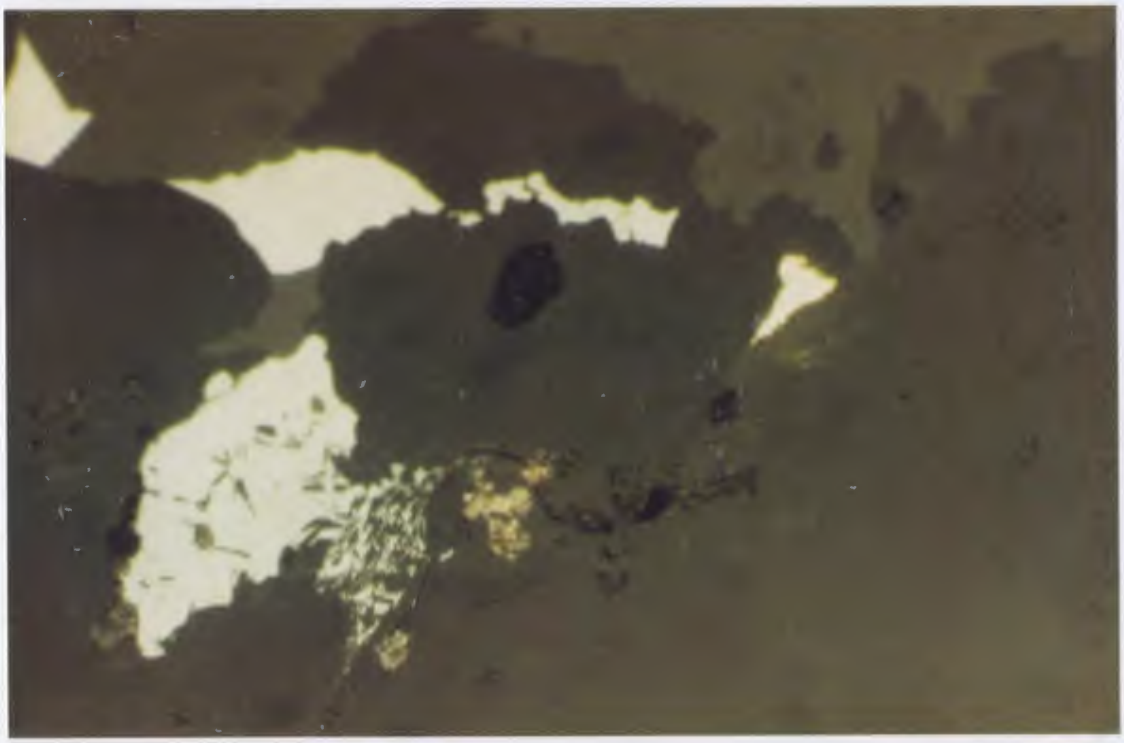

Plate 3.7. Photomicrograph of native gold occurring in quartz gangue (right center) in association with a chalcocite grain. L-type vein (x40)

returned values as low as 70 ppb Au.

### 3.2.2 Style of Mineralization:

The three known L-type veins are small, with maximum strike length of 5 metres and 0.4 metre width. The veins cross cut the fabric in the host rock and show no evidence of deformation. Although there are several areas within the talc-magnesite altered ultramafic rocks that are cut by late quartz veins, the orientations of the mineralized veins are distinct from barren veins, always striking from 110 -120°. The barren veins are also distinctive in that they are usually carbonate-poor, contain no sulphides, are often composed of coarsely crystalline, vuggy quartz and are more continuous, narrow, sheeted features. The mineralized veins may represent a conjugate set with an intersection lineation plunging 14° toward 116°. The approximately 120° orientation is identifiable on a regional scale as major lineaments within both the Cape St. John Group and the ophiolite and may be important to exploration. Some important showings of LPW-type mineralization occur along a major 120° lineament as well.

### 3.2.3 Alteration:

The L-type veins occur within the regionally

talc-magnesite altered ultramafic rocks. The distribution of this alteration zone is shown on map 87-01. Talc and magnesite are the principle constituents of this zone with ratios of talc to magnesite averaging 0.75:1. Opaque minerals consist of specular hematite, magnetite and chromite. Specular hematite as subhedral to euhedral crystals is the most abundant.

In thin section, the magnesite occurs as large (up to 5mm) crystals and crystal aggregates. The talc is always found interstitial to magnesite. Hematite is the latest of the opaque phases and is probably contemporaneous with the formation of carbonate. Magnetite is a corroded residual phase from serpentinite and chromite is a corroded residual phase from the primary magmatic rocks.

Where quartz veins cross cut the talc-magnesite wall rocks, local silicification combined with intense carbonatization occurs in the wallrocks to the veins (Plate 3.8). Quartz, talc and chlorite occur interstitial to magnesite in the silicified wall rocks (Plate 3.9).

The talc-magnesite rock has a very distinctive weathered surface (Plates 3.10 and 3.11). Carbonate, being most susceptible to chemical weathering, forms pits on the surface with talc remaining as steel blue protruding knobs. Where the talc-magnesite has been silicified, the


Plate 3.8. Pervasively carbonatized and silicified ultramafic rock (listwaenite) adjacent to a quartz-magnesite vein which cross cuts the talc-magnesite assemblage. Bright green is chlorite as seen in Plate 3.9.

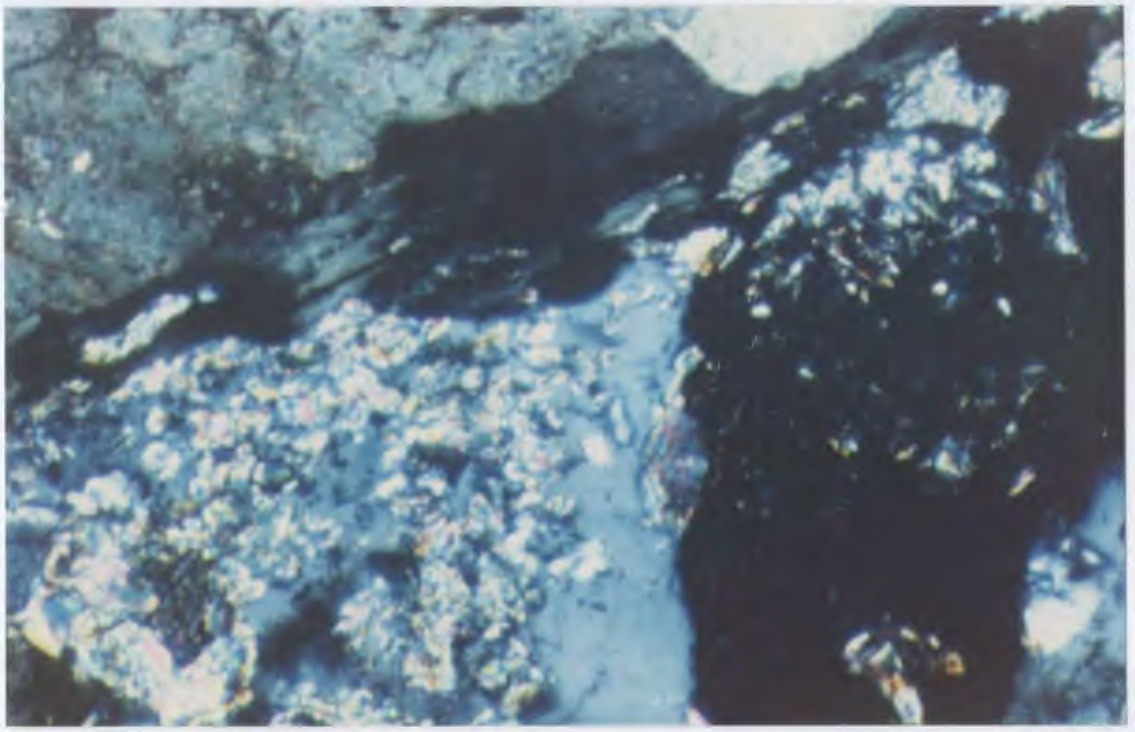

Plate 3.9. Photomicrograph of the alteration assemblage adjacent to a quartz-magnesite vein in talc-magnesite. Quartz (dark grey) and talc (pink, yellow and blue) occur interstitial to magnesite (light and dark brown). (x10)

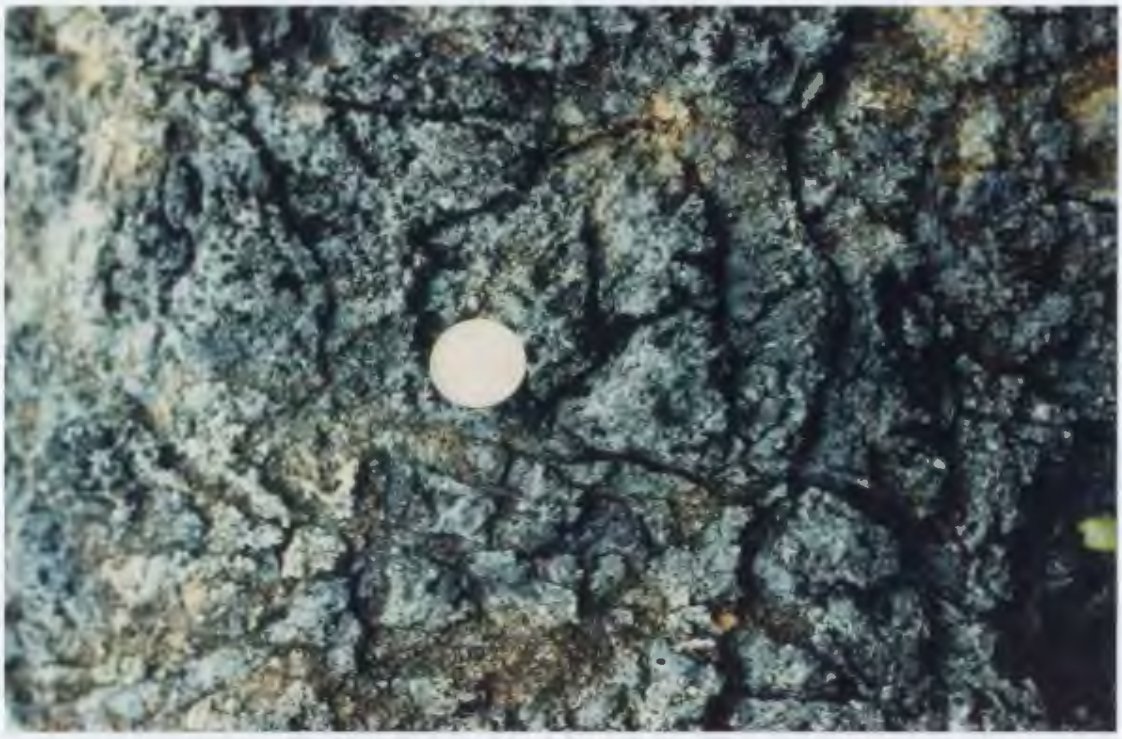

Plate 3.10. Typical weathered surface of talc-magnesite altered ultramafic rocks. Magnesite weathers chemically leaving soft, blue protrusions of talc.

Plate 3.11. Silicified talc-magnesite schist. Magnesite weathers chemically leaving pale green-white protrusions of silica.

protruding knobs take on a frosted sugary appearance. An overall rusty-brown colour is imparted by oxidized iron in the magnesite.

## 3.3 Long Pond West-Type Mineralization:

### 3.3.1 Long Pond West #1:

#### 3.3.1a Mineralogy:

The Long Pond West #1 showing occurs in highly altered ultramafic rocks. The host mineralogy is ferroan dolomite, ankerite, quartz and fuchsite. The dolomite occurs as intergrown patches of irregular crystal aggregates with some fine grained quartz and is replaced by quartz, ankerite and fuchsite in a complex crosscutting network of veins (Plate 3.12). Ankerite occurs in the veins as euhedral crystals and crystal aggregates up to 1 mm across. Fuchsite is present as thin (<0.25 mm) segregations parallel to vein margins.

Euhedral chrome-rich magnetite grains and rare, highly corroded chromite grains are commonly associated with the fuchsite. Specular hematite is found only in the dolomite. All of the above mineral phases are interpreted to be products of hydrothermal activity with the exception of chromite.

One grain of gold has been observed within a quartz

Plate 3.12. LPW-type vein mineralization from Long Pond West #1 showing. Note the quartz-fuchsite vein material cross cutting the earlier quartz-dolomite alteration assemblage (red-brown).

veinlet from this showing. Gold is known to be associated with the carbonate from this zone as well since detrital gold with negative carbonate crystal imprints occurs within regolith over the showing (Plate 3.13).

### 3.3.1b Style of Mineralization:

The mineralization at this showing is of a stockwork type and occurs within the ultramafic rocks at the contact with pyroclastic rocks of the Cape St. John Group. The pyroclastic rocks are deformed (Plate 3.14) but alteration is less well developed than in the ultramafic rocks. Southward, away from the contact with the Cape St. John Group, the density of quartz, ankerite, fuchsite veins decreases and the hematite-rich, dolomite-quartz assemblage prevails.

### 3.3.1c Alteration:

The alteration peripheral to the Long Pond West #1 showing consists of pervasive, almost complete carbonatization and hematization of ultramafic rocks in a narrow (<25 m) belt confined to the fault contact between ophiolitic ultramafic rocks and the Cape St. John Group. The carbonatization combined with the hematite results in a rusty brown to bright red colouration of the outcrop. The carbonate mineral in this alteration zone is ferroan


Plate 3.13. Scanning electron micrograph of detrital gold grain from overburden above LPW-type vein. Negative carbonate crystal imprint attests to an association between carbonate and gold in the vein.

Plate 3.14. Deformed pyroclastic rocks of the Cape St. John Group adjacent to the contact with ultramafic rocks hosting LPW-type mineralization at Long Pond.

dolomite. Minor pervasive silicification accompanied this alteration as well. Chromite and magnetite are present as highly corroded grains, obvious precursor phases to the carbonate assemblages.

The alteration described above preceded the mineralization as indicated by replacement of the dolomite-bearing alteration assemblage by ankerite and fuchsite-bearing quartz veins which contain gold. The carbonate compositions change from Ca, Mg +/- Fe (dolomite) carbonate in the alteration zone to Ca, Mg, Fe, Mn carbonate (ankerite) in the mineralized zone (Table 3.1).

### 3.3.2 Other Long Pond West-Type Showings:

#### 3.3.2a Mineralogy:

The three showings considered in this section; the Long Pond West # 2, the Tom showing and the Red Cliff Pond North showing, occur as veins within shear zones in Cape St. John Group rocks. The mineralogy of these showings varies little between locations. Gold occurs in quartz veins containing medium to coarse grained specular hematite and sericite. The amount of hematite may vary from 5 - 10% and usually occurs in domains parallel to the vein walls rather than disseminated throughout. Sericite is more erratically distributed in the veins and also occurs outside of them, parallel to the vein walls as an alteration envelope.

Table 3.1. Average electron microprobe analyses of alteration and vein mineral compositions.

Listwaenite Mineralization

| | Carb. (a) | Carb.(v) | Chlorite(a) |
|---|---|---|---|
| No. Sa's | 15 | 8 | 6 |
| $SiO_2$ | | | 45.00 |
| $Al_2O_3$ | | | 9.55 |
| $TiO_2$ | | | 0.29 |
| $Fe_2O_3$ | 7.44 | 7.76 | 4.45 |
| MnO | 0.05 | 0.09 | 0.04 |
| MgO | 40.73 | 40.63 | 24.29 |
| CaO | 0.11 | 0.21 | 5.74 |
| $Na_2O$ | | | 0.42 |
| $K_2O$ | | | 0.01 |
| $Cr_2O_3$ | | | 1.64 |
| NiO | | | 0.73 |
| Total | 48.32 | 48.69 | 92.16 |

Long Pond West-Type Mineralization

| | Carb. (a) | Carb.(v) | Chlorite(v) | Sericite(v) | Fuchsite(v) |
|---|---|---|---|---|---|
| No. Sa's | 17 | 6 | 15 | 9 | 5 |
| $SiO_2$ | | | 26.03 | 49.21 | 48.04 |
| $Al_2O_3$ | | | 23.25 | 31.20 | 26.55 |
| $TiO_2$ | | | 0.11 | 0.58 | 0.14 |
| $Fe_2O_3$ | 0.17 | 5.39 | 24.53 | 2.42 | 4.48 |
| MnO | 0.17 | 1.20 | 0.23 | 0.01 | 0.01 |
| MgO | 20.69 | 16.34 | 15.07 | 1.69 | 1.54 |
| CaO | 31.07 | 28.59 | 0.01 | 0.02 | 0.04 |
| $Na_2O$ | | | 0.02 | 0.20 | 0.16 |
| $K_2O$ | | | 0.03 | 8.73 | 9.47 |
| $Cr_2O_3$ | | | 0.01 | 0.00 | 2.68 |
| NiO | | | 0.14 | 0.03 | 0.26 |
| Total | 52.11 | 51.52 | 89.43 | 94.10 | 93.36 |

Notations (a) and (v) denote occurrence of the mineral in the altered wall rock (a) or in the mineralized vein (v). All values are in weight percent.

Very minor pyrite, chalcopyrite, bornite, galena and molybdenite have been found in polished sections of the Tom showing veins (Plates 3.15, 3.16 and 3.17). Pyrite is the most abundant sulphide.

Patches of hydrothermal chlorite commonly comprise up to 2-3 percent of the veins. When sulphides are present they are usually associated with the chlorite and are often mantled by specularite rims. Similar assemblages, noted by Barton et. al. (1977) in the Creede mining district of Colorado were used to estimate activities of $O_2$ and $S_2$ in the fluid.

### 3.3.2b Style of Mineralization:

The mineralization is confined to type 2 and 3 auxilliary structures, as defined in Chapter 2. In most cases, the origin of the host rock prior to shearing is not clear but textural and local relationships point to a variety of lithologies ranging from sedimentary to felsic pyroclastic and mafic volcanic rocks (Plates 3.18 and 3.19). There is no evidence that the mineralization is host rock specific. The mineralization appears to be structurally controlled. The veins occur in zones of intense shearing and alteration but the gold bearing veins cross cut the main shear fabric. This crosscutting characteristic of mineralized veins is commonly observed in

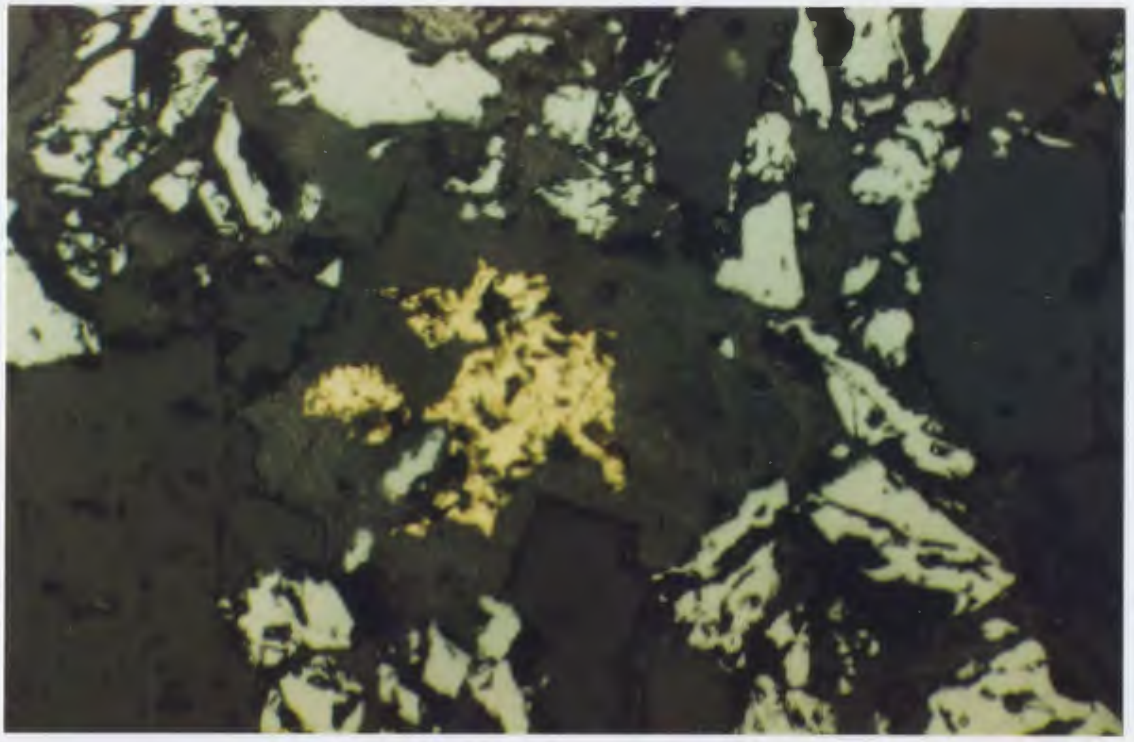

Plate 3.15. Pyrite with specularite in an LPW-type quartz-chlorite vein assemblage. (x40)

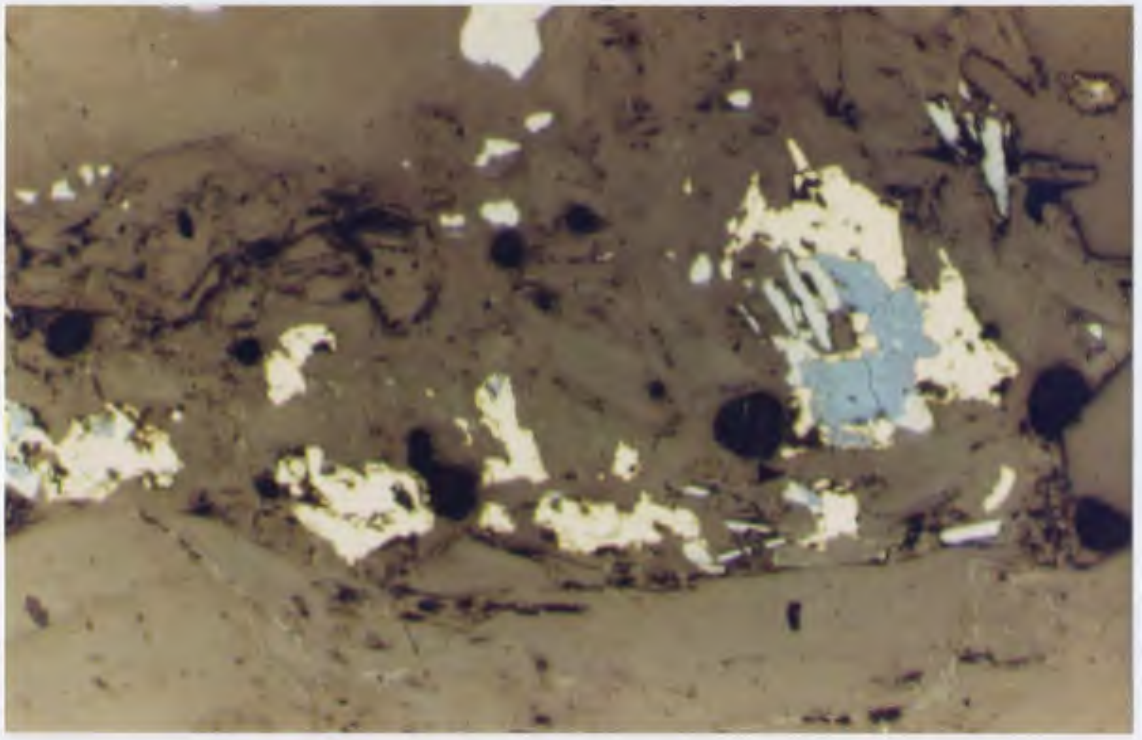

Plate 3.16. Chalcopyrite (yellow), bornite (blue), galena, (white) and specularite (grey) in an LPW-type quartz-chlorite vein assemblage. Note the specularite mantling the chalcopyrite-bornite grain. (x10)

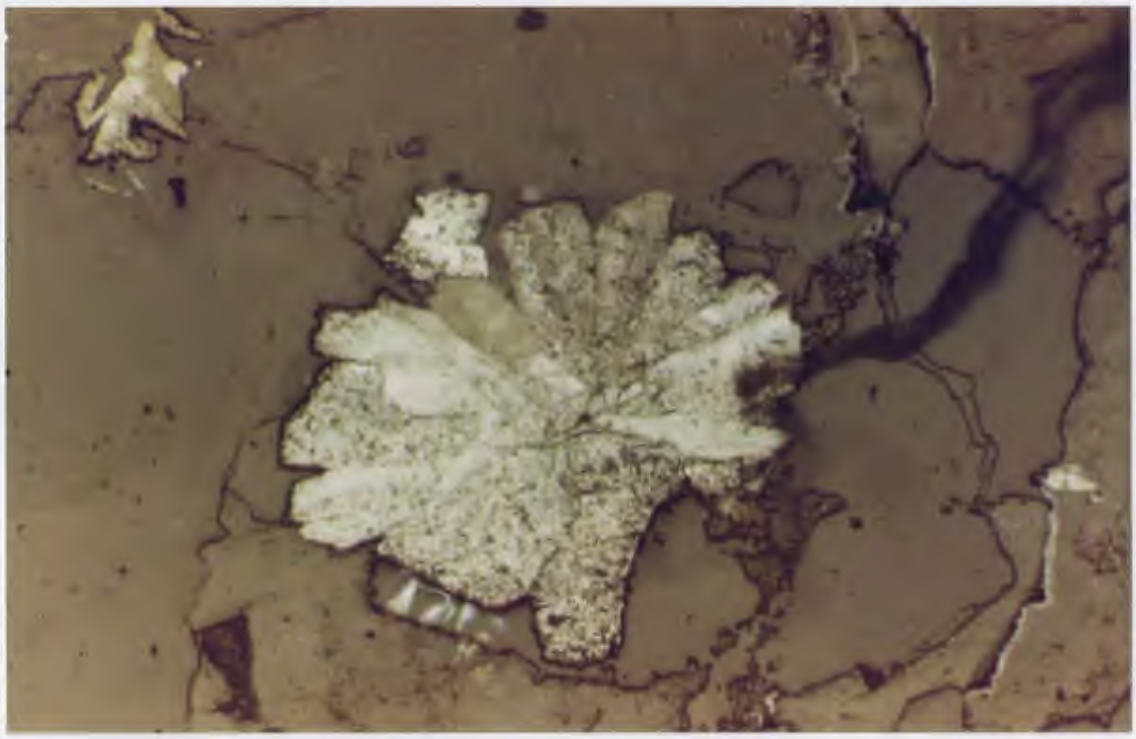

Plate 3.17. Molybdenite rosette in an LPW-type quartz-chlorite vein assemblage. (x40)


Plate 3.18. Penetratively sheared conglomeratic sedimentary rock hosting LPW-type mineralization. Clasts are best defined on cleavage planes. Grey colour of outcrop is due to pervasive hematization.

Plate 3.19. Pervasive alteration of mafic volcanic rock adjacent to LPW-type vein at Long Pond West. Bleaching (sericitization) is the first stage followed by hematization (dark purple) which overprints the sericitic alteration.

many lode-gold-type deposits (Colvine, et. al., 1984; Hodgson, 1987, in press). The veins found to date are all less than 0.5 metres thick and are widely spaced (see Plates 3.20 and 3.21). They appear to pinch out with distance away from the shear zone which suggests a relationship between shearing and mineralization.

### 3.3.2c Alteration:

The alteration associated with the Long Pond West-Type mineralization is distinctive and easily recognized in the field. The alteration intensity correlates with the degree of shearing in the host rock.

The alteration process involves the introduction of silica, potassium and iron to the rocks. The silica occurs as pervasive silicification and as discreet veins. The veins vary from 1mm to 0.5 metres wide. The quartz veins occur as a continuum from early folded and transposed veins to late crosscutting veins, again indicating a syndeformational origin. The pervasive silicification occurs as a microcrystalline matrix to altered and often fractured, primary lithic fragments and quartz and feldspar crystals (Plate 3.22). The microcrystalline quartz is often domainal and outlines the shear fabric within the rocks.

Plate 3.20. Typical LPW-type vein in the Cape St. John Group. Attitude of the vein is oblique to the shear zone boundary. Note the pervasive hematization of the host rocks (black) and the specularite in the vein.

Plate 3.21. Quartz-specularite veins cross cutting sericite-hematite altered sedimentary rocks of the Cape St.John Group. Note the distinctive style of alteration.

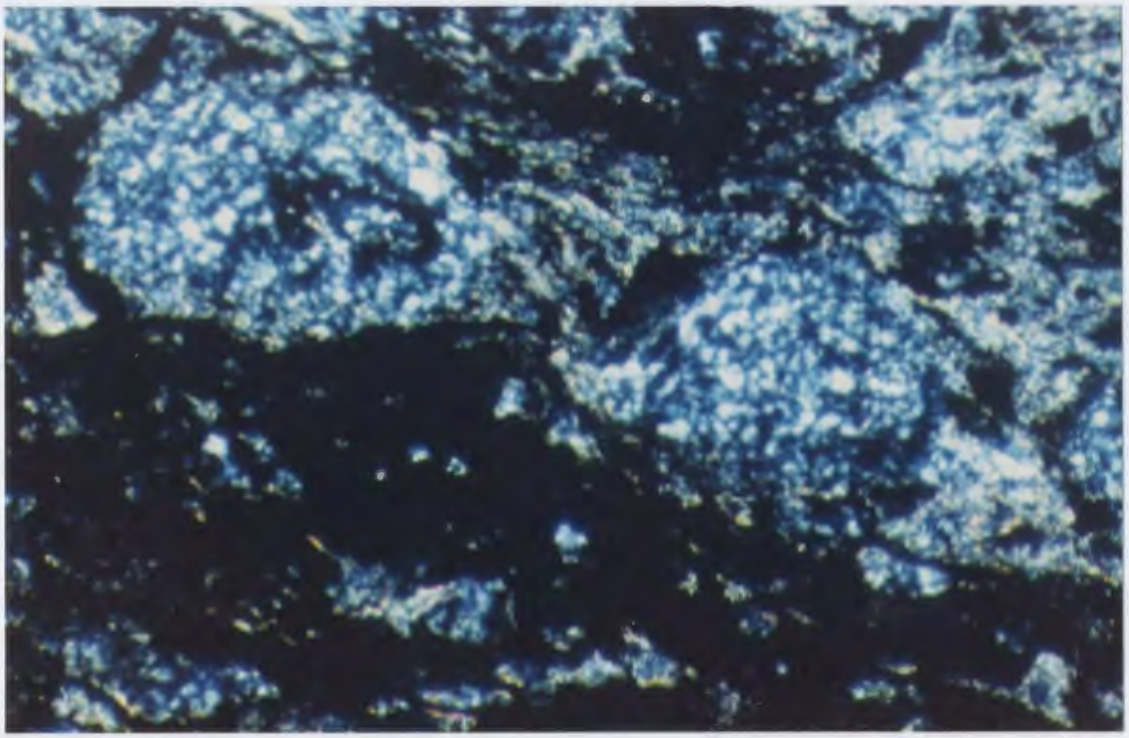

Plate 3.22. Photomicrograph of hematite alteration in Cape St. John Group pyroclastic rock. Black domains are hematite. Quartz and sericite are intimately intergrown in the light coloured domains. Note the complete recrystallization of the clast in the center. (x10)

Pervasive sericite and hematite alteration occurs coincident with silicification. In the pervasively altered shear zone the sericite and hematite exist as foliation parallel domains (Plate 3.22). Sericite also forms pseudomorphs after feldspar. The distribution of the hematite is somewhat irregular, causing a mottled purple and buff coloured appearance (see Plates 3.19 and 3.21). The apparent syndeformational age of the mineralization and coincident alteration implied by the range of deformed and undeformed quartz veins is supported by the occurrence of both deformed and undeformed, initially fracture controlled, domains of hematite alteration (Plates 3.23 and 3.24).

Accessory mineral phases found in the quartz-sericite-hematite zone include very minor fuchsite and rare carbonate which occur both in the veins and in the sheared host rocks. In the alteration associated with the Red Cliff Pond showing, chlorite commonly occurs as radiating patches on the schistosity planes.

### 3.3.3 Long Pond East:

A gold showing occurs on the east shore of Long Pond in deformed argillite. The argillite is interbedded with the pillow lava of the Betts Cove Complex. Little work was carried out on this showing during the course of the

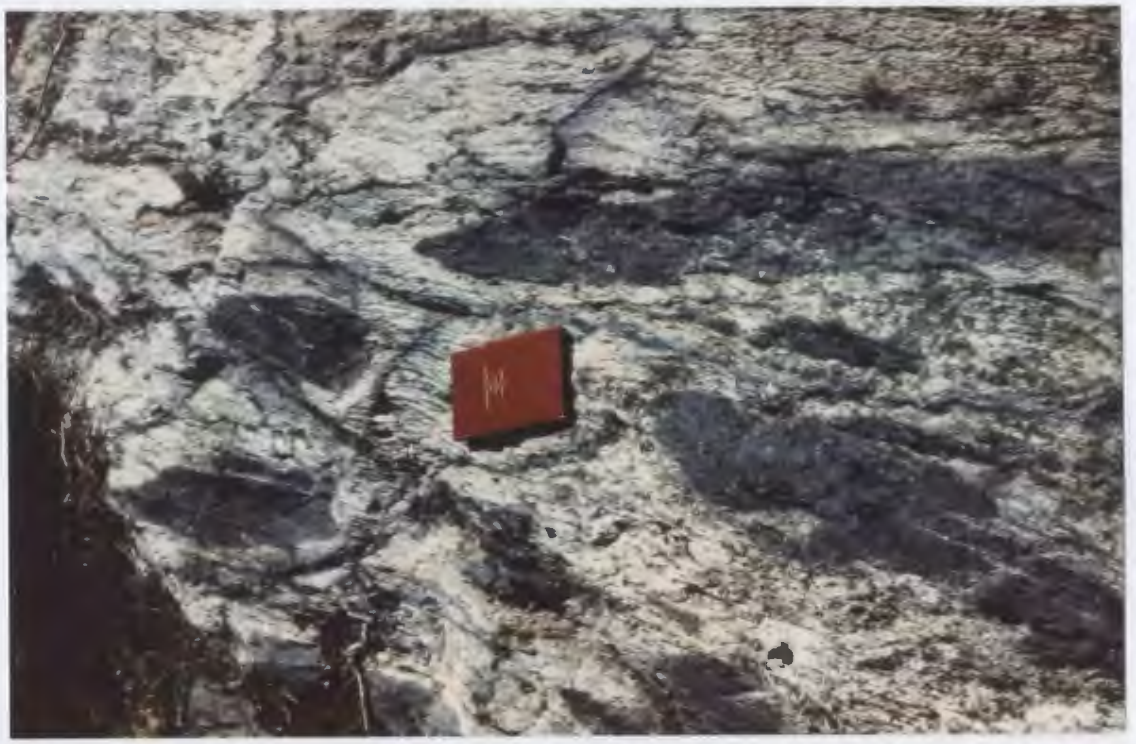

Plate 3.23. Deformed domains of hematite alteration. Fold closures are evident in the ends of the hematite-rich lenses.

Plate 3.24. Undeformed, fracture controlled hematite alteration. Plates 3.23 and 3.24 are from the same outcrop.

study. Small veins of quartz and sericite up to 2 cm wide occur randomly within fractured and slightly sheared argillite. The host rocks display pervasive hematite and carbonate alteration but pyrite is the principle metallic phase in the gold-bearing veinlets.

## 3.4 Other Areas of Gold Mineralization Potential:

Four areas (Map 87-01) located northwest of West Pond, on the south shore of Bar Pond, at the northwest end of East Pond and on the southern shore of Goat Pond, display alteration and mineralization analagous to showings described above but have not returned any significant gold values upon analysis. These zones are all characterized by some degree of sericite-carbonate alteration as well as the occurrence of sulphide-hematite/magnetite assemblages.

Northwest of West Pond, pyrite and specularite occur in a quartz-carbonate altered zone confined to a type 1 auxilliary structure (see Chapter 2) in felsic crystal tuffs. Pyrite within this zone is mantled by iron oxides, similar to the sulphides in the Long Pond West-Type mineralized veins (Plate 3.25).

On the south shore of Bar Pond there are heavily sheared and carbonatized mafic volcanic rocks of the Cape St. John Group which contain minor pyrite mantled by

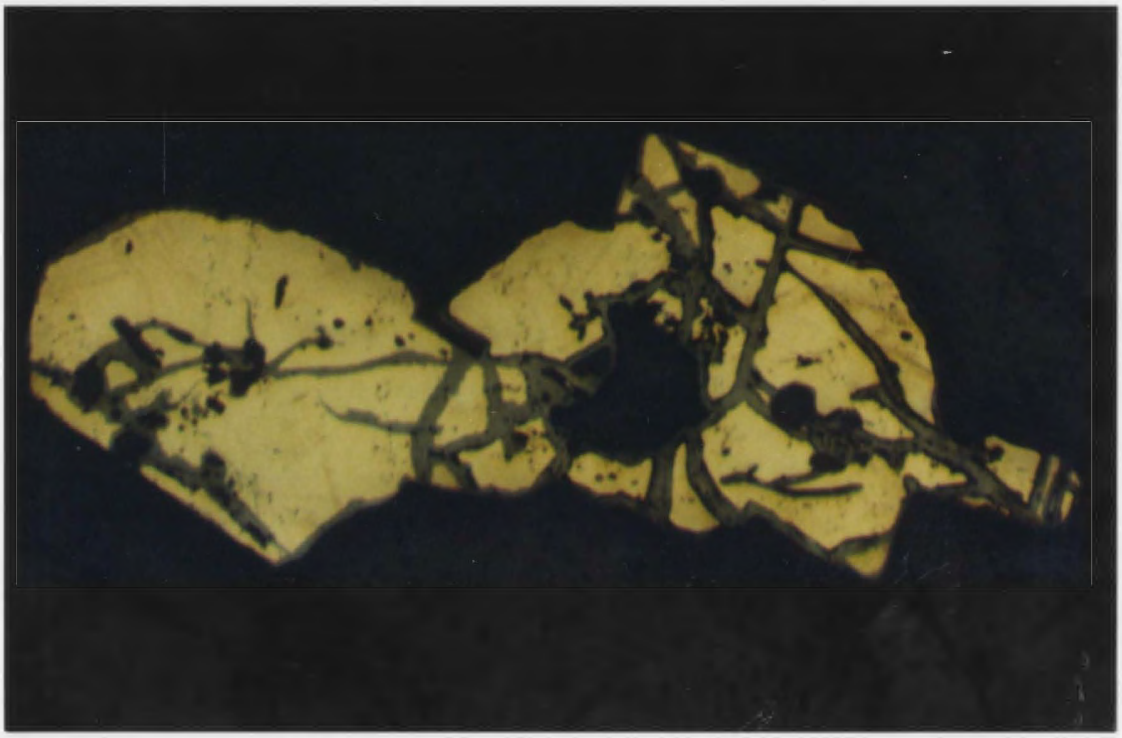

Plate 3.25. Pyrite replaced by magnetite in an alteration zone at the northwest end of West Pond. This paragenetic sequence is common to all the mineralized veins.

hematite or magnetite. Barren quartz veins cut the alteration zone.

In an inlet at the northwest end of East Pond a quartz vein up to 2.5 metres thick occurs subparallel to ophiolite hosted argillite. The quartz vein contains pyrite, specularite, K-feldspar, carbonate, sericite and patches of hydrothermal chlorite.

On the southern shore of Goat Pond a sheared contact between felsic pyroclastic rocks to the north, and mafic volcanic rocks to the south, displays pervasive hematite alteration as well as sporadic quartz, carbonate and sericite. Hematization of the mafic volcanic rocks imparts a deep green, purple colour. Hematization of the felsic pyroclastic rocks creates textural features identical to those seen in the pervasively altered host rock to the Long Pond West Type mineralization described above.

## 3.5 Summary of Mineralization:

Two types of gold mineralization are established on the basis of distinctive characteristics, yet certain features are common to both. The L-type mineralization occurs exclusively within ultramafic rocks, while the LPW-type occurs in ultramafic rocks, and the Cape St. John Group sedimentary and felsic volcanic rocks. Copper sulphides

are the principal metallic mineral in L-type veins. Specular hematite is the principal metallic phase in LPW-type veins. Magnesite-carbonate occurs in L-type veins while ankerite-carbonate occurs in LPW-type veins. Sericite and fuchsite are associated with the LPW-type veins but not the L-type.

The two types of mineralization are similar in that the earliest metallic mineral phases in all veins are sulphides, which were subsequently mantled by iron-oxides (magnetite and/or hematite). Sulphide mineral paragenesis displays iron enrichment from chalcocite to bornite and chalcopyrite in L-type veins and from bornite to chalcopyite and pyrite in LPW-type veins. Small quantities of galena are present in both vein types. The wall rock alteration assemblages for both types consist of silica-carbonate and specular hematite.

Distinction of the two types of mineralization is justified because the similarities mentioned above are not evident in the field.

# CHAPTER 4

# GEOCHEMISTRY

## 4.1 General:

The aim of the geochemical studies carried out is to characterize the element signatures of the stages of alteration from fresh to altered host rocks, as well as the mineralization itself. With the establishment of signatures, it may be possible to define geochemical pathfinders for gold mineralization in similar environments elsewhere. The element signatures may also be supportive of a suspected link between regional carbonate alteration and gold mineralization. Strontium isotope and rare earth element (REE) geochemistry are utilized to provide insight into the source of mineralizing fluids and gold.

## 4.2 Analytical Procedures:

A large variety of elements have been analysed including major element oxides, gold and platinum group elements, REE and various other trace elements. The data is included in Appendix I.

Major element oxides were determined by conventional atomic absorption techniques. Precious metals - Au and platinum group elements (PGE) - were determined by ICP-MS

with fire assay preconcentration in a NiS bead. The method is described by Jackson et. al. (in prep.). Trace elements were determined by a combination of conventional XRF techniques or ICP-MS. The procedure of ICP-MS determination is described by Longrich et. al. (in prep.). Low level REE analysis of the ultramafic rocks is done by dissolving 1 gram of sample in doubly-distilled hydrofluoric and nitric acid under clean lab conditions. Cation exchange columns were used to remove most of the $^{+}1$ and $^{+}2$ valency cations in order to concentrate the REE and reduce plasma matrix affects due to high amounts of total dissolved solids. Matrix affects were further monitored by using the standard addition method of analysis. Whole-rock ultramafic standard PCC-1 was analysed also.

## 4.3 Ultramafic Rocks:

The ultramafic rocks were studied most extensively because of their relatively simple chemistry. The rocks referred to as unaltered are those displaying primary cumulate textures despite some serpentinization. It was assumed that detection of changes attributable to the alteration and mineralization processes would be easiest by monitoring the less complicated ultramafic rock composition through the stages of these processes.

Evaluation of the unaltered ultramafic rock geochemistry reveals that many elements display fractionation trends when plotted against $Al_2O_3$; other elements form fields that are assumed to represent a normal distribution (Figures 4.1a and b). Immobility of $Al_2O_3$ is assumed and supported by its position along a straight line joining immobile elements in the isochon diagram in Figure 4.2. On isochon diagrams (Grant, 1986), altered rock compositions are plotted versus the composition of the unaltered protolith. Elements that are immobile during alteration plot along a straight line (isochon) through the origin. When the protolith composition is represented by the X-axis, elements that are enriched or depleted in the altered rock plot above and below the isochon respectively. Changes of volume accompanying alteration are reflected by changes in slope of the isochon.

The units on the axes of the isochron diagram are arbitrary. The average concentration of an element in the altered and unaltered rocks, is multiplied by a value that causes the respective data point to plot within the range of the axes.

The ultramafic rock geochemistry is evaluated in terms of: 1/ alteration-related major and trace element fluctuations relative to established fields and fractionation trends; 2/ REE behaviour in fresh versus

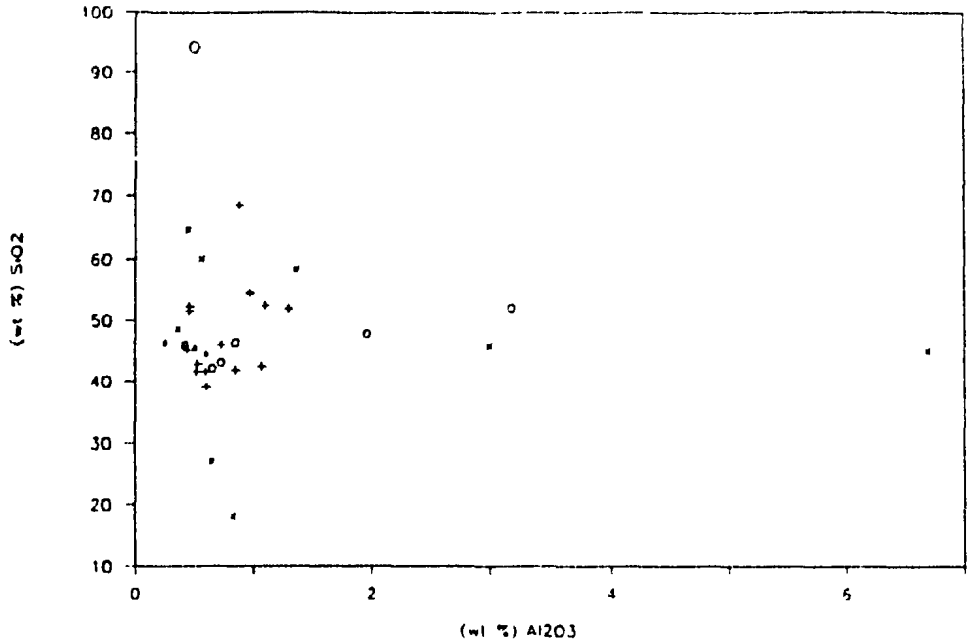


a)

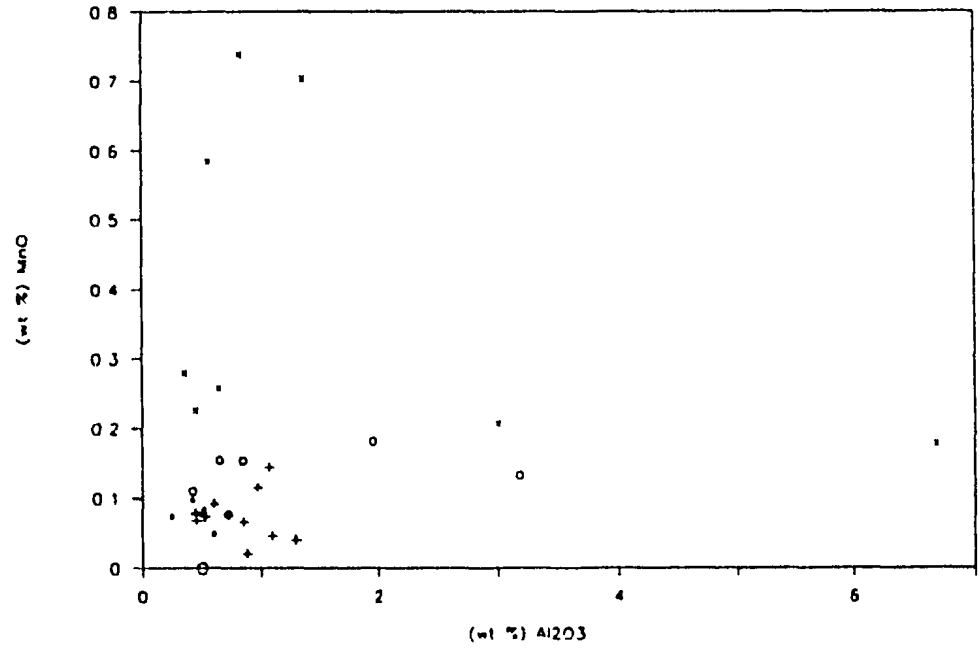


b)

Figure 4.1. Plot of $SiO_2$ vs $Al_2O_3$ a) and MnO vs $Al_2O_3$ b) for all ultramafic rocks. Considering the cumulate rocks, the linear relationship in a) is interpreted as a fractionation trend, data in b) defines a range of normal distribution in unaltered rocks. Cumulate rocks (o), Talc-magnesite (+), Serpentine-magnesite (*), Quartz-hematite-dolomite (x).

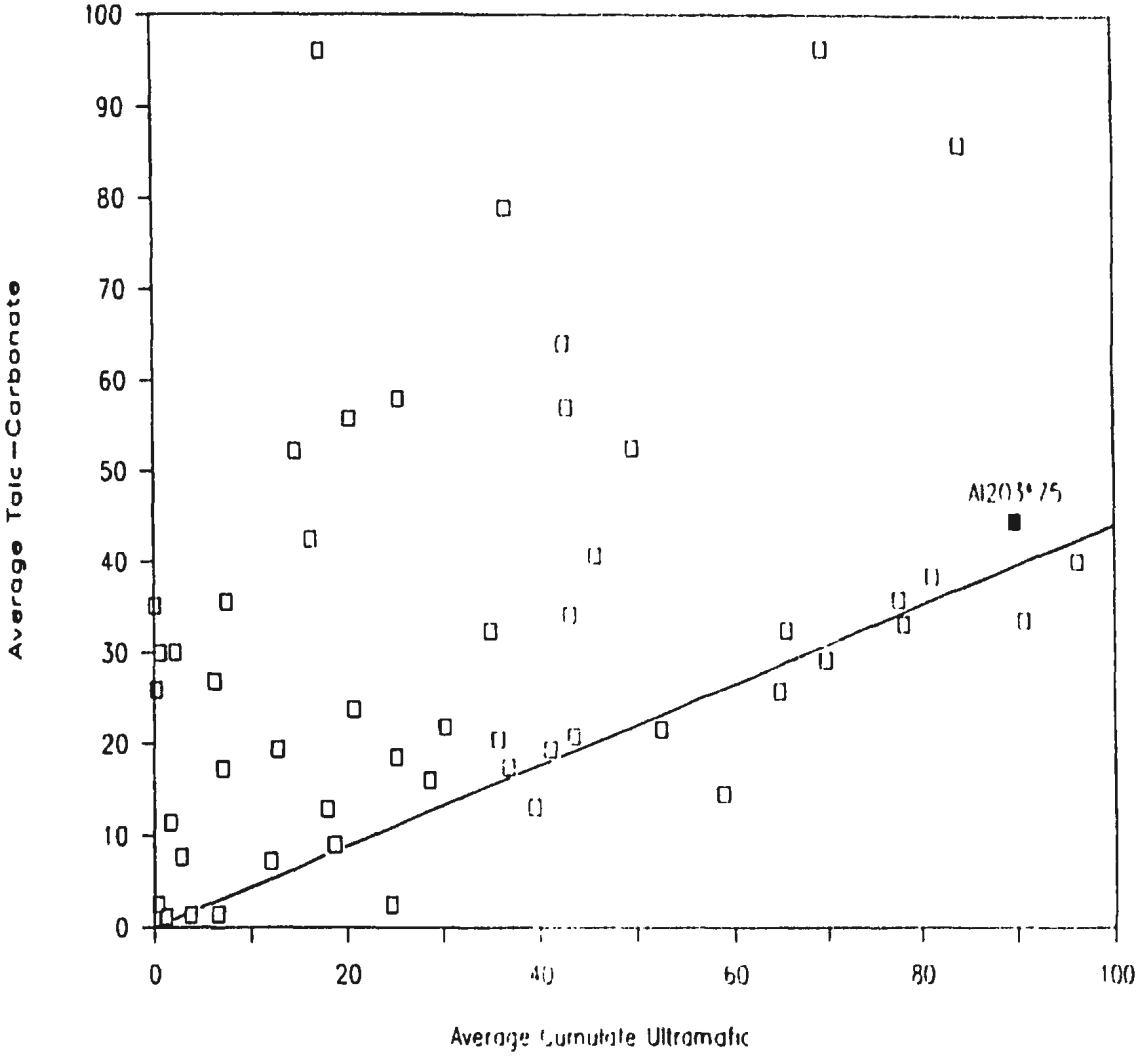


Figure 4.2. Isochon diagram, Grant (1986). Points represent altered vs unaltered element concentrations of Betts Cove Complex ultramafic rocks. Diagram demonstrates element immobility for elements plotting on the straight line indicated. Note the position of $Al_2O_3$ very near the line.

altered rock; 3/ gold concentration in the fresh and altered rocks and 4/ PGE variations with increasing degrees of alteration.

### 4.3.1 Major and Trace Elements:

Plots of selected major and trace elements versus $Al_2O_3$ for all ultramafic rock types are presented in Figures 4.3a-k.

#### 4.3.1a Cumulate Ultramafic Rocks:

The major and trace element data from the cumulate rocks display fractionation trends for $SiO_2$, MgO, CaO, Sc, V, Cr and Ni. Most other elements are distributed within a definable field which is interpreted to represent a range of background concentration in the cumulate rocks. The presence of these trends and fields suggests that the rocks have undergone only minor alteration from their primary igneous composition, despite some serpentine alteration, and supports the use of these data as a reference for assessing chemical changes in altered rocks.

#### 4.3.1b Serpentine-Magnesite:

Subtle chemical changes result from alteration of fresh ultramafic rock to the serpentine-magnesite assemblage.

The alteration results in Cr, Zn depletion and P, As and Sb enrichment. Hydrothermal mobility of Cr is indicated by the presence of chrome-bearing mica in altered rocks in the

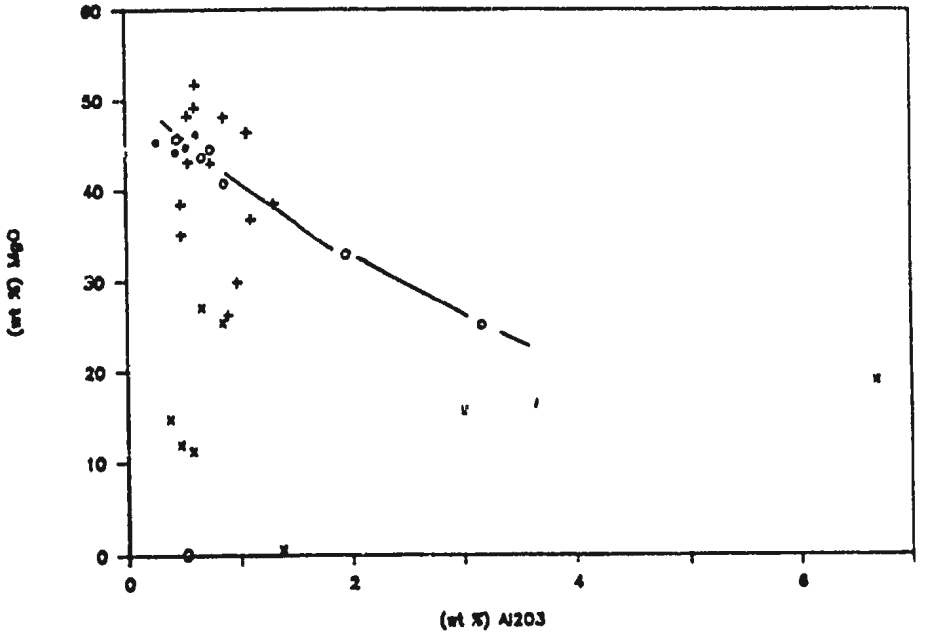


a)

Figure 4.3. Some plots of major and trace elements vs $Al_2O_3$. $Al_2O_3$ is used as an index of fractionation against which many elements display fractionation trends for the least altered samples (eg. MgO). Where coherent fractionation trends are not evident (eg. $K_2O$) the data outlines a normal range of values for unaltered samples. Deviations from these trends and fields are interpretyed to result from secondary alteration effects. Cumulate ultramafic rocks (o); Serpentine-magnesite (*); Talc-magnesite (+); Quartz-hematite-dolomite (x).

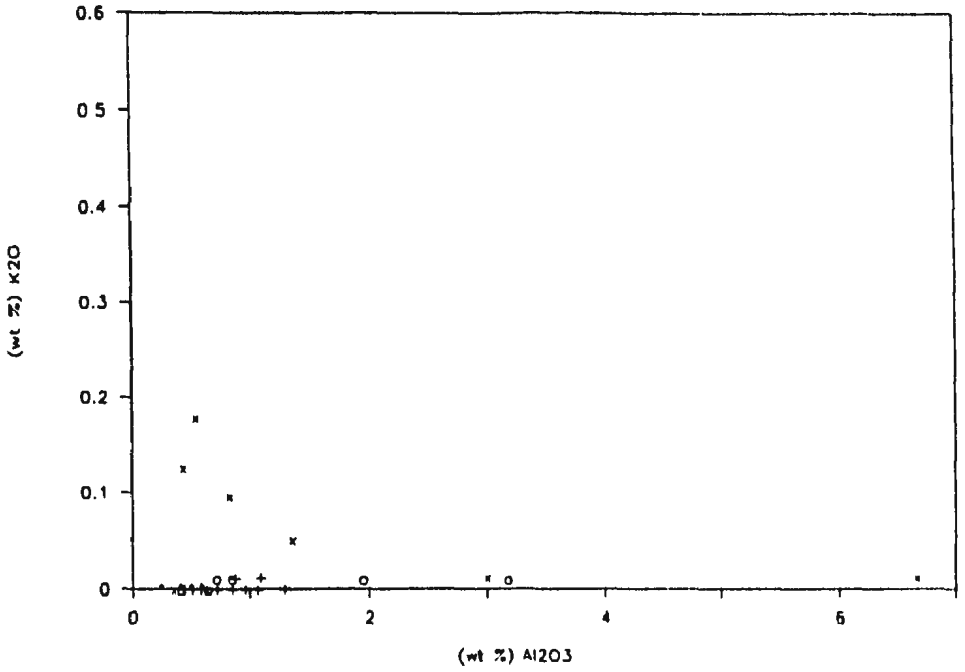
0.6
0.5
0.4
0.3
0.2
0.1
0
(wt %) K2O
0
2
4
6
(wt %) Al2O3

b)

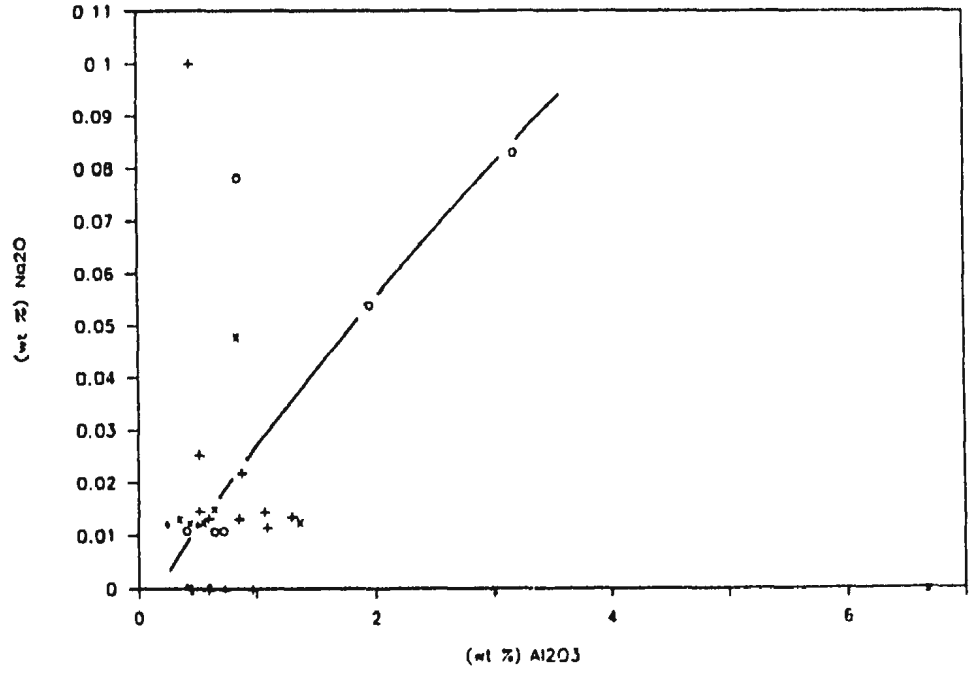
0.11
0.1
0.09
0.08
0.07
0.06
0.05
0.04
0.03
0.02
0.01
0
(wt %) Na2O
0
2
4
6
(wt %) Al2O3

c)

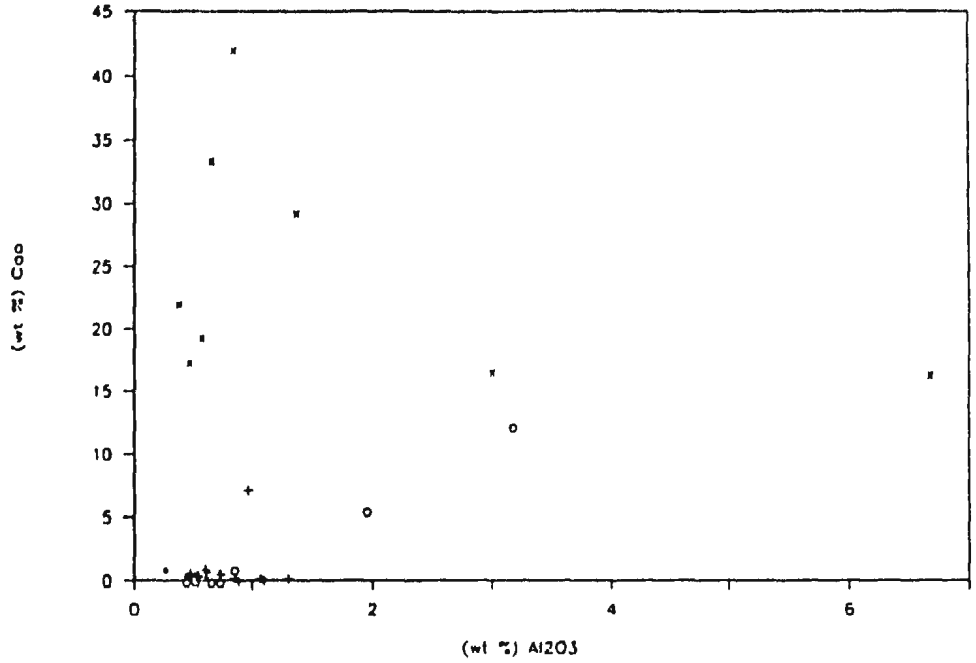
45
40
35
30
25
20
15
10
5
0
(wt %) CaO
0
2
4
6
(wt %) Al2O3

d)

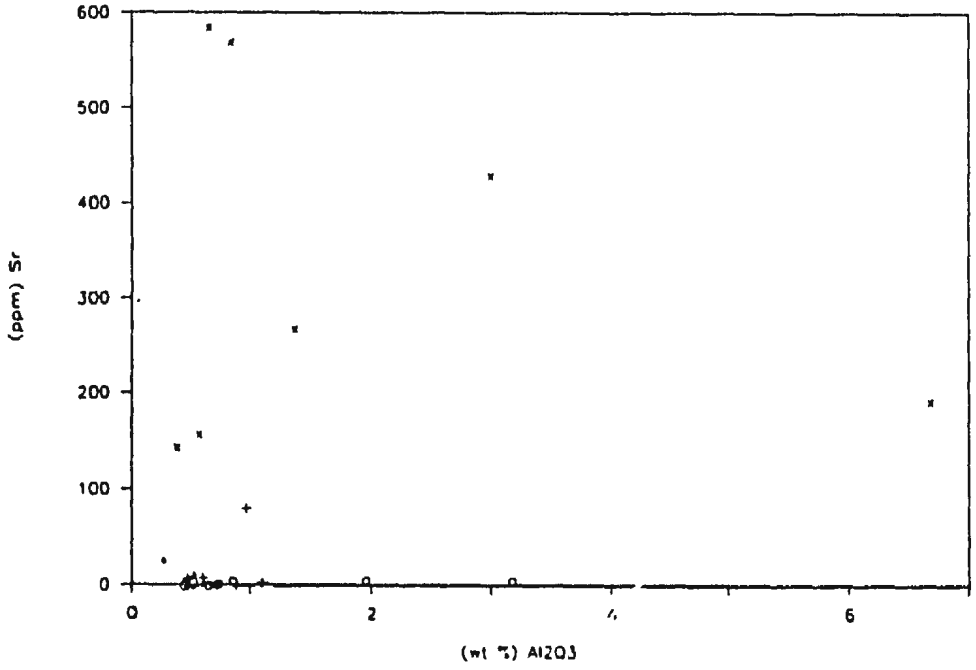
600
500
400
300
200
100
0
(ppm) Sr
0
2
6
(wt %) Al2O3

e)

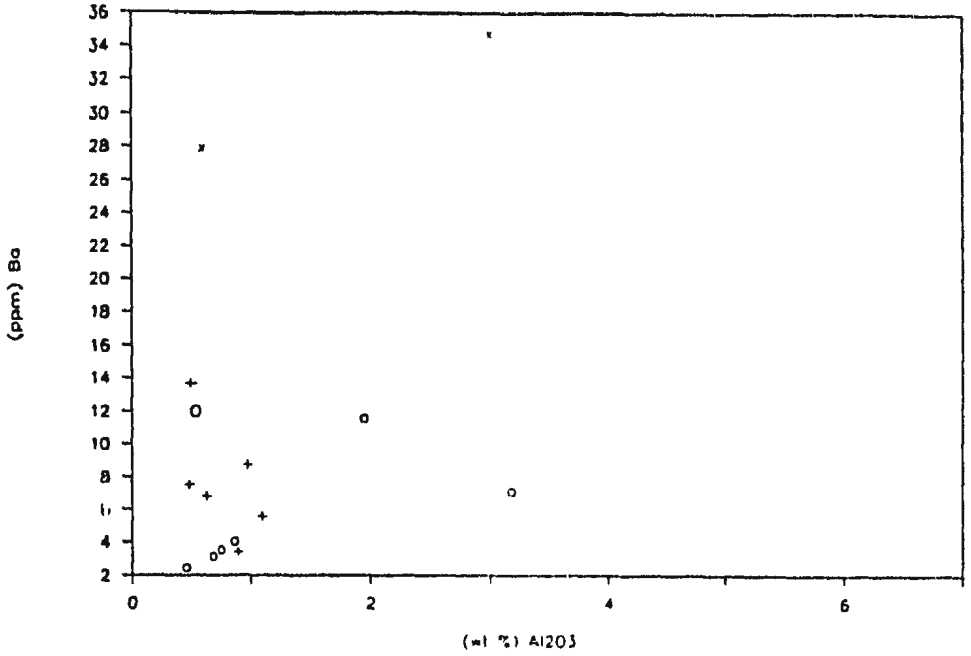
(ppm) Ba
(wt %) Al2O3
36
34
32
30
28
26
24
22
20
18
16
14
12
10
8
4
2
0
2
4
6

f)

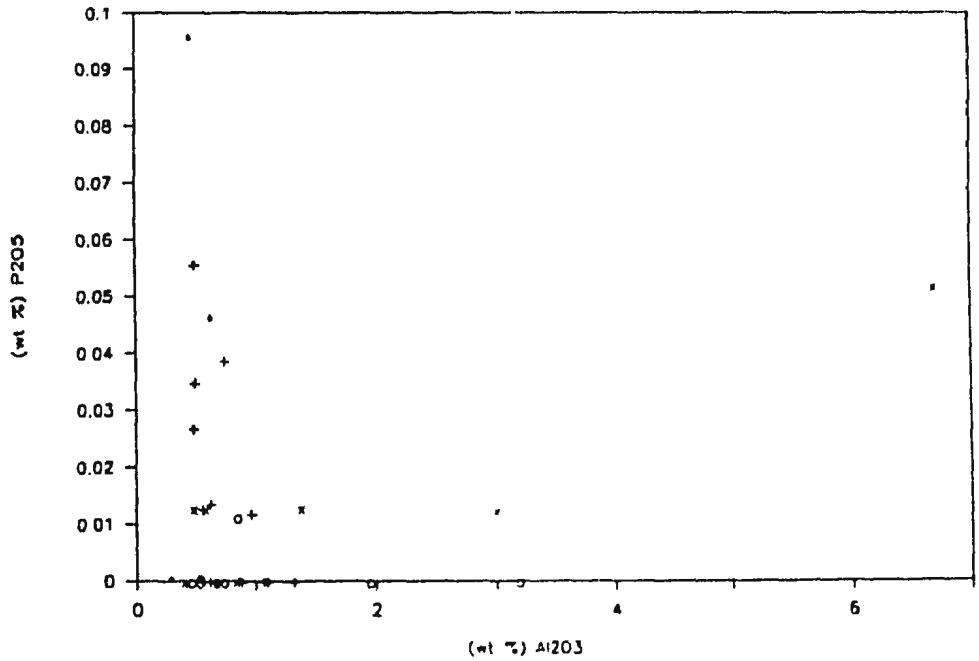
(wt %) P2O5
(wt %) Al2O3
0.1
0.09
0.08
0.07
0.06
0.05
0.04
0.03
0.02
0.01
0
0
2
4
6

g)

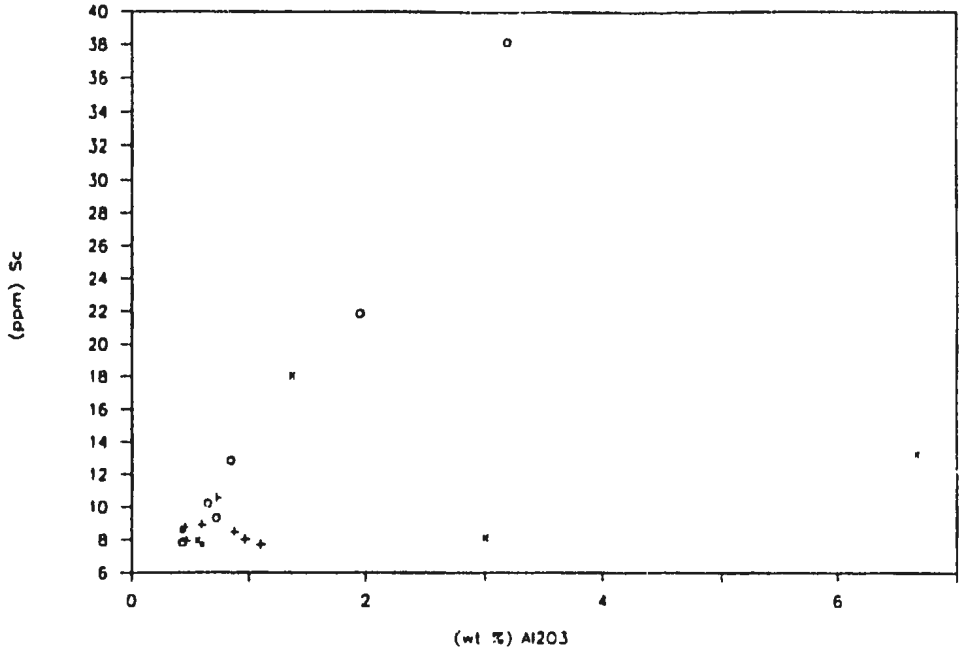
(ppm) Sc
40
38
36
34
32
30
28
26
24
22
20
18
16
14
12
10
8
6
0
2
4
6
(wt %) Al2O3

h)

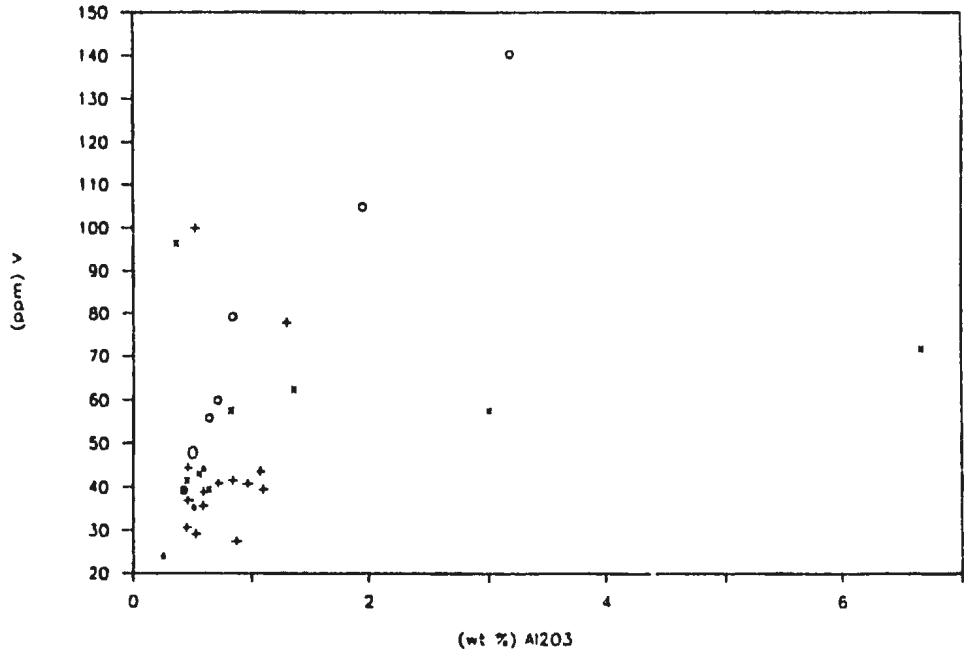
(ppm) V
150
140
130
120
110
100
90
80
70
60
50
40
30
20
0
2
4
6
(wt %) Al2O3

i)

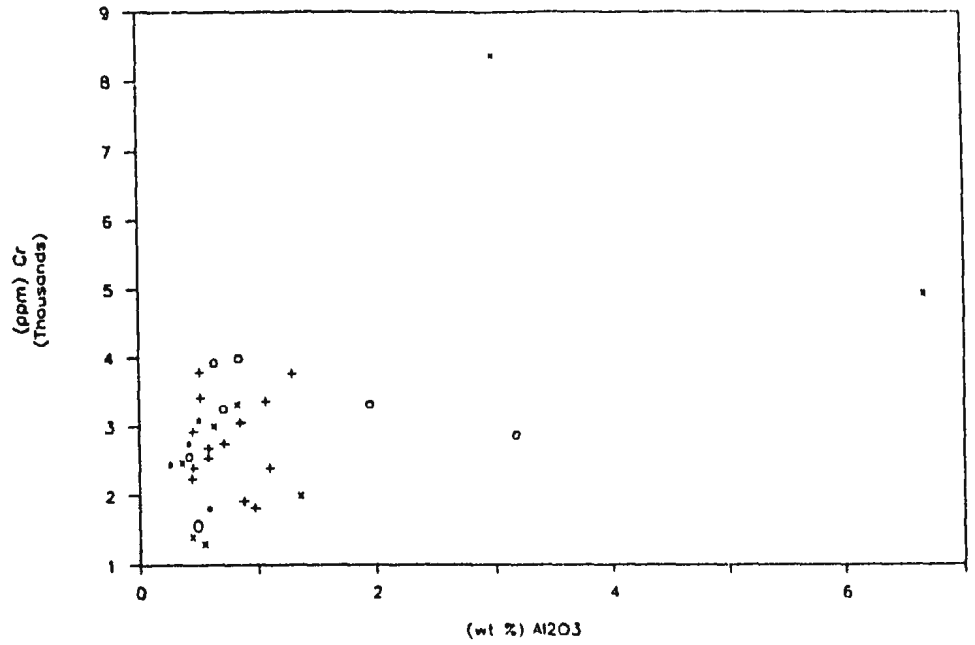
(ppm) Cr
(Thousands)
9
8
7
6
5
4
3
2
1
0
2
4
6
(wt %) Al2O3

j)

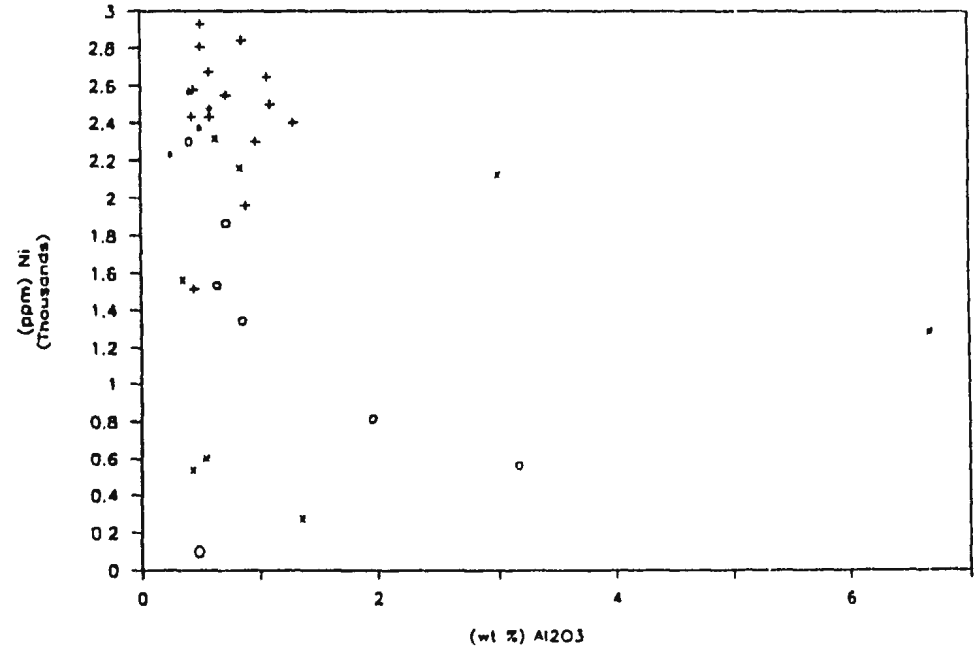
(ppm) Ni
(Thousands)
3
2.8
2.6
2.4
2.2
2
1.8
1.6
1.4
1.2
1
0.8
0.6
0.4
0 2
0
0
2
4
6
(wt %) Al2O3

k)

area. Enrichment of P, a high field strength element, may be attributed to increased mobility of high field strength elements in $CO_2$-bearing systems (Murphy and Hynes, 1986).

#### 4.3.1c Talc-Magnesite:

The enrichments and depletions of various elements in serpentine-magnesite, relative to the cumulate rocks, are also manifest in the chemistry of the talc-magnesite alteration. In addition, Si, Te, Ba, Cu, Pb, Th, Sn and Ni are enriched and Mn, Sc, Zn and Zr are depleted.

#### 4.3.1d Quartz-Hematite-Dolomite:

The geochemical transition from serpentine-magnesite to talc-magnesite reflects a progressive change. Discontinuities are present in the transition between talc-magnesite and quartz-hematite-dolomite. In the talc-magnesite zone, Ni, Si, Te, Th and Cu showed enrichment but in the quartz-hematite-dolomite, Ni, Si, Te and Th show no pattern and Cu is depleted. Similarly, Cd, Mn, Zn and Zr are depleted in talc-magnesite zone but all are enriched in quartz-hematite-dolomite.

The geochemical discontinuity between the talc-magnesite and quartz-hematite-dolomite alteration is

illustrated in Figure 4.4 where Mg/Fe+Mg+Mn+Ca is plotted versus Fe/Fe+Mg+Mn+Ca. A straight line relationship exists between samples of serpentine-magnesite and talc-magnesite while samples of quartz-hematite-dolomite deviate from the line. Carbonate mineral compositions are responsible for the observed deviation (Figure 4.5).

### 4.3.2 Rare Earth Elements:

#### 4.3.2a Cumulate Ultramafic Rocks:

The fresh ultramafic rocks show characteristic, U-shaped chondrite normalized patterns at levels in the range of 0.1 of typical chondrite abundances (Figure 4.6). Overall abundances range between a low in dunite and a high in clinopyroxene-bearing peridotite. There is a slight skewness in these patterns with the light - middle REE being of lowest abundance. One sample displays a large negative Ce anomaly.

The U-shaped cumulate ultramafic rock REE patterns are much different than the typical light rare earth element (LREE) depleted patterns often associated with mantle material. High abundances of LREE in similar rocks have been postulated to be a result of metasomatic processes occurring in the mantle, over a subduction zone (Hamlyn et.al., 1985).

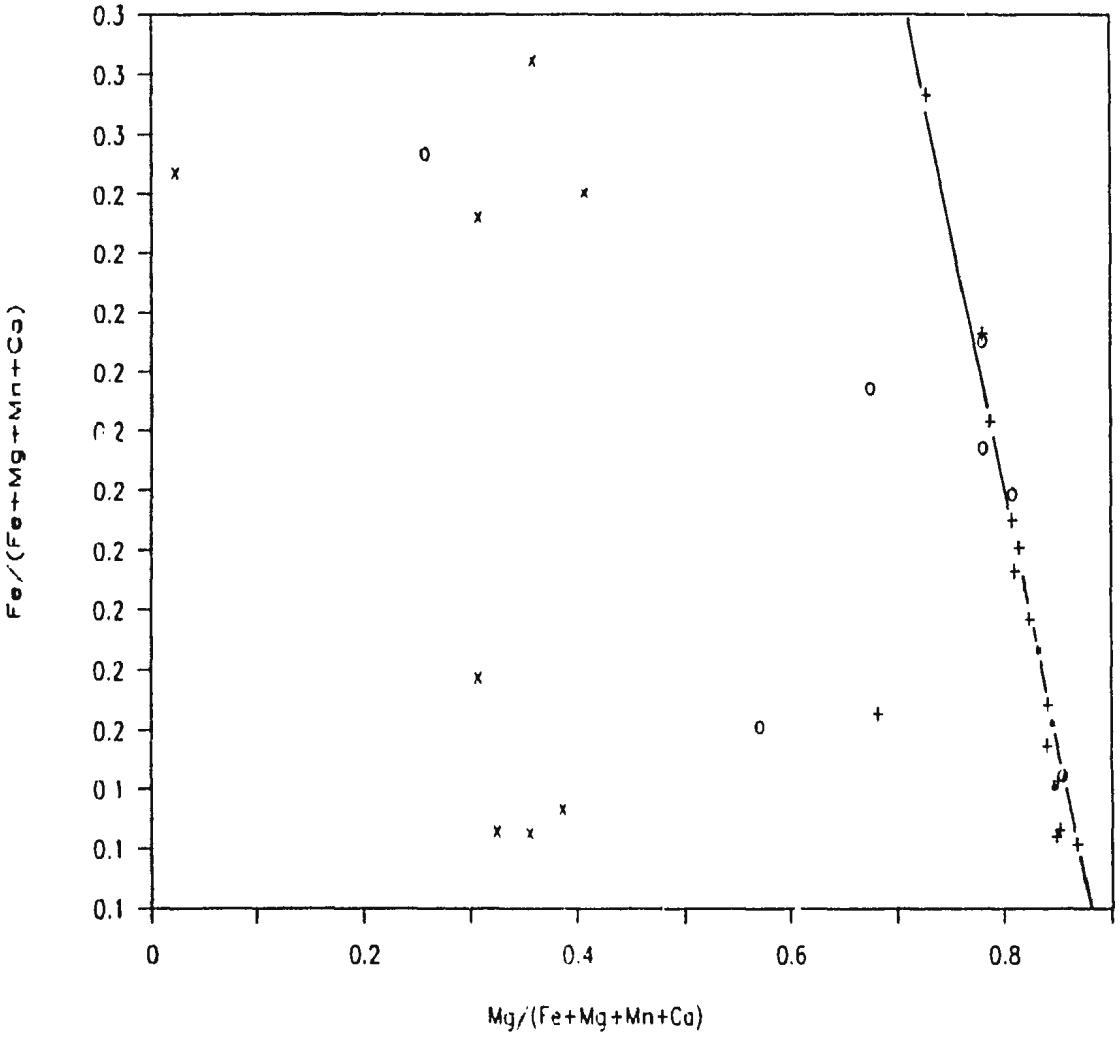


Figure 4.4. Plot of whole rock Fe/(Fe+Mg+Mn+Ca) vs. Mg/(Fe+Mg+Mn+Ca). Distribution shows the discontinuity between the talc-magnesite (+) and the quartz-hematite-dolomite (x) alteration assemblages. Carbonate compositional differences are responsible for this pattern. L-type (*) and LPW-type (o) mineralized veins are included for comparison.

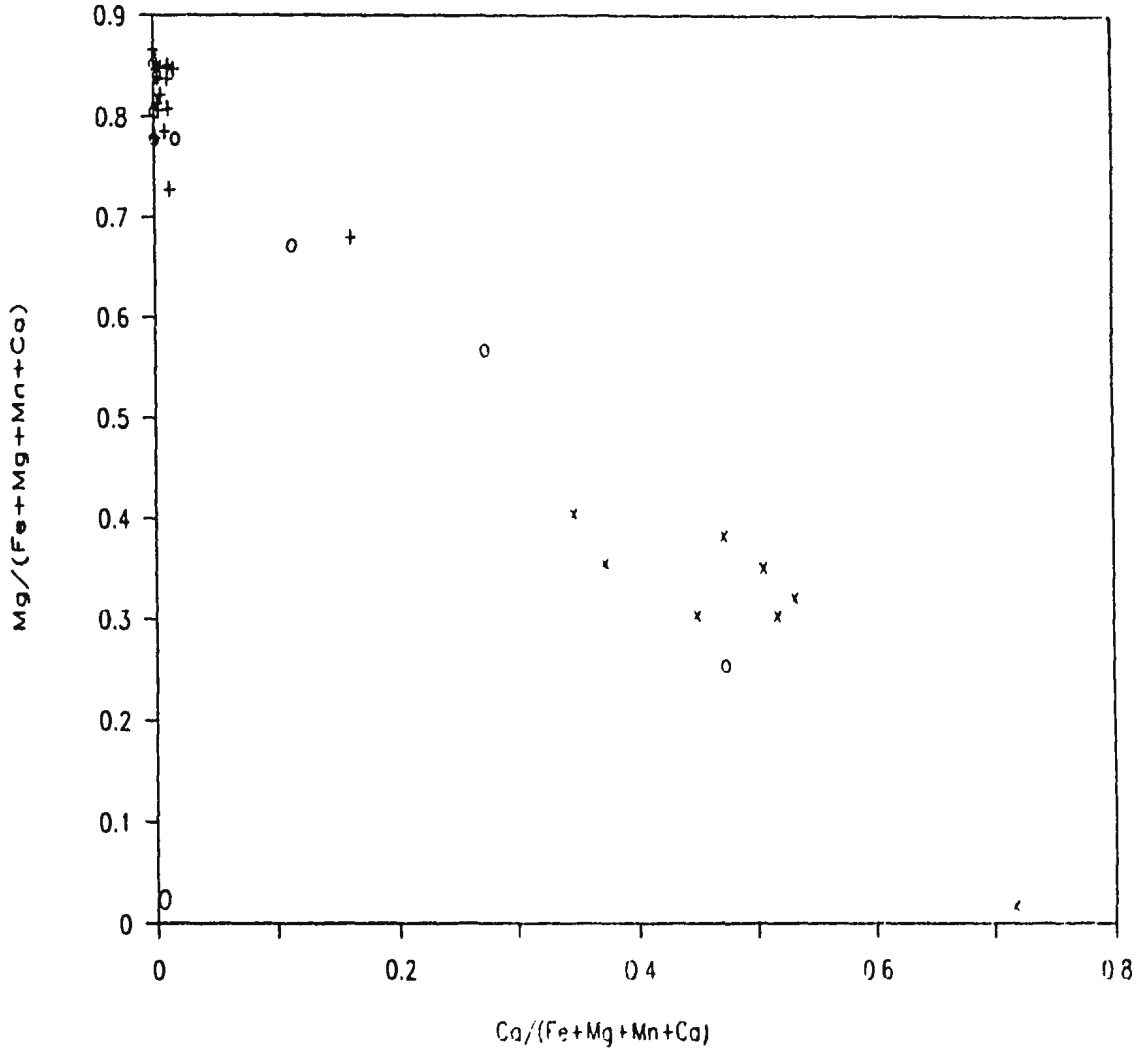


Figure 4.5. Plot of whole rock Mg/(Fe+Mg+Mn+Ca) vs. Ca/(Fe+Mg+Mn+Ca). Distribution shows the extent to which Ca has replaced Mg during alteration to form dolomite, in the quartz-hematite-dolomite altered zone. Serpentine-magnesite (*); Talc-magnesite (+); quartz-hematite-dolomite (x); LPW-type vein (o).

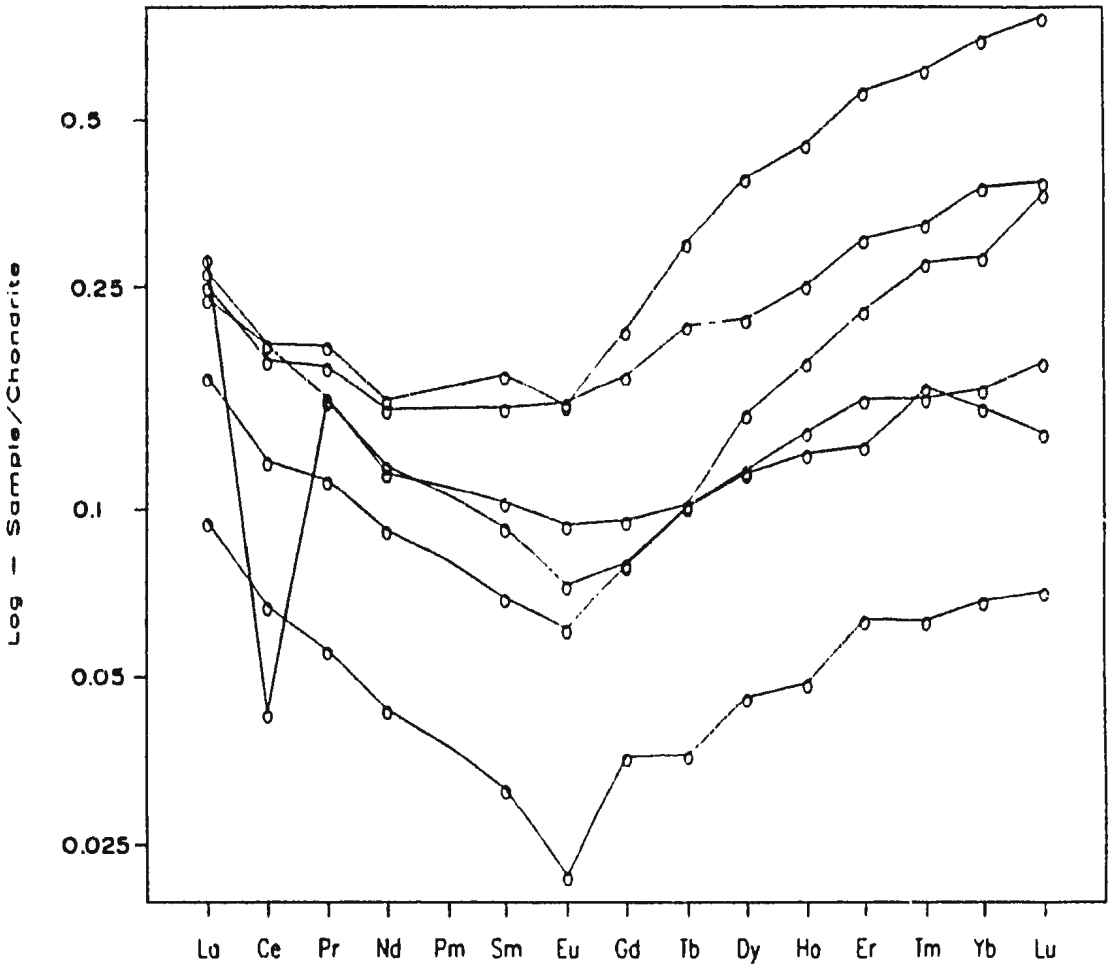


Figure 4.6. Rare earth element plot for cumulate ultramafic rocks normalized to chondrite values. Chondrite values from Taylor and McLennan, 1985.

The patterns exhibited by the fresh ultramafic rocks are utilized as background levels for monitoring changes due to alteration. The behaviour of the REE in hydrothermal alteration systems has been studied by a variety of authors, (Graf, 1977), (Kerrich and Fryer, 1979), (McLennan and Taylor, 1979), (Taylor and Fryer, 1982; 1983a), (Strong, 1984b; Strong et. al., 1984), (Wilton, 1985), (Michard and Albarede, 1986), (Fryer and Taylor, 1987). These studies document the occurrence of fractionation patterns within the REE due to hydrothermal alteration processes.

#### 4.3.2b Talc-Magnesite:

The REE patterns displayed by talc-magnesite altered ultramafic rock are very similar to those displayed by the fresh ultramafic rocks (Figure 4.7). The major differences are an elevation in the LREE and the occurrence of both positive and negative Eu anomalies. Enrichment of LREE is manifest in higher La/Gd ratios (Figure 4.8). There is a small negative Ce anomaly in one sample.

The REE abundances are varied between samples of talc-magnesite. This variation may be partly due to hydrothermal affects but is probably related mostly to variations in primary igneous abundances due to the initial presence or absence of evolved mineral phases such as

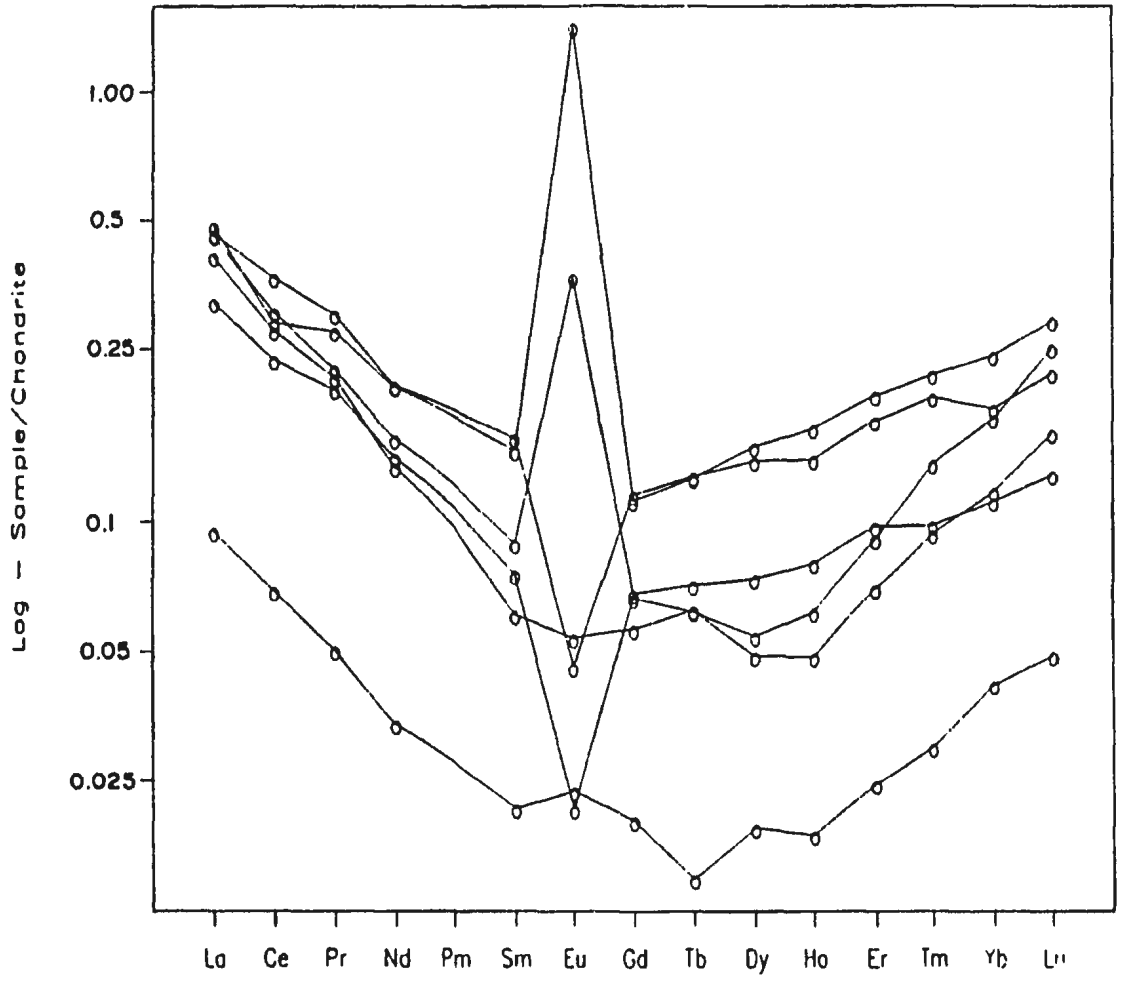


Figure 4.7. Rare earth element plot for samples of talc-magnesite schist normalized to chondrite values (Taylor and McLennan, 1985). Note the somewhat stronger depletion in middle REE compared to the cumulate ultramafic rocks in Figure 4.6.

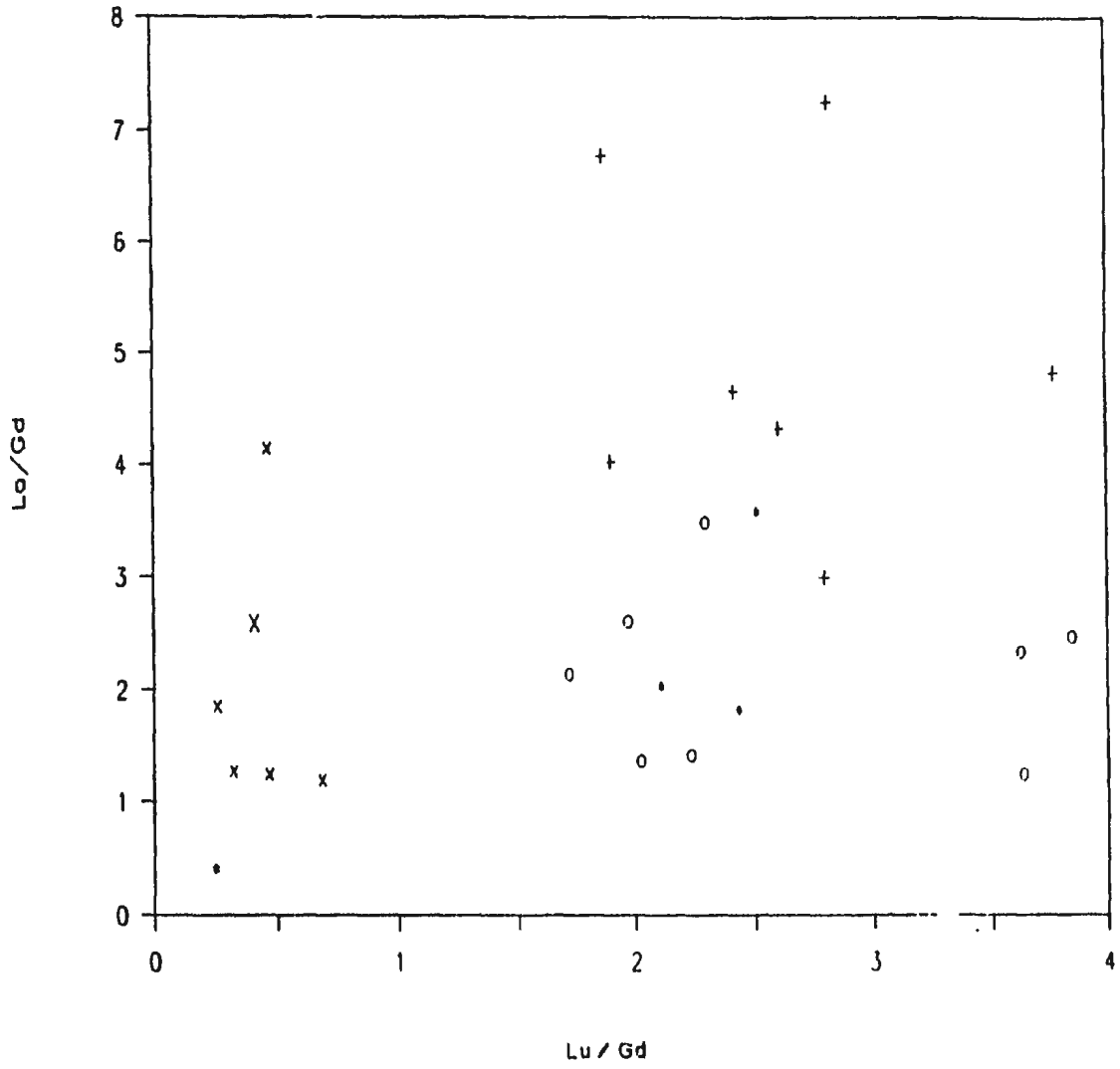


Figure 4.8. Plot of La/Gd vs. Lu/Gd for all ultramafic rocks. Only a slight change is observed for the talc-magnesite (+) while the quartz-hematite-dolomite (x) shows a marked separation attributable to middle REE enrichment. Cumulate ultramafic rocks (o); Jasper clast in Cape St. John Group conglomerate (X).

clinopyroxene. The similarity between the talc-magnesite patterns and the fresh ultramafic patterns may indicate that the fluid interaction with rocks other than ultramafic rocks was limited, since interaction with different rocks of higher REE abundance would be expected to elevate the REE.

Fryer and Taylor (1987) implicate the fluid oxidation state as a control on the generation of Eu anomalies in altered rocks . In the present data, Eu shows the greatest deviance from the other REE in samples affected by reducing fluids. The sample with the highest Eu anomaly (Eu/Eu*=11.02) in Figure 4.7 has been altered by reducing fluids and contains abundant sulphide. The sample with the other positive anomaly, and one of the samples with a negative anomaly, contain no sulphides but are from the fringes of a pyrite-rich zone at the contact of talc-magnesite and pillow lava. The remaining samples are specular hematite-bearing, indicating an oxidized hydrothermal fluid.

#### 4.3.2c Quartz-Hematite-Dolomite:

The REE patterns from samples of the quartz-hematite-dolomite altered zone differ from those of the fresh and talc-magnesite altered rocks (Figure 4.9). Although absolute abundances are similar, the light, and

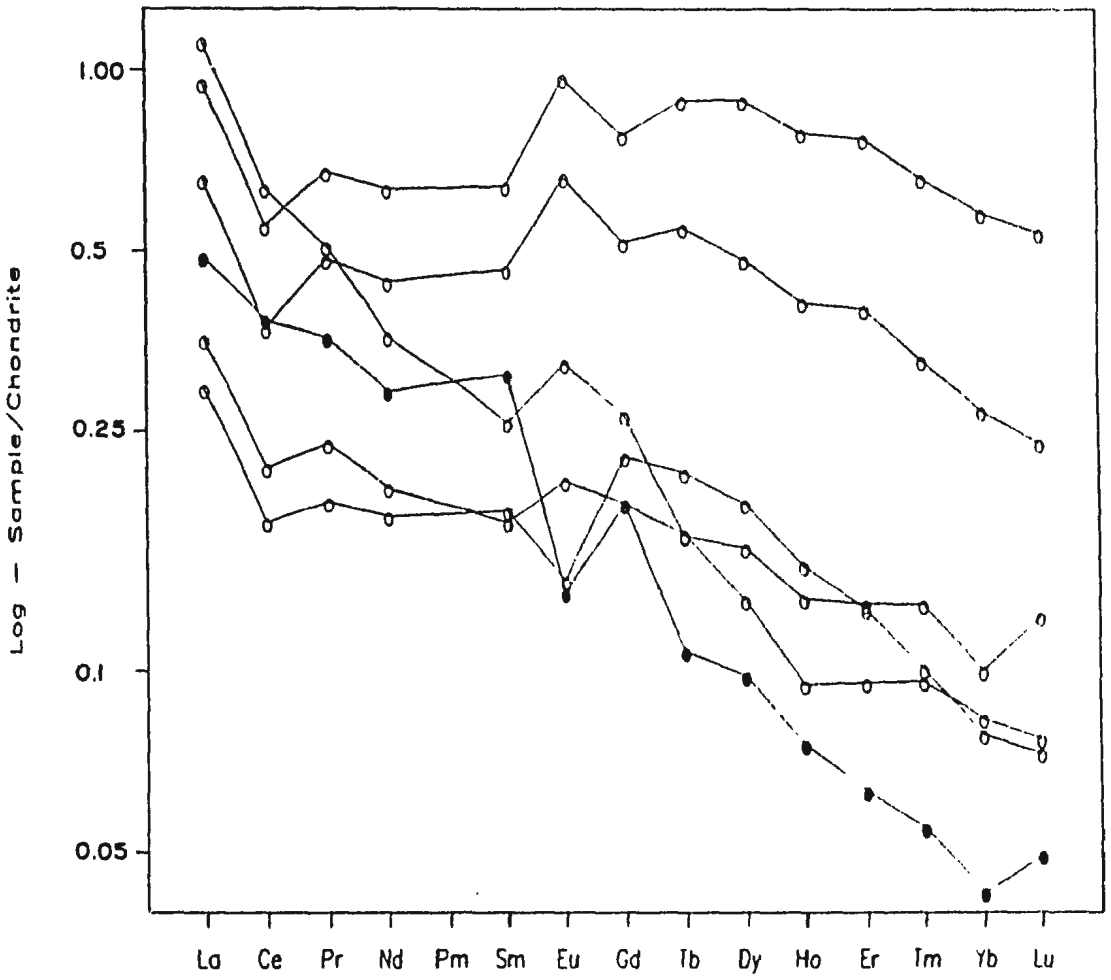


Figure 4.9. Rare earth element plot for quartz-hematite-dolomite altered ultramafic rocks (x) normalized to chondrite values (Taylor and McLennan, 1985). Note the pronounced middle REE enrichment relative to the other types of ultramafic rocks. The solid circle represents a clast of similarly altered material within Cape St. John Group sediments.

especially the middle REE (MREE) are significantly enriched. The heavy rare earth elements (HREE) are least changed, with Lu appearing immobile. The strong MREE enrichment is manifest by slightly decreased La/Gd ratios despite an increase in La abundance and strongly decreased Lu/Gd ratios compared to talc-magnesite schist (Figure 4.8). Negative Ce anomalies are present in most of the samples.

Similar MREE enrichment is reported by Kerrich and Fryer, (1979) for mid-Atlantic Ridge rodingite. Rodingite is a Ca and $CO_3$ altered rock formed by metasomatic processes involving low temperature, ultramafic-derived fluids (Coleman, 1977).

Most samples show moderate, positive Eu anomalies. These Eu anomalies may result from preferential precipitation of $Eu^{2+}$ in dolomite - $Eu^{2+}$ being of similar charge and ionic radius to Ca - while excluding the other REE of $3^+$ charge. General enrichment of total Eu in the fluid is not indicated by a REE pattern for a mineralized vein within this altered zone (Figure 4.10).

The REE pattern displayed by the jasper clast in Figure 4.9 is identical to those of the quartz-hematite-dolomite alteration zone. The clast is from conglomerate within a shear zone at the contact of the ophiolite and Cape St.

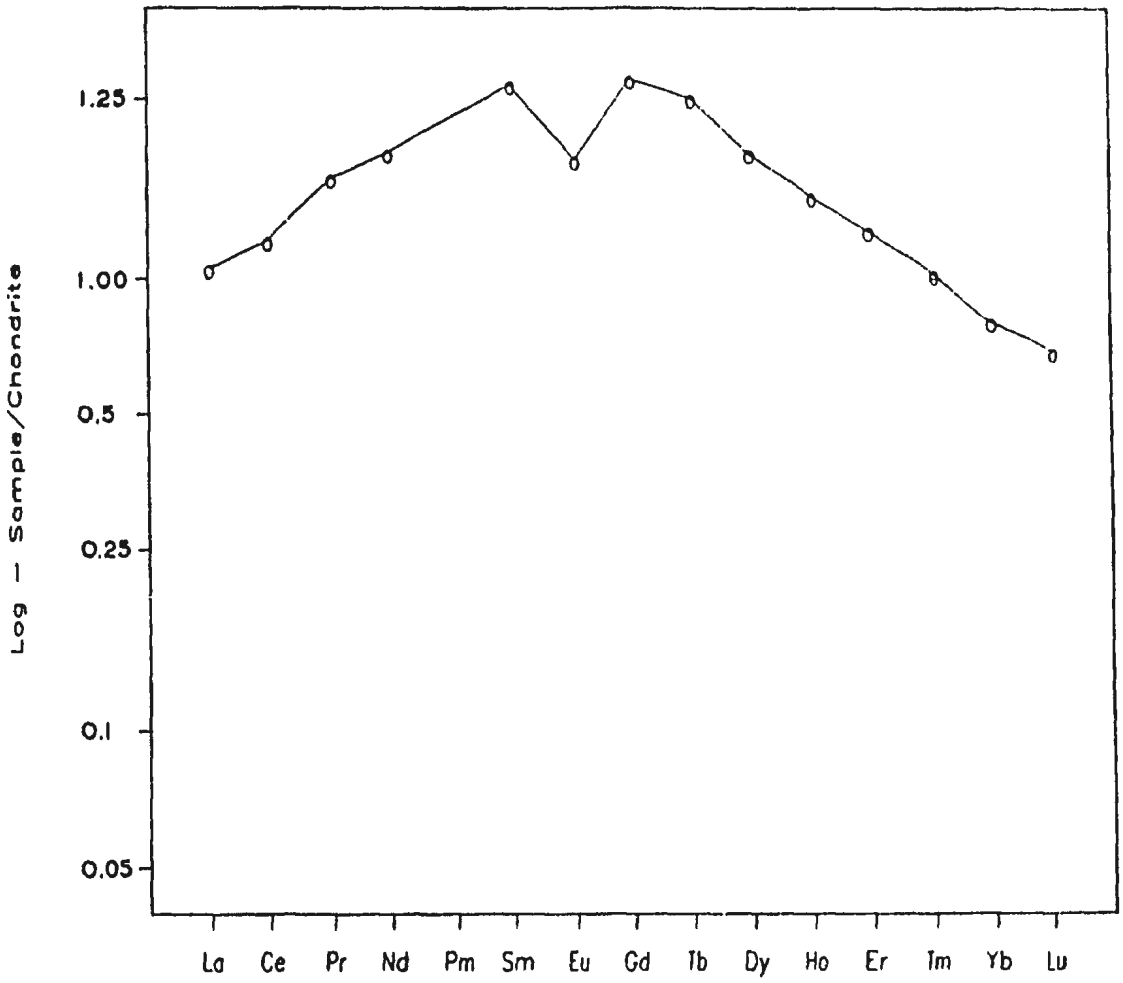


Figure 4.10. Chondrite-normalized REE plot for LPW-type vein at Long Pond West #1 showing. Chondrite values from Taylor and McLennan, 1985.

John Group.

### 4.3.3 Precious metals:

#### 4.3.3a Gold:

The gold contents of fresh ultramafic rocks, serpentine-magnesite, talc-magnesite and quartz-hematite-dolomite altered rocks have been determined. Table 4.1 summarizes the gold and PGE geochemistry of the ultramafic rocks.

Only 5 determinations of gold in fresh ultramafic rocks were made but in all cases none was detected. These data corroborate evidence from Buisson and LeBlanc (1987) that gold contents of mantle peridotite are low; their data suggests contents in the range of 3 to 5 ppb.

There is a correlation between elevated gold values and carbonate alteration. This association is the only positive correlation with Au evident from the data for all ultramafic rocks. This correlation has been recognized by authors elsewhere such as Goncharenko (1970) and Buisson and LeBlanc (1985; 1986; 1987). Figure 4.11 illustrates the strong fractionation of Au into the carbonate altered ultramafic rocks.

Table 4.1. Summary of precious metal geochemical data on ultramafic rock types.

| Element | n | Range | Mean | Std. Dev. |
|---|---|---|---|---|
| | | Cumulate Ultramafic Rocks | | |
| Pt | 6 | 0-17.2 | 10.6 | 6.1 |
| Pd | 6 | 0-30 | 9.1 | 10.1 |
| Ru | 6 | 0- 5.9 | 2.3 | 2.0 |
| Rh | 6 | 0- 1.8 | 1.4 | 0.6 |
| Ir | 6 | 0- 2.5 | 0.5 | 0.9 |
| Au | 6 | NA | 0.0 | 0 |
| | | Serpentine-Magnesite | | |
| Pt | 4 | 5 - 9.5 | 7.3 | 1.7 |
| Pd | 4 | 2.5-10.9 | 7.3 | 3.4 |
| Ru | 4 | 4.4- 8.3 | 6.4 | 1.8 |
| Rh | 4 | 0.9- 2.7 | 1.7 | 0.8 |
| Ir | 4 | 2.3- 4.0 | 3.0 | 0.7 |
| Au | 4 | 0 -16.5 | 7.4 | 6.6 |
| | | Talc-Magnesite | | |
| Pt | 14 | 2.2- 9.1 | 5.1 | 1.9 |
| Pd | 14 | 0.4-15.7 | 4.9 | 4.0 |
| Ru | 14 | 3.0- 8.0 | 7.1 | 1.7 |
| Rh | 14 | 0.4- 1.9 | 1.4 | 0.4 |
| Ir | 14 | 1.6- 4.3 | 3.2 | 0.8 |
| Au | 14 | 0.7-300 | 44.6 | 82.3 |
| | | Quartz-Hematite-Dolomite | | |
| Pt | 8 | 1.5- 9.0 | 5.4 | 5.0 |
| Pd | 8 | 1.4- 4.4 | 2.7 | 1.3 |
| Ru | 8 | 1.9- 7.3 | 4.1 | 1.9 |
| Rh | 8 | 0.5- 2.2 | 1.1 | 0.6 |
| Ir | 8 | 0.6- 4.0 | 2.0 | 1.1 |
| Au | 8 | 7.6-127 | 46.3 | 51.1 |

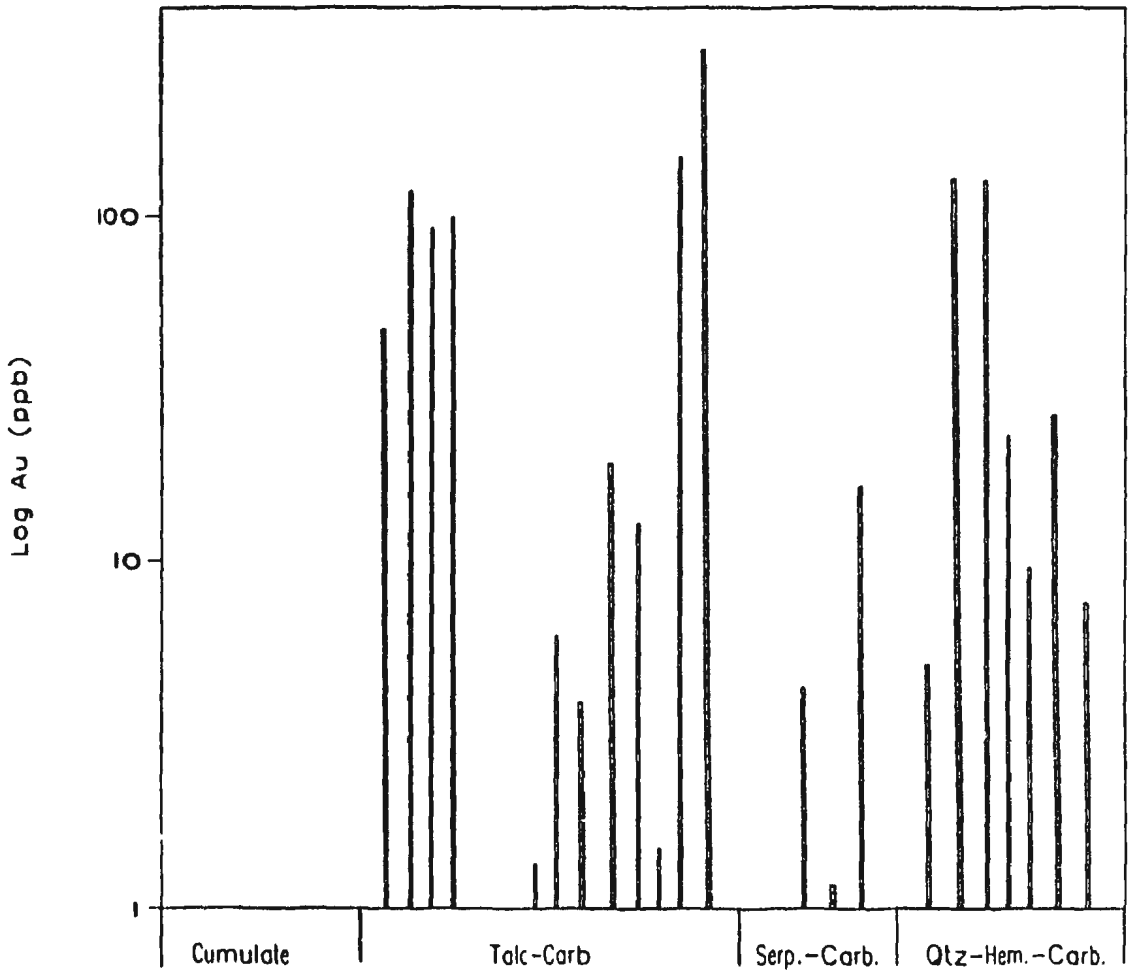


Figure 4.11. Plot of Au content from all samples of ultramafic rocks. Distribution shows the strong correlation between carbonate alteration and elevated gold content.

### 4.3.3b Platinum Group Metals:

There are no high values for the PGE in any samples analysed, however, there is a consistent fractionation observed within the group which correlates with carbonate alteration intensity. Figure 4.12a is a plot of average PGE values for the various ultramafic rocks. Figure 4.12b is a plot of the average PGE values in the 3 altered types of ultramafic rock, normalized to the average PGE values in the fresh ultramafic rocks. The normalized patterns best show a consistent Pt and Pd depletion and Ru, Ir enrichment within the altered rocks. Rhodium levels show little change. Fractionation of Pt and Pd from Ir has been observed in several studies. Stumpfl (1986) discusses Pd, Ir decoupling by hydrothermal ($H_2O$ - $CO_2$) processes in Fe, Ni, Cu veins at Kambalda. Crocket and Mac Rae (1986) report separation of Pt and Pd from Ir by primary igneous processes - greater compatibility of Ir in fractionating phases within komatiitic and tholeiitic volcanic rocks in Monroe township, Ontario. Brugmann et. al. (1987) give evidence for compatible behaviour of Au and Pd and incompatible behaviour of Ir, Os and Ru in komatiitic melts leading to Pd fractionation from Ir, Os and Ru.

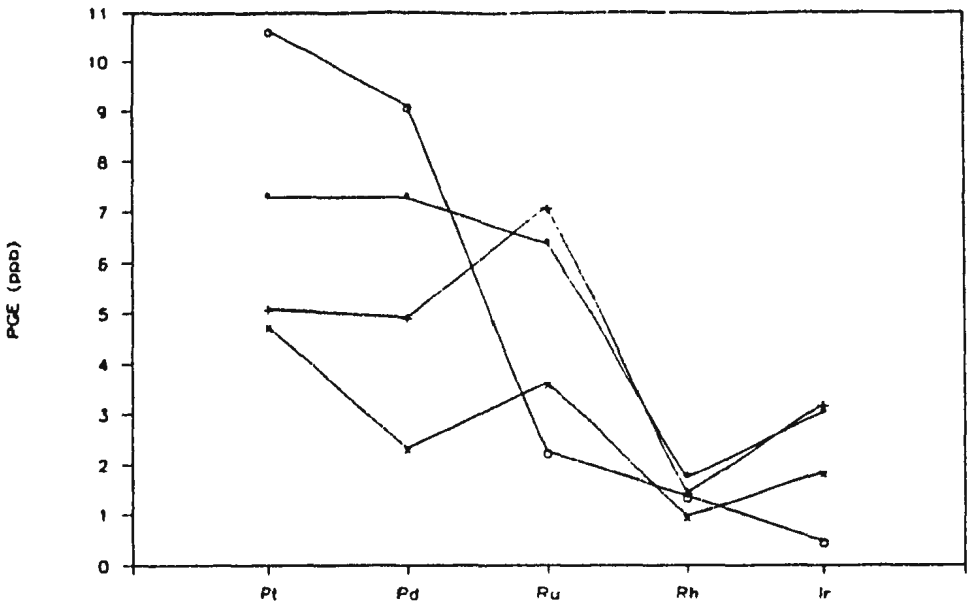


a)

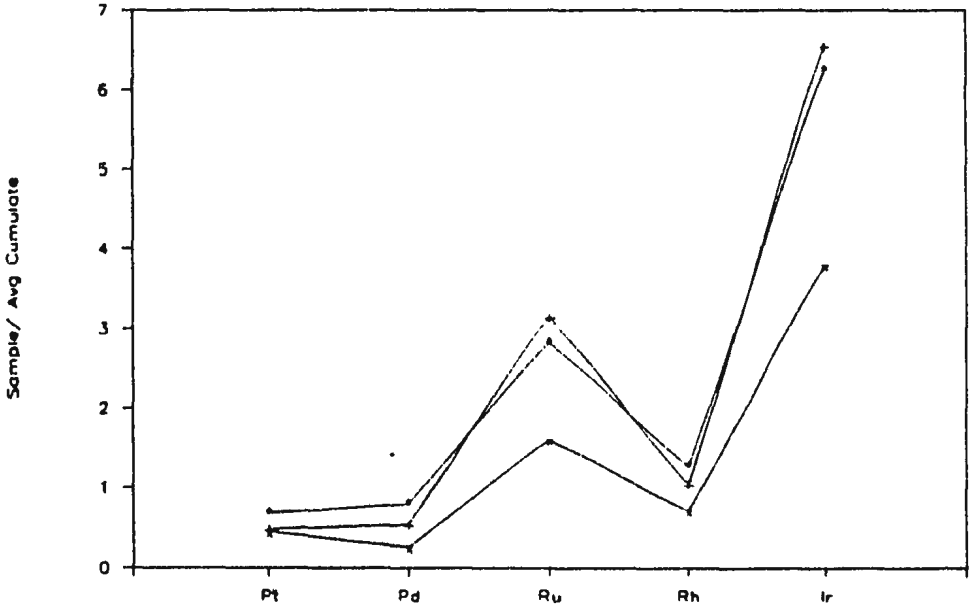


b)

Figure 4.12. a) Average PGE contents of the various ultramafic rock types from Table 4.1. b) Average PGE contents from a) above, normalized to average PGE contents in cumulate (unaltered) ultramafic rocks. Cumulate rocks (o); Serpentine-magnesite (*); talc-magnesite (+); Quartz-hematite-dolomite (x).

The depletion of Pt and Pd occurs only within ultramafic rocks that have been affected by carbonate alteration. This implicates a hydrothermal mechanism for mobilizing the Pt and Pd. The coincidental concentration of Ir and Ru is not well understood but may relate to similar processes as those responsible for Au mobilization.

## 4.4 Mineralized Veins:

### 4.4.1 Major and Trace Elements:

The chemistry of L-type and LPW-type veins reflects the chemistry of the talc-magnesite and quartz-hematite-dolomite respective host rocks. In Figure 4.13, the major and selected trace element values determined for the L-type veins are plotted with respect to their range in the talc-magnesite rocks. Most of the observed deviations of vein chemistry from host rock chemistry can be attributed to concentration or dilution by $SiO_2$ and carbonate. There are, however, some obvious mineralization-associated chemical signatures. Cu and S correlate with gold mineralization. Cu is enriched relative to the altered host rocks by a factor of 200 times. The only other element which shows any correlation with gold mineralization is Bi which displays enrichment factors of 40 to 50 times background.

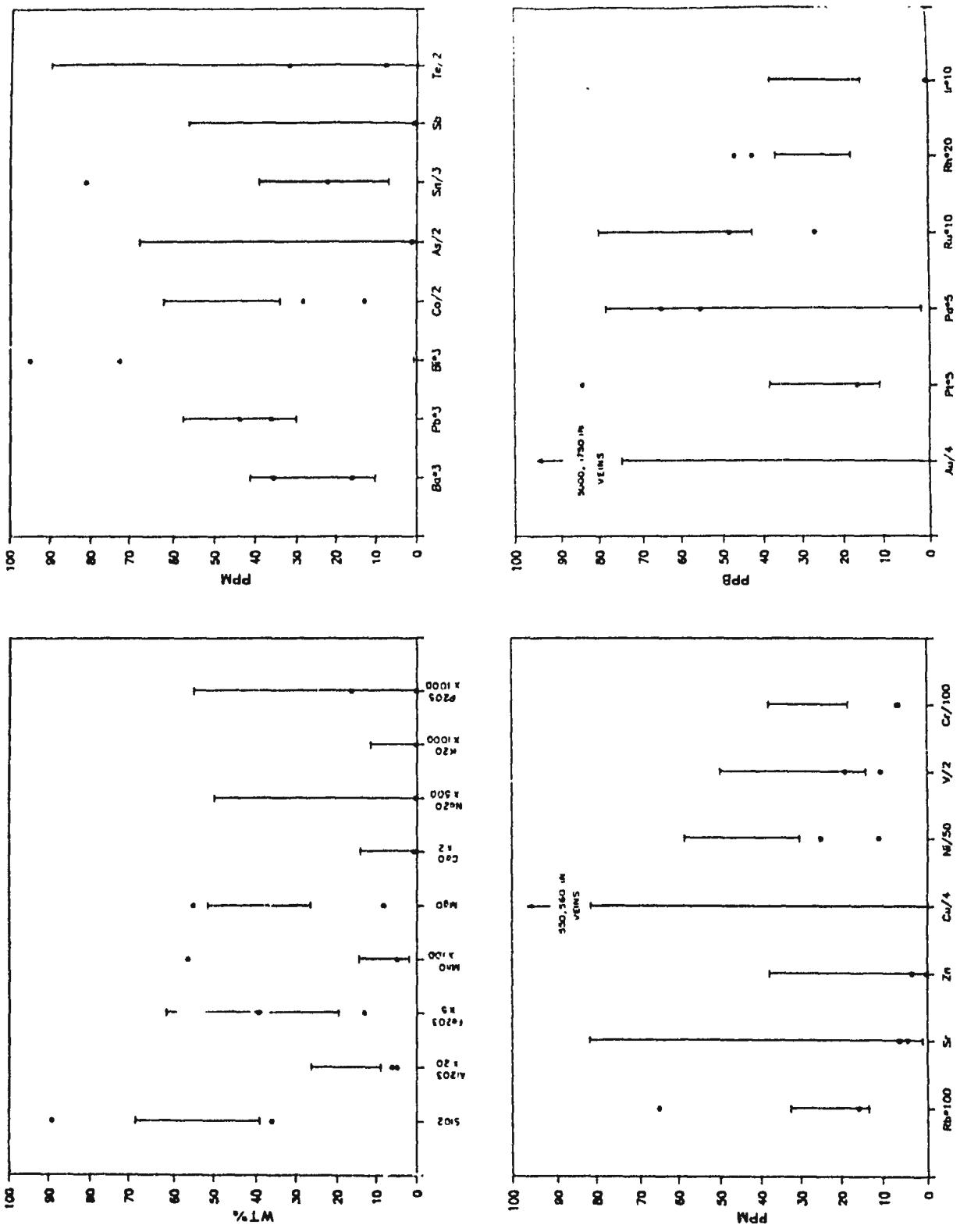


Figure 4.13. Major and selected trace element data for L-type gold-bearing veins (*) referenced against their range in the talc-magnesite host rock.

Based on one sample, the LPW-type vein shows elemental signatures which are distinct from those of the L-type veins. Figure 4.14 displays the LPW-type vein chemistry in the same manner as Figure 4.13. $SiO_2$ is the major component of the vein and is therefore strongly enriched. Cr, $K_2O$ and Rb are co-enriched due to the formation of fuchsite.

4.4.2 Rare Earth Elements:

REE patterns for the mineralized veins are shown in Figures 4.10 and 4.15. L-type vein patterns are characterized by abundances between 0.05 and 0.1 of chondrite levels. The patterns are U-shaped but there is an inflection point at Tm where the slope decreases toward Lu. Except for the inflection point at Tm, the L-type vein patterns are identical to those of the enclosing host talc-magnesite schists, suggesting that the fluid responsible for formation of the veins was the same fluid that caused the talc-magnesite alteration.

The pattern for the LPW-type vein, at the Long Pond West #1 showing, displays a very strong MREE enrichment similar to the MREE enrichment in the peripheral alteration zone to the vein. The overall abundance of REE is highest in this sample compared to all other ultramafic samples, ranging from slightly less, to five times chondrite

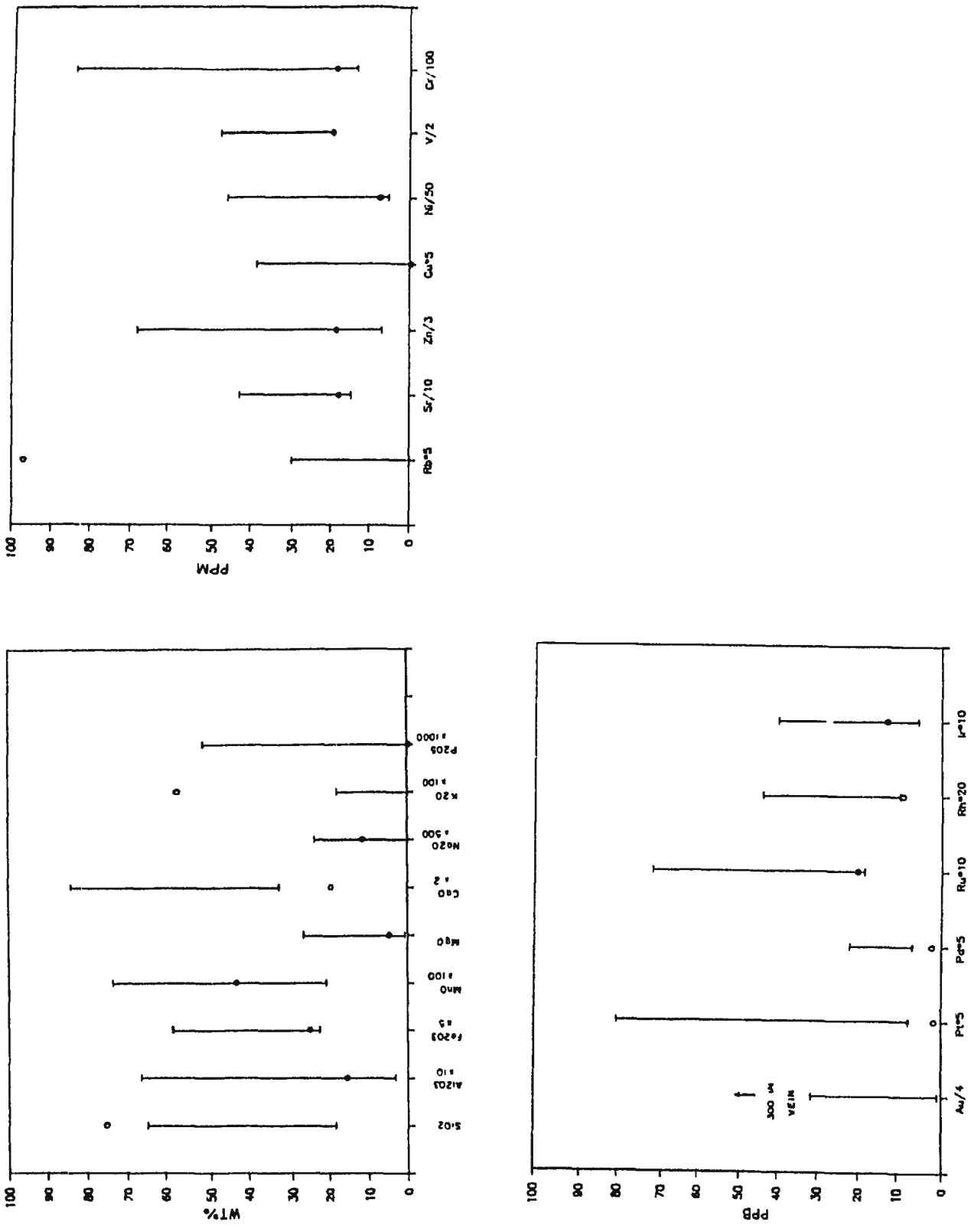


Figure 4.14. Major and selected trace element data for LPW-type veins (o) referenced against their range in the quartz-hematite-dolomite host rock.

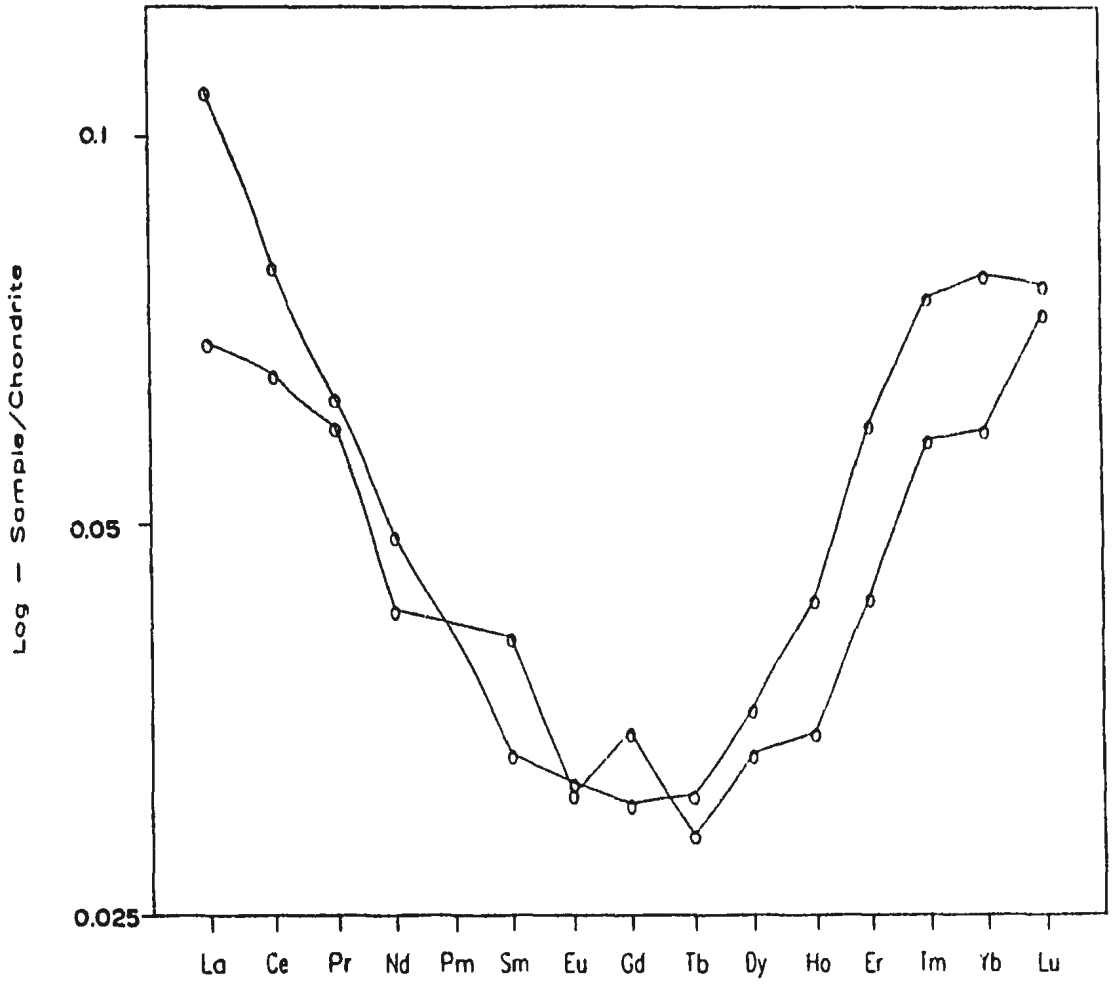


Figure 4.15. Chondrite-normalized rare earth element plot for L-type veins. Chondrite values from Taylor and McLennan, 1985.

levels. There is a weak negative Eu anomaly (Eu/Eu*=0.67) which may be a result of depletion of Eu in the fluid as a result of preferential precipitation in dolomite formed during alteration of the host rocks.

### 4.4.3 Precious Metals:

Gold enrichment factors in the mineralized veins range from 6000 to 10,000 for the L-type veins and 500 to 600 in the LPW-type veins. These are typical of enrichment factors in many lode gold deposits (Kerrich, 1983).

In the L-type veins, Pt, Pd and Rh are enriched and Ru and Ir are depleted relative to the talc-magnesite host rocks. In the LPW-type vein, all PGE are at low levels relative to the range of PGE in the quartz-hematite-dolomite altered host rocks. These characteristics may be seen in Figures 4.13 and 4.14.

## 4.5 Cape St. John Group:

Limited geochemical study of the showings in the Cape St. John Group has been undertaken because the mineralized shear zones are within lineament controlled, clastic sedimentary rocks which are a poor sample medium from which to obtain coherent, mineralization-related geochemical trends. The major, and most trace element data are

inconsistent due to variable proportions of detrital material of mixed composition. The REE show some features which may be attributed to the mineralization process and are discussed below.

4.5.1 Rare Earth Elements:

REE patterns for highly sheared and altered clastic sediments on the northeast shore of Red Cliff Pond, mineralized by LPW-type veins, are shown in Figure 4.16. The patterns represent samples in a transect from the fault contact with talc-magnesite altered ultramafic rocks at the central part of the shear zone, outward toward the shear zone boundary. The samples of lowest abundance are from fault gouge where mixing of ultramafic rocks and Cape St. John Group sedimentary rocks has occurred. The fault gouge has been overprinted by intense carbonate-fuchsite alteration.

The three samples in the carbonate-altered fault gouge are LREE depleted relative to the samples from the less altered fringe of the shear zone. The heavy REE from Dy to Lu are consistent with the samples outside of the carbonate alteration despite slightly lower abundances. Strong negative Eu anomalies are present in two of the carbonate altered samples.

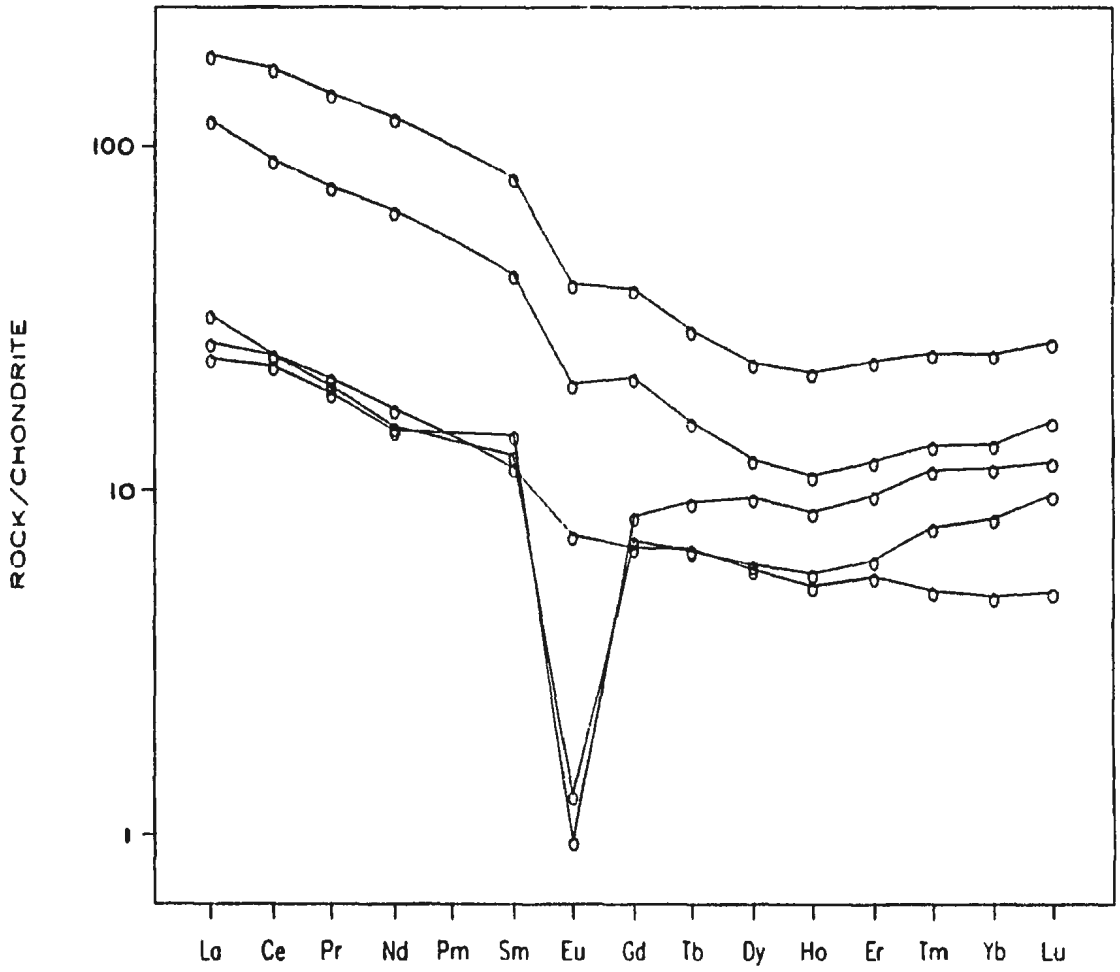


Figure 4.16. Chondrite-normalized rare earth element plot for highly sheared and altered clastic sediments of the Cape St.John Group. Chondrite values from Taylor and McLennan, 1985.

The two least altered samples are identical except for slight differences in abundance. It is likely that the REE patterns of all the samples were similar and the LREE depletion and the Eu anomalies are a result of hydrothermal alteration. Physical mixing of Cape St. John rocks with REE-deficient ultramafic rocks in the core of the shear zone, may have contributed to the lower abundances of REE in the altered samples which are closest to the ultramafic contact.

## 4.6 Rb/Sr Isotope Systematics:

Isotope data were obtained from 10 samples for the purposes of dating LPW-type mineralization and alteration and to determine the fluid source. The data are listed in Table 4.2.

### 4.6.1 Rb/Sr Dating:

An attempt was made to obtain an Rb/Sr mineral isochron date using carbonate and fuchsite from the LPW-type mineralization at the Long Pond West #1 showing, following the procedure of Bolke and Kistler (1986). A whole rock isochron was also attempted by sampling the enclosing quartz-hematite-dolomite alteration zone which has a variable fuchsite content.

Table 4.2. Rb/Sr isotopic data.

| Sa.# | $^{87}Rb$ (ppm) | $^{86}Sr$ (ppm) | $^{87}Sr/^{86}Sr$ Measured | $^{87}Rb/^{86}Sr$ | Sa. Type |
|---|---|---|---|---|---|
| 28-1 | 5.6 | 14.9 | 0.71084 +/-0.00018 | 0.3689 | LPW-type vein |
| 28-3 | ND | 13.3 | 0.70910 +/-0.00016 | 0.0051 | qtz-carb.-hematite |
| 28-4 | 1.2 | 10.1 | 0.70983 +/-0.00011 | 0.1196 | qtz-carb.-fuchsite-hematite |
| 28-5 | ND | 40.0 | 0.70877 +/-0.00007 | 0.0055 | qtz-carb.-hematite |
| 28-6 | 0.9 | 38.2 | 0.70823 +/-0.00027 | 0.0232 | qtz-carb.-fuchsite-hematite |
| LPW-C | 1.7 | 7.7 | 0.71059 +/-0.00032 | 0.2192 | LPW vein ankerite |
| LPW-F | 38.3 | 6.3 | 0.75468 +/-0.00072 | 6.0379 | LPW vein fuchsite |

| Sa# | Sr (ppm) | Rb (ppm) | $^{87}Sr/^{86}Sr$ Measured | Sa. Type |
|---|---|---|---|---|
| SA-5 | 4.88 | 0.17 | 0.70996 +/-0.00028 | talc-carb. schist |
| V-1 | 0.40 | 3.69 | 0.70994 +/-0.00064 | L-type vein |
| V-2 | 0.13 | 3.55 | 0.70934 +/-0.00019 | L-type vein |

Note: $^{87}Rb$ and $^{86}Sr$ concentrations determined by isotope dilution; total Rb and Sr concentrations determined by ICP-MS.

ND - not detected

The whole rock data in Figure 4.17 are not concordant to an acceptable degree and field evidence implies a post-Cape St. John Group age for the mineralization, therefore the date from this study is not accepted as representing the age of mineralization. It is probably coincidental that the date obtained by this method (430.7 +/- 90 ma) is similar to an Rb/Sr date obtained by Pringle (1978) of 429 +/- 50 ma for ignimbrite in the Cape St. John Group near the mineralized zone dated here, and a recent U/Pb zircon date on the Cape St. John Group of approximately 430 ma (Coyle, pers. comm.).

The fuchsite-carbonate mineral isochron age of 528.5 +/- 19.7 ma is also contradictory to the post-Cape St. John Group age for mineralization indicated by field evidence. Removal of Rb from the fuchsite during post-mineralization processes could be responsible for steepening the slope of the isochron and increasing the apparent age of the sample.

4.6.2 Sr Isotope Data:

Whole rock Sr isotopic data for alteration assemblages and veins with below detection limit Rb (XRF detection limit of 4 ppm) are used in this section to aid in determining the fluid source. When no appreciable Rb is present in the system the Sr isotopic composition should not change from the time it is set during an igneous,

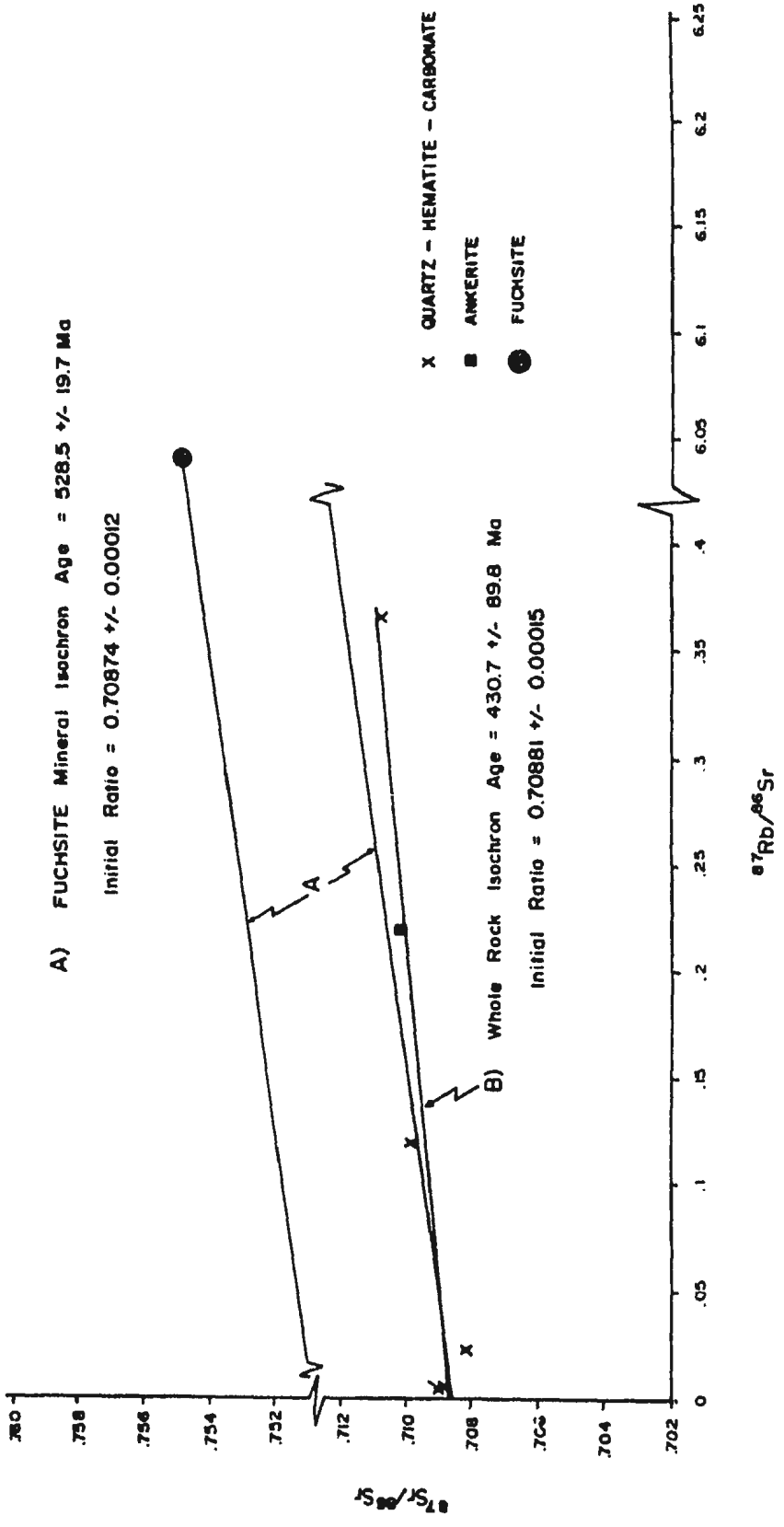


Figure 4.17. Rb/Sr isochron for whole rock and mineral samples from LPW-type mineralization in ultramafic rocks.

metamorphic or mineralizing process. In this case where altered rocks are examined, the Sr isotopic composition should reflect the composition of the fluid responsible for the alteration or mineralization. Sr isotopes have been used similarly by various authors such as Taylor and Fryer (1983b), Norman and Landis (1983), Bolke and Kistler (1986), Kimball and Gerlach (1986) and Kerrich et. al., (1987).

Figure 4.18 is a plot of the range of Sr isotopic data for the samples analysed. Superimposed on this data are the Sr isotopic ranges for the most likely fluid sources. Primary igneous Sr obtained through interaction with the ultramafic rocks may be ruled out since mantle values at the time of ophiolite formation (490 ma) were much too low. Isotopic values for the Burlington Granodiorite and the Cape St. John Group - prior to isotopic resetting at 343 ma - were also much too low to have reacted with the fluid to contribute to the Sr values in the altered and mineralized samples. Three Sr sources that could contribute the Sr to the fluid are the isotopically reset Cape St. John Group at 343 +/- 15 ma, the Cape Brule Porphyry (possibly reset at 393 +/- 25 ma) and sea water at 490 ma.

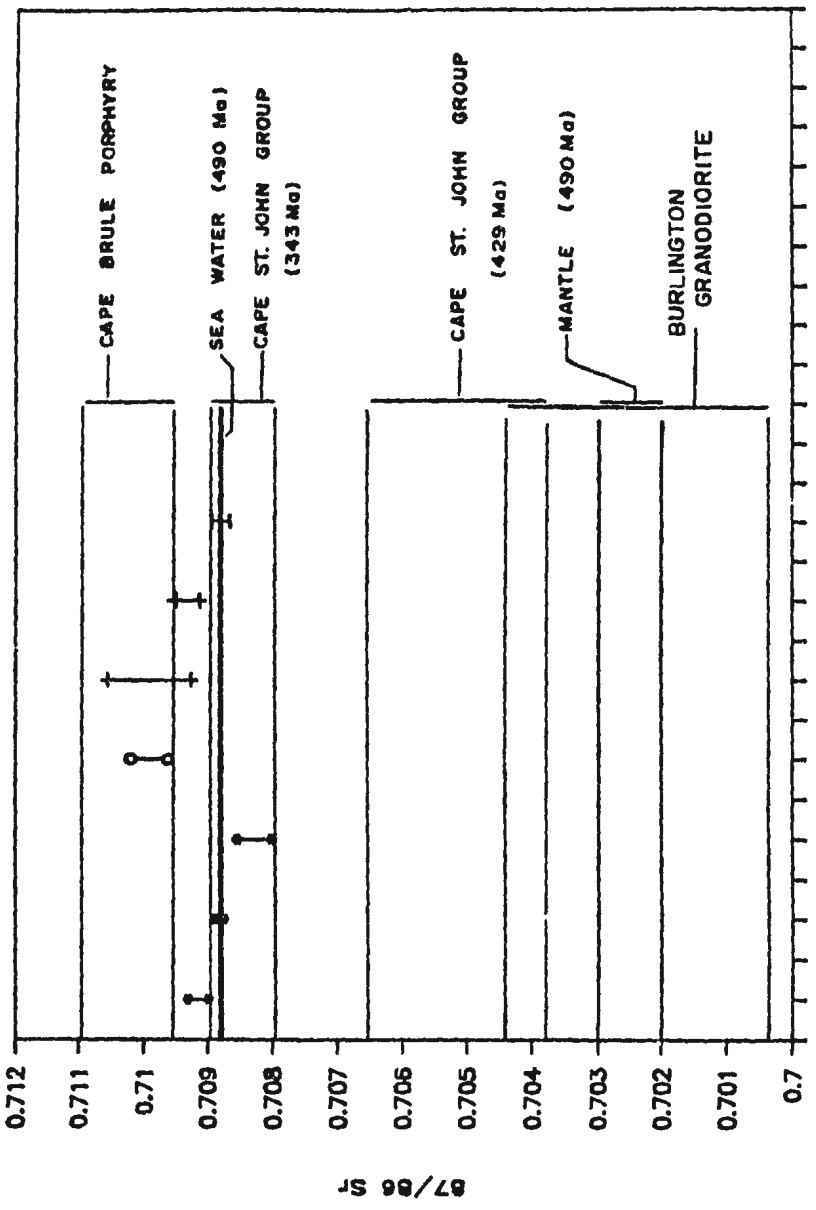


Figure 4.18. Sr isotopic composition of Rb-poor altered rocks compared to Sr isotopic compositions of nearby lithologies, Ordovician sea water and Ordovician mantle. (*) Qtz- hem.-carb., (o) talc-carb., (+) L-type veins, (-) initial ratio for whole rock qtz-hem.-carb. isochron. Sea water and mantle values from Faure (1986), other values from Pringle (1978).

## 4.7 Discussion:

Table 4.3 summarizes the geochemistry of the ultramafic rocks in terms of enrichments or depletions of specific elements in the alteration assemblages. Geochemical manifestations of alteration in the ultramafic rocks are cumulative as alteration progresses from fresh cumulate rocks through serpentine-magnesite and talc-magnesite. Alteration to the quartz-hematite-dolomite assemblage results in abrupt shifts in the geochemical behavior of various elements relative to the serpentine-magnesite and talc-magnesite. Despite the contrasts displayed between the quartz-hematite-dolomite and other ultramafic rocks, all the alteration may be related to the same hydrothermal system. The contrast in the geochemistry of the different alteration stages can be explained by changing physical-chemical conditions in the hydrothermal system.

The best regional scale indicators of gold mineralization are the carbonate alteration and coincident gold enrichment. The carbonate alteration is the most useful indicator since it can be identified easily in the field. Increased content of $SiO_2$, $K_2O$, CaO, Sr and MnO coupled with decreased MgO are only associated with LPW-type gold mineralization. The $SiO_2$ and $K_2O$ metasomatism is evident in the field.

Table 4.3. Behaviour of various elements during the observed stages of alteration.

## Enrichments

| | Serpentine Magnesite | Talc Magnesite | Qtz-Hematite Dolomite |
|---|---|---|---|
| Weak | Sb | Si Te | Cd Sn Zr |
| Moderate | P | Ba Cu Pb P Sb Th | P Sb |
| Strong | As | As Sn Ni | As Ba Ca K Mn Pb Sr Zn |

## Depletions

| | | | |
|---|---|---|---|
| Weak | Zn | Cr Mn Sc Zn Zr Cd V | Cr Li Na |
| Moderate | | Fe | Fe Sc V |
| Strong | | | Cu Mg |

## Immobile

| | | | |
|---|---|---|---|
| | Ca Cd Cu Ni K Li Mg Sc Si Sn Sr V Te Ti | Ca K Li Mg Na Sr Ti Y | Ti |

## No Clear Pattern

| | | | |
|---|---|---|---|
| | Ba Cs Pb Th U Y Mn Na Zr Fe | Cs U Co | Cd Cs Si Te Th U Y Co Ni |

Platinum group element mobility is indicated from the geochemical data. Increasing carbonate alteration has the effect to lower the Pt, Pd contents and increase the Ru, Ir contents of the ultramafic rocks. The ultimate destination of the Pt and Pd removed from the system is unknown but has implications for the formation of hydrothermal PGE deposits. Relatively high PGE values in the Long Pond East showing (Appendix I-4) may result from remobilization of PGE from the ultramafic rocks by hydrothermal processes.

The geochemical data present several clues to the source of the fluid responsible for the alteration and mineralization and a possible source rock for the gold.

1) The REE data from all ultramafic rocks are characterized by abundances equal to or less than chondrite values and REE patterns in the talc-magnesite and associated mineralization are nearly identical to those from fresh ultramafic samples. A fluid source that had interacted with rocks other than ultramafic rocks would be expected to have much higher abundances of REE than that observed.

2) Patterns in the quartz-hematite-dolomite and associated mineralization are similar to one from Mid-Atlantic-Ridge rodingite (Kerrich and Fryer, 1979). Patterns similar to rodingite may be indirect evidence of an ultramafic influence on the fluid since rodingite is formed by metasomatism from ultramafic-derived fluids.

3) Negative Ce anomalies are present in the REE from all of the ultramafic rocks as would be expected if seawater formed a component of the hydrothermal fluid (Haskin and Paster, 1979).

4) Strontium isotopic data indicate an $^{87}Sr/^{86}Sr$ composition for the fluid which compares well with seawater at 490 ma, the time of ophiolite formation.

The data implicate sea water as the dominant fluid in the hydrothermal system and an ultramafic source rock for the gold. Hydration of ultramafic rocks during ophiolite formation, through sea floor hydrothermal activity, would create a suitable fluid reservoir. Subsequent dehydration of the ultramafic rocks during regional metamorphism could initiate a hydrothermal system capable of causing the type of alteration and mineralization observed.

There is an apparent contradiction between REE evidence that indicates the mineralizing fluids are ultramafic-derived, and gold values below detection in the presumed fresh ultramafic "source" rocks. Only five samples of fresh ultramafic rocks were analysed and it is expected that with a larger sample group, the average gold content of these rocks would be closer to the 3-5 ppb value published by Buisson and LeBlanc (1987) for similar rocks. The pervasive alteration of the ultramafic rocks indicates nearly 100% access to the rock by the fluid. Under these

conditions, a rock with 3-5 ppb gold could act as an effective source rock.

# CHAPTER 5

# SUMMARY AND GENETIC MODEL

## 5.1 Summary:

### 5.1.1 Geology:

The study area is centered on the contact of the Ordovician Betts Cove Ophiolite with the Silurian Cape St. John Group and consanguineous Cape Brule Porphyry. Ultramafic rocks at the contact occur as a thin, fault-bounded sliver along the contact length. The Silurian also unconformably overlies the ultramafic rocks locally. The gabbroic and sheeted dyke units of the ophiolite are missing in most places and the pillow lava is in fault contact with the ultramafic rocks. The Cape St. John Group consists of subaerial volcanic and intermixed sedimentary rocks. A distinctive conglomerate unit is spatially related to the fault bounded ultramafic unit and contains abundant clasts of altered ultramafic detritus.

The effects of two metamorphic events are recognized in the different lithologies of the area. Spilitic assemblages in the ophiolitic rocks result from sea floor hydrothermal processes active during ocean spreading and ophiolite formation. The second event was metasomatic and

locally affected all rock types. Pervasive carbonate and quartz-carbonate alteration of ultramafic rocks and quartz-sericite-hematite alteration of shear zones within the Cape St. John Group result from the metasomatic event.

Four types of structures are recognized as important for gold mineralization. The fault zone containing the altered ultramafic rocks controls deformation, alteration and mineralization. Three sets of auxilliary structures to the ultramafic bounding fault (UBF) are defined. These auxilliary structures are also important loci of alteration and mineralization.

5.1.2 Alteration and Mineralization:

Cumulate ultramafic rocks occur in the southwest. Some serpentinization is ubiquitous in these rocks. Shearing and coincident carbonate alteration affects the cumulate rocks progressively toward the northeast. Serpentine-magnesite assemblages are formed at the onset of $CO_2$ metasomatism. With increased shearing and higher fluid $CO_2$ content, talc-magnesite becomes the dominant assemblage. Superimposed on the talc-magnesite alteration locally, is a distinctive quartz-hematite-dolomite assemblage. Fluids responsible for the alteration were oxidizing as evidenced by the ubiquitous presence of specular hematite.

Alteration is also related to shear zones in the Cape St. John Group near the fault contact with the ultramafic rocks. The shear zones contain mylonite which is altered to quartz, sericite, hematite assemblages.

Two types of mineralization are present. Listwaenite-type mineralization is hosted by talc-magnesite schist and contains native gold in quartz, magnesite, sulphide veins. Long Pond West-type mineralization is hosted by quartz-hematite-dolomite altered ultramafic rocks and the altered shear zones within the Cape St. John Group. Native gold, minor sulphide, magnetite and specular hematite, occur within quartz-sericite-fuchsite veins.

### 5.1.3 Geochemistry:

Geochemical studies of the ultramafic rocks are effective for determining elemental changes related to mineralization, due to their predictable chemistry. The following sections 5.1.3 a-c refer to the chemistry of the ultramafic rocks only.

#### 5.1.3a Major and Trace Elements:

Few chemical signatures specific to the mineralization can be identified from the major and trace element chemistry. Listwaenite-type (L-type) mineralization

displays obvious enrichments of Cu, S and Bi relative to the host talc-magnesite. Except for Bi, these enrichments are obvious from the vein mineralogy. Long Pond West-type (LPW-type) mineralization is characterized by Si, K, and Rb enrichments relative to the host quartz-hematite-dolomite altered rocks. These chemical signatures are manifest in the mineralogy as well.

### 5.1.3b Rare Earth Elements:

Low overall abundances of REE in the veins and vein-REE patterns which mimic those in unaltered ultramafic rocks, indicate an ultramafic source for the mineralizing fluids.

Normalized patterns in the alteration zone associated with Long Pond West-type mineralization match with a pattern from a jasperoid clast within a conglomerate unit in the Cape St. John Group. The conglomerate unit is spatially associated with the ultramafic bounding faults and subsidiary lineaments. The conglomerates are locally deformed and contain LPW-type veins. The field evidence above and confirmation from REE geochemistry that the clasts are related to the altered ultramafic rocks constrains the age of the alteration and mineralization to the waning stages of the last deformation event.

### 5.1.3c Precious Metals:

Gold geochemistry illustrates the pronounced association between $CO_2$ metasomatism and gold enrichment. This correlation between $CO_2$ metasomatism and gold enrichment demonstrates the importance of large-scale carbonate alteration as an indicator of gold mineralization potential.

Platinum group element data demonstrate consistent fractionations within the group due to hydrothermal processes. In all samples affected by $CO_2$ metasomatism, Pt and Pd are depleted while Ru and Ir are enriched; Rh remains immobile. Platinum group element values in the mineralized veins are low, and comparable to the host rock abundances.

### 5.1.3d Rb/Sr Isotope Systematics:

Whole rock and mineral Rb/Sr isochron dating was attempted on the alteration and mineralization at Long Pond West. The isochrons were not concordant and the dates obtained are of little value.

Samples of Rb-poor rocks (less than 4 ppm by XRF analysis ) were used for Sr isotope studies aimed at defining a source of the mineralizing fluid. The Sr

isotope data for such samples cluster closely around the value of sea water $Sr^{87/86}$ at 490 ma. Values are also similar to the range defined by the Cape Brule Porphyry and Cape St. John Group $Sr^{87/86}$, reset by the Acadian Orogenic event (Pringle, 1978).

## 5.2 Comparison to Known Gold Camps:

The mineralization in the study area resembles many gold environments in that there is a large associated carbonate alteration zone (Boyle, 1979; MacGeehan and Hodgson, 1982), gold occurs in quartz-carbonate vein lodes within structurally controlled shear zones (Thomson, 1948; MacGeehan and Hodgson, 1982; Hodgson 1987), and ultramafic rocks are associated (MacGeehan and Hodgson, 1982; Roberts, 1987; Phillips, 1986; Landefield and Silberman, 1986). The examples described here compare best to gold mineralization in the California Mother Lode district (Knopf,1929; Landefield and Silberman, 1986) and ophiolites of Morroco and Saudi Arabia (Buisson and LeBlanc, 1985, 1986, 1987). These examples occur in association with ophiolites which are confined to large scale structural zones.

## 5.3 Genetic Model:

Any model proposed to explain the occurrence and generation of the gold mineralization in the study area

must address several questions.

1) What are the fluid characteristics?

2) What are the chief controls on mineralization?

ie. Is it lithologic?

Is it structural?

What is the gold transport mechanism?

How was the gold precipitated?

3) What is the fluid source and how was the fluid generated?

4) What is the age of mineralization?

Each is dealt with in turn below.

5.3.1 Fluid Characteristics:

The presence of iron oxides mantling sulphide in L-type and minor sulphides with ubiquitous specular hematite in LPW-type mineralization indicates that the fluid evolved from reducing to oxidizing in both cases. Barton et. al. (1977) use the oxide, sulphide and iron-rich chlorite assemblage to determine the range of fluid $aO_2$ and pH. This assemblage is present in most LPW-type veins. With referrence to Figure 5.1, the possible range of $aO_2$ and pH with this mineral assemblage is narrowly constrained. The pH would be in the range of 4.5 - 5.5 and Log $aO_2$ would be -34 to -35. The L-type mineralization is less easily constrained based on mineralogy alone. The trend from reduced to oxidized fluids manifest by all vein

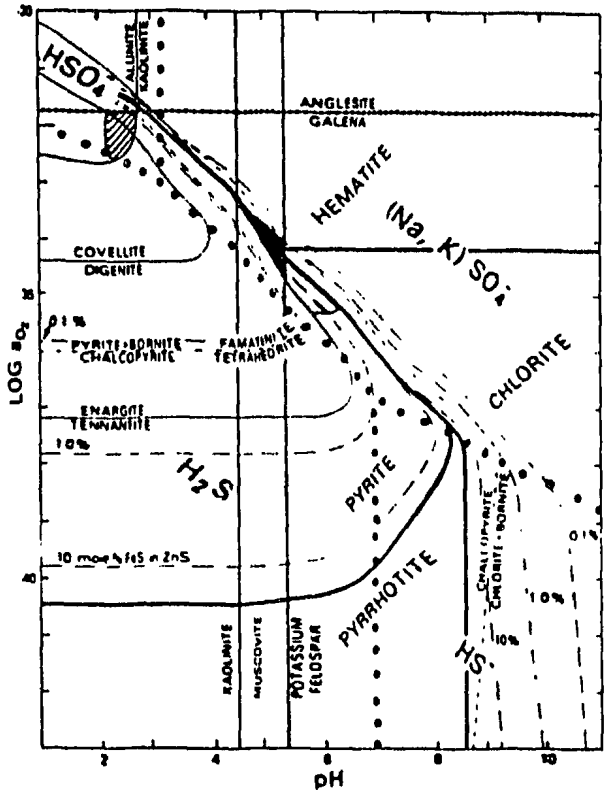


Figure 5.1. Log $aO_2$-pH diagram at 250°C, [S= 0.02 molal, salinity = 1, Na/K = 9 (from Heald et. al, 1987 after Barton et. al 1977). LPW-type mineralization contains the principle assemblage pyrite-chalcopyrite-galena, hematite, muscovite and Fe-chlorite. Fluid $aO_2$ and pH are thus constrained within the shaded area. Thick-solid lines separate dominant mineral species, pyrite, pyrrhotite, hematite and chlorite. Dots separate fields of dominant ionic species.

assemblages is interpreted to result from progressive carbonatization of the ultramafic rocks. Eckstrand (1975) demonstrates the reduced to oxidized fluid evolution which takes place during carbonate alteration of serpentinized ultramafic rocks through reactions like that shown below.

$$\underset{\text{serpentine}}{18Mg_3Si_2O_5(OH)_4} + \underset{\text{magnetite}}{Fe_3O_4} + 30CO_2 =$$

$$9MgSi_4O_{10}(OH)_2 + 30(Mg_{0.9}Fe_{0.1})CO_3 + 27H_2O + 1/2O_2$$

talc — magnesite

The oxygen that is released when the Fe in magnetite reacts to form magnesite causes an increase in the fluid $fO_2$ proportional to the degree of carbonatization.

The fluid responsible for the mineralization and alteration in both types of mineralization was obviously a $CO_2$ - $H_2O$ mixture as evidenced by the extensive development of carbonate mineral assemblages.

$Ca^{2+}$, Sr, Rb and $K_2O$ were major cations contained within the LPW-type mineralizing fluid and are manifest in the dolomite and fuchsite-rich alteration zone.

Sr isotopic compositions of the vein fluids and Ordovician sea water are similar (see Figure 4.16).

### 5.3.2 Controls on Mineralization:

All known mineralization occurs in vein lode or stockwork form within shear zones. Vein formation usually post dates deformation, but in some cases veins are affected by the deformation. The host lithologies are extremely variable and probably have little or no control on the location of mineralization, except to the extent that competency differences may allow for preferential shear zone development and vein formation in certain lithologies.

The implication of seawater in the mineralizing process leads to the conclusion that $Cl^-$ was a major anionic species available for complexing and transporting gold. Henley (1973) provides experimental data pertaining to gold solubility as chloride complexes. His data demonstrate the amenability of $Cl^-$ to complex gold in oxidized fluids. Thio-sulphide complexing of gold may be a factor, especially in the sulphide-rich listwaenite veins (Seward, 1973; 1982).

A schematic model for gold precipitation is presented in Figure 5.2. Gold-bearing $H_2O$-$CO_2$ fluid ascending within faults and shear zones causes extensive carbonate alteration and lesser amounts of silicification. Because of the oxidized character of the fluid involved,

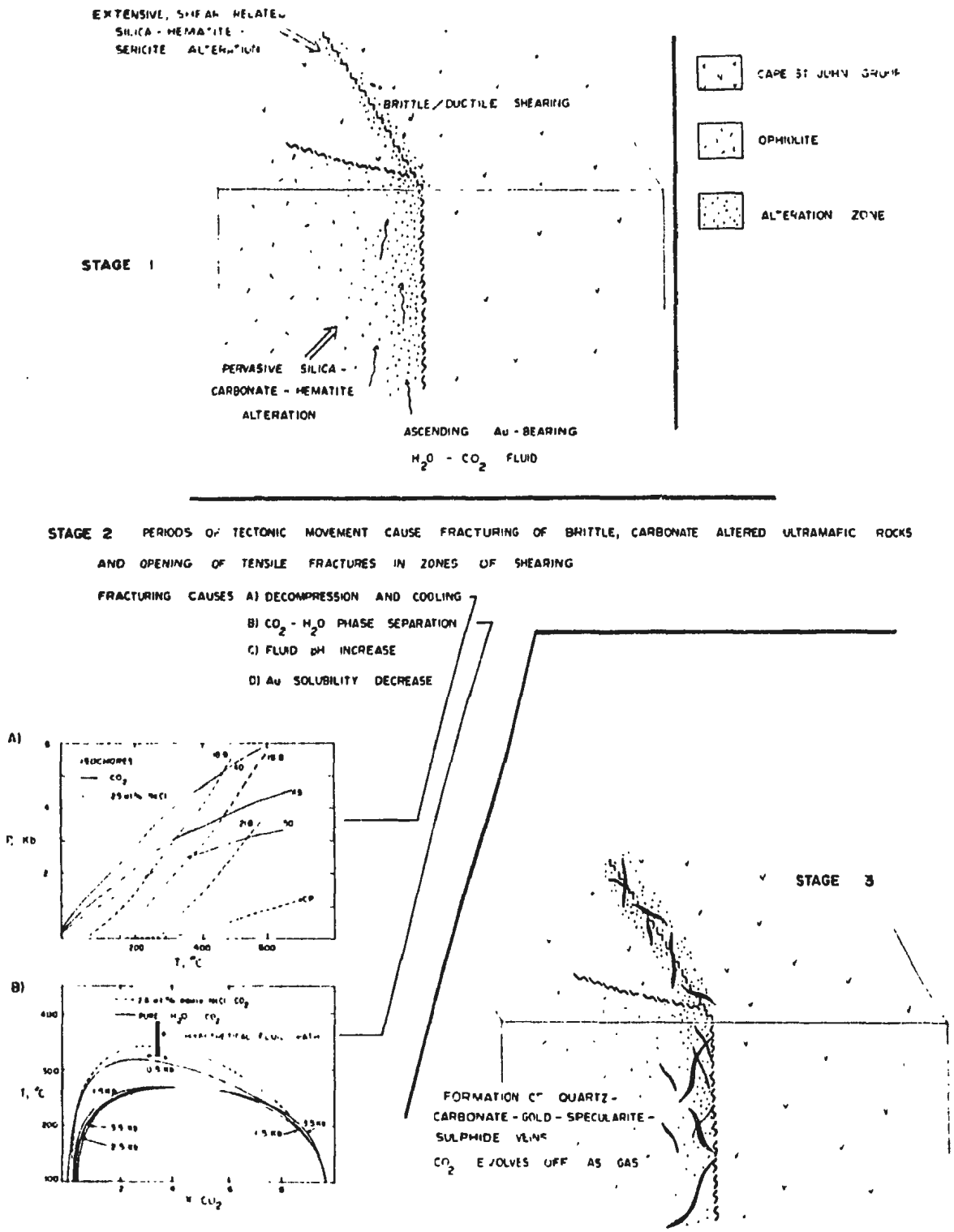


Figure 5.2. Schematic model proposed for alteration and mechanism of gold deposition. Isochore and $CO_2$-$H_2O$ solvus data from Crawford, (1981).

hematization is common as well. The fluid migration occurs coincident with some degree of deformation, resulting in development of brittle fractures in the competent, carbonate altered ultramafic rocks, and tensile fractures in the ductile shear zones. Fracturing causes decompression, cooling and $CO_2$-$H_2O$ phase separation, with resulting pH increase. Cooling is a process implicated in gold deposition for $Cl^-$ or $HS^-$ complexed gold (Henley, 1973; Seward, 1973, 1982). Increase in pH would cause chloride complexed gold, only, to precipitate (Seward, 1982).

### 5.3.3 Fluid Source and Mobilization Mechanism:

Evidence from Sr isotopes and REE indicate Ordovician sea water was the dominant fluid involved in the alteration and mineralization. The sea water was trapped as connate water in hydrated mineral phases during sea floor hydrothermal activity and released by metamorphic dehydration reactions during Acadian orogenesis.

### 5.3.4 Age of Mineralization:

The appearance of quartz-hematite-dolomite altered clasts within the Cape St. John Group indicates a pre-Cape St. John Group age for the LPW-type mineralization. Since LPW-type mineralization also crosscuts the Cape St. John

Group between Red Cliff and Long Ponds, the evidence is conflicting. It is possible that there was more than one period of similar alteration and mineralization, however, a simpler explanation is favourable. Another alternative is that the alteration and mineralization event post dates the Cape St. John Group and the conglomerate unit formed along an active fault scarp; the fault acting to focus fluid migration.

A U/Pb zircon date from the base of the Cape St. John Group (430 ma; Coyle, pers. comm., 1988) provides a lower age limit for the mineralization. $^{40}Ar/^{39}Ar$ cooling dates on the eastern portion of the peninsula give ages clustering around 350 ma (Hibbard, 1983). This age is taken as the minimum age of mineralization.

The L-type veins are undeformed and therefore post date the major deformation event(s) is the area. The metallic mineral paragenesis in the L-type veins is the same but possibly less evolved than in the LPW-type veins. These similarities between the two vein types suggest that they are synchronous.

5.3.5 Geologic and Metallogenic Development:

Figure 5.3a-d is a schematic representation of the geologic and metallogenic development envisaged for the

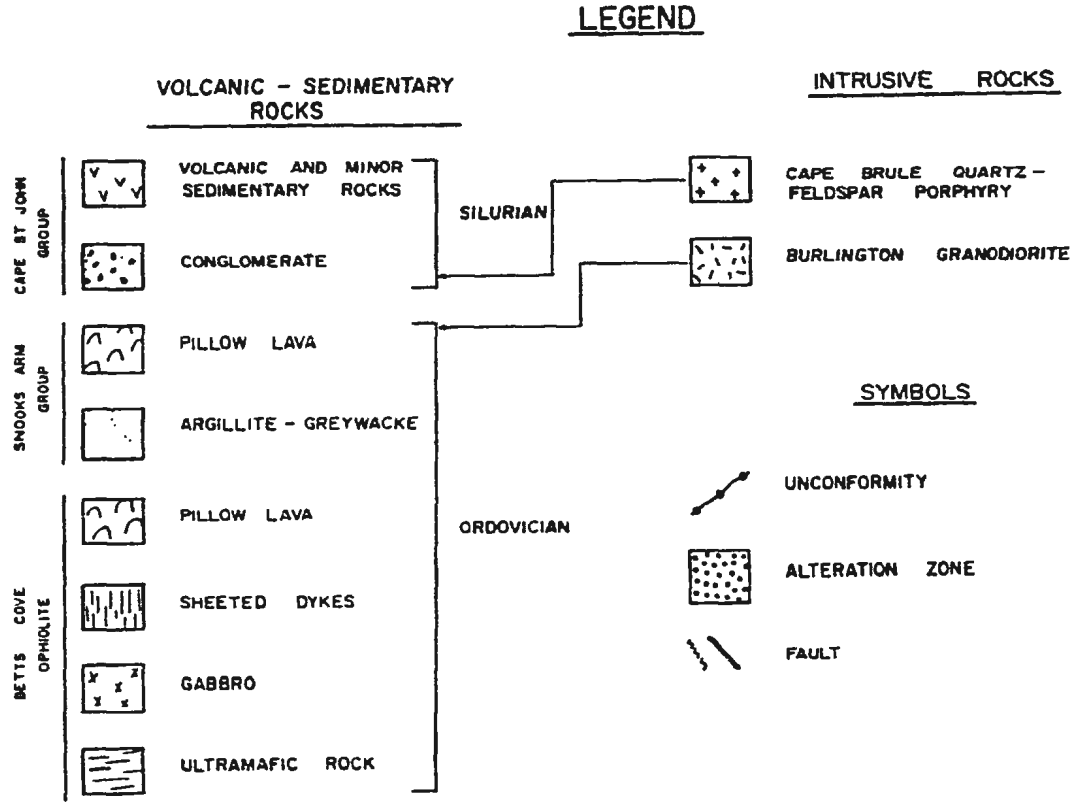
LEGEND
VOLCANIC - SEDIMENTARY ROCKS
INTRUSIVE ROCKS
CAPE ST JOHN GROUP
VOLCANIC AND MINOR SEDIMENTARY ROCKS
CONGLOMERATE
SNOOKS ARM GROUP
PILLOW LAVA
ARGILLITE - GREYWACKE
BETTS COVE OPHIOLITE
PILLOW LAVA
SHEETED DYKES
GABBRO
ULTRAMAFIC ROCK
SILURIAN
ORDOVICIAN
CAPE BRULE QUARTZ - FELDSPAR PORPHYRY
BURLINGTON GRANODIORITE
SYMBOLS
UNCONFORMITY
ALTERATION ZONE
FAULT

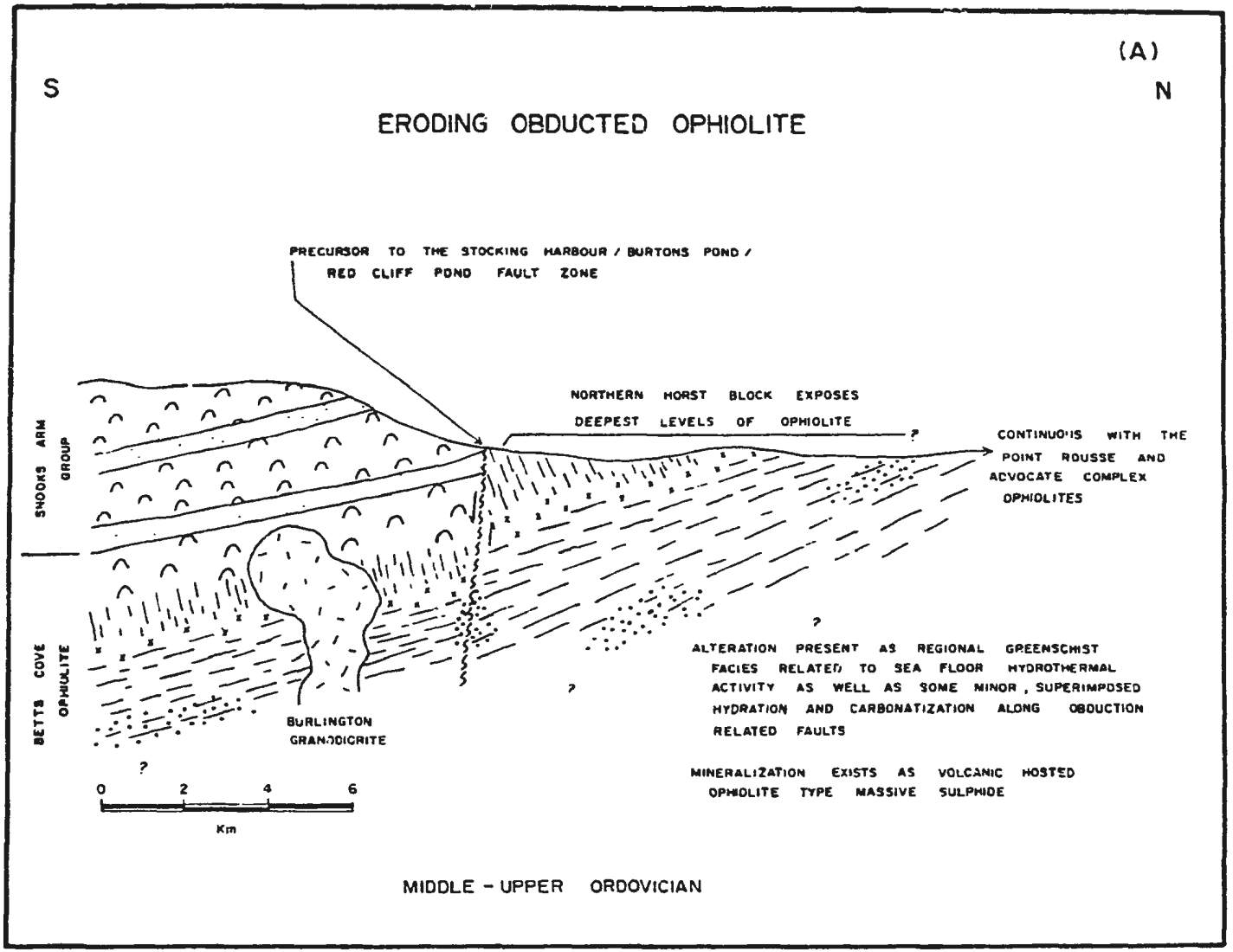
(A)
S
N
ERODING OBDUCTED OPHIOLITE
PRECURSOR TO THE STOCKING HARBOUR / BURTONS POND / RED CLIFF POND FAULT ZONE
NORTHERN HORST BLOCK EXPOSES DEEPEST LEVELS OF OPHIOLITE
?
CONTINUOUS WITH THE POINT ROUSSE AND ADVOCATE COMPLEX OPHIOLITES
SNOOKS ARM GROUP
BETTS COVE OPHIOLITE
BURLINGTON GRANODIORITE
?
?
?
ALTERATION PRESENT AS REGIONAL GREENSCHIST FACIES RELATED TO SEA FLOOR HYDROTHERMAL ACTIVITY AS WELL AS SOME MINOR, SUPERIMPOSED HYDRATION AND CARBONATIZATION ALONG OBDUCTION RELATED FAULTS
MINERALIZATION EXISTS AS VOLCANIC HOSTED OPHIOLITE TYPE MASSIVE SULPHIDE
0 2 4 6
Km
MIDDLE - UPPER ORDOVICIAN

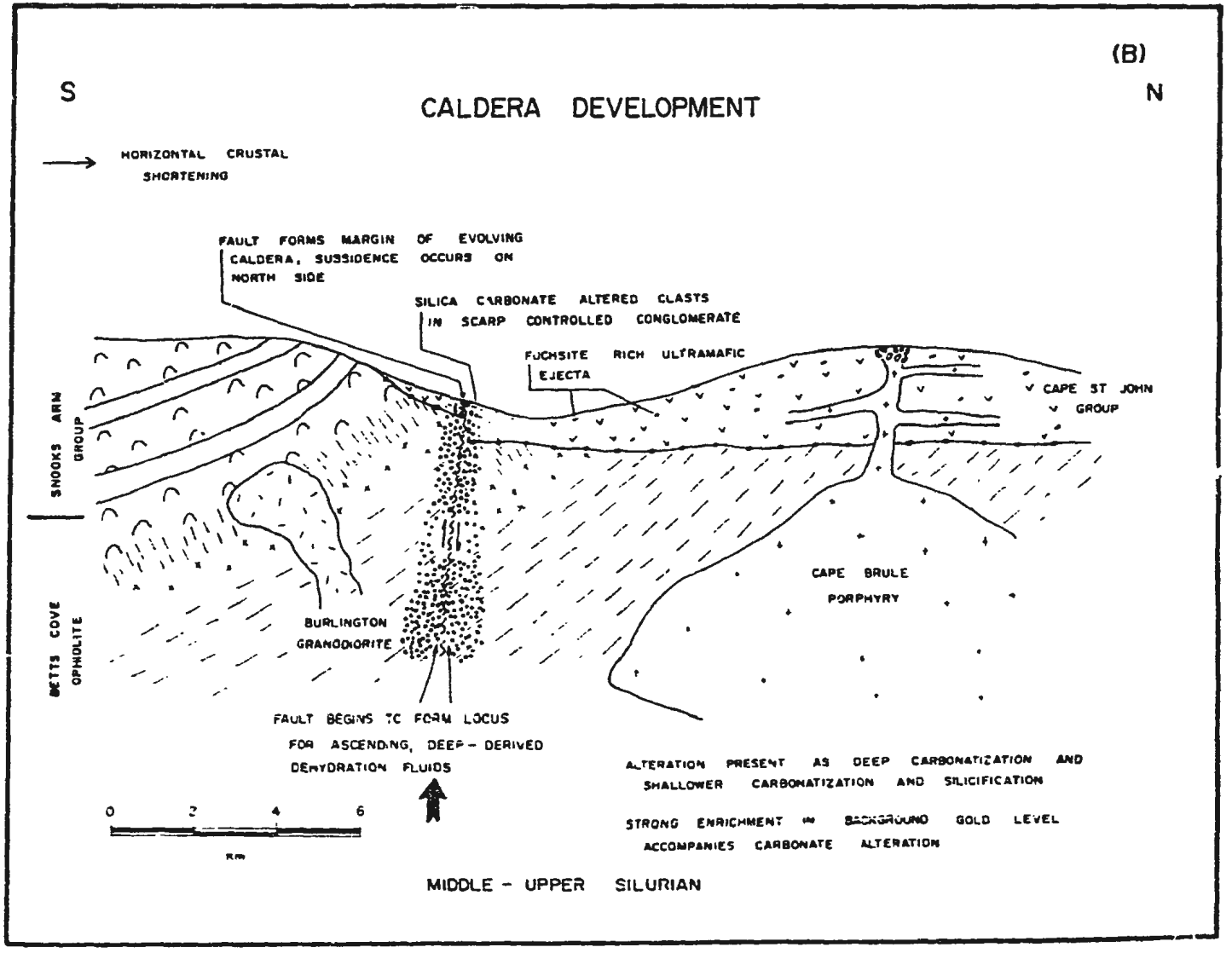
(B)
S
N
CALDERA DEVELOPMENT
HORIZONTAL CRUSTAL SHORTENING
FAULT FORMS MARGIN OF EVOLVING CALDERA, SUBSIDENCE OCCURS ON NORTH SIDE
SILICA CARBONATE ALTERED CLASTS IN SCARP CONTROLLED CONGLOMERATE
FUCHSITE RICH ULTRAMAFIC EJECTA
CAPE ST JOHN GROUP
SNOOKS ARM GROUP
BETTS COVE OPHOLITE
BURLINGTON GRANODIORITE
CAPE BRULE PORPHYRY
FAULT BEGINS TO FORM LOCUS FOR ASCENDING, DEEP-DERIVED DEHYDRATION FLUIDS
0 2 4 6
km
ALTERATION PRESENT AS DEEP CARBONATIZATION AND SHALLOWER CARBONATIZATION AND SILICIFICATION
STRONG ENRICHMENT IN BACKGROUND GOLD LEVEL ACCOMPANIES CARBONATE ALTERATION
MIDDLE - UPPER SILURIAN

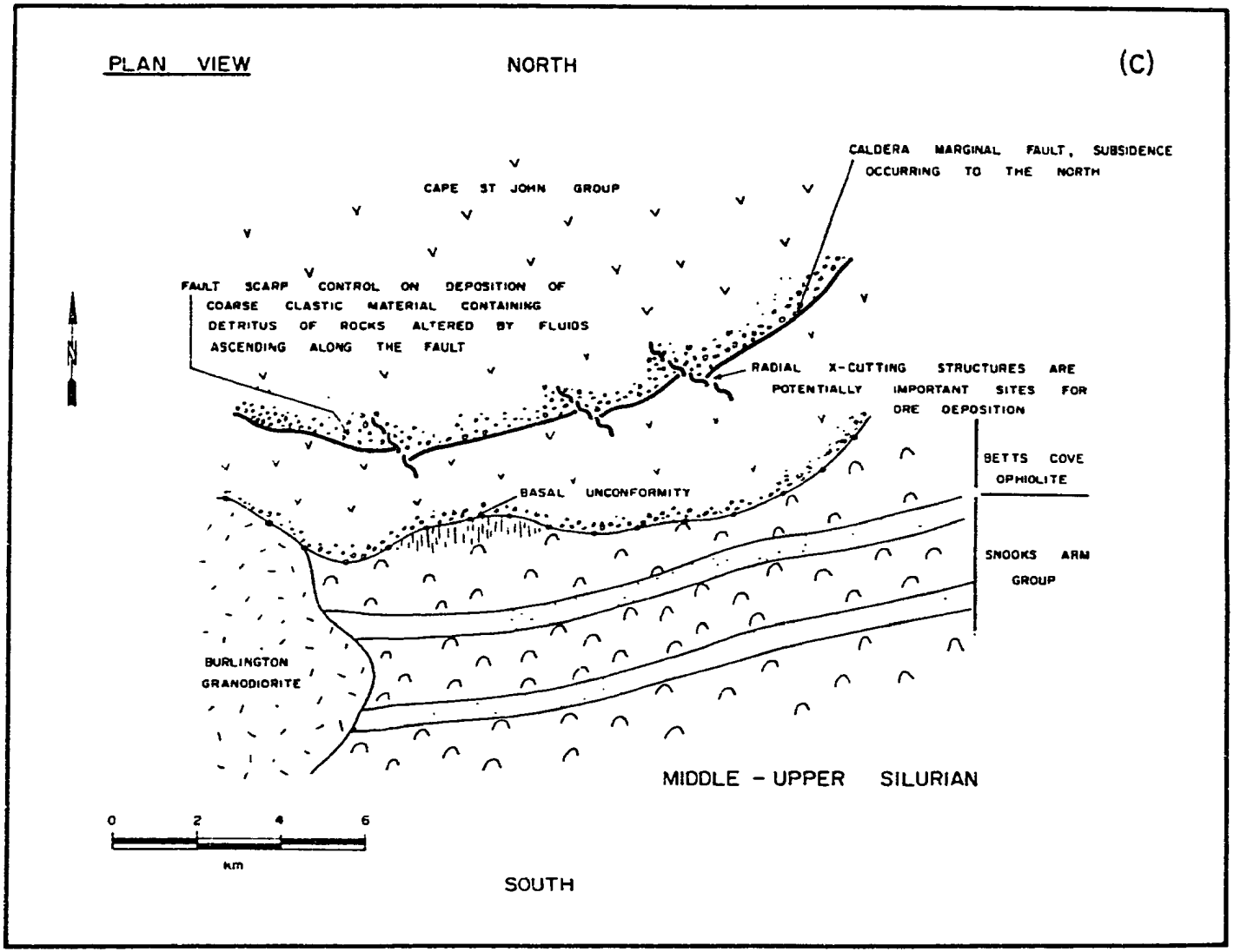
PLAN VIEW
NORTH
(C)
CALDERA MARGINAL FAULT, SUBSIDENCE OCCURRING TO THE NORTH
CAPE ST JOHN GROUP
FAULT SCARP CONTROL ON DEPOSITION OF COARSE CLASTIC MATERIAL CONTAINING DETRITUS OF ROCKS ALTERED BY FLUIDS ASCENDING ALONG THE FAULT
RADIAL X-CUTTING STRUCTURES ARE POTENTIALLY IMPORTANT SITES FOR ORE DEPOSITION
BETTS COVE OPHIOLITE
BASAL UNCONFORMITY
SNOOKS ARM GROUP
BURLINGTON GRANODIORITE
MIDDLE - UPPER SILURIAN
0 2 4 6
km
SOUTH

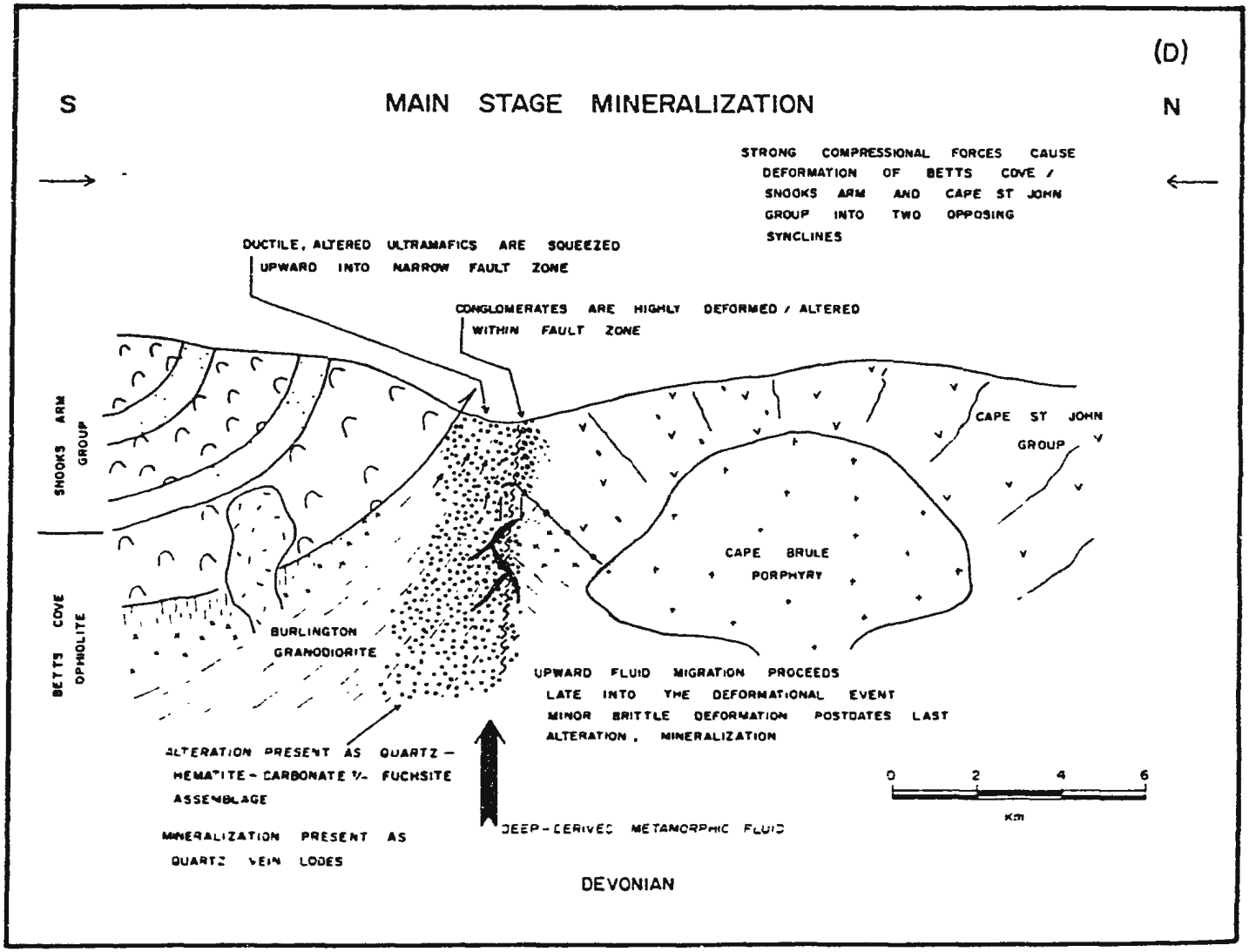
(D)
S
MAIN STAGE MINERALIZATION
N
STRONG COMPRESSIONAL FORCES CAUSE DEFORMATION OF BETTS COVE / SNOOKS ARM AND CAPE ST JOHN GROUP INTO TWO OPPOSING SYNCLINES
DUCTILE, ALTERED ULTRAMAFICS ARE SQUEEZED UPWARD INTO NARROW FAULT ZONE
CONGLOMERATES ARE HIGHLY DEFORMED / ALTERED WITHIN FAULT ZONE
SNOOKS ARM GROUP
BETTS COVE OPHIOLITE
BURLINGTON GRANODIORITE
CAPE BRULE PORPHYRY
CAPE ST JOHN GROUP
UPWARD FLUID MIGRATION PROCEEDS LATE INTO THE DEFORMATIONAL EVENT
MINOR BRITTLE DEFORMATION POSTDATES LAST ALTERATION, MINERALIZATION
ALTERATION PRESENT AS QUARTZ - HEMATITE - CARBONATE +/- FUCHSITE ASSEMBLAGE
MINERALIZATION PRESENT AS QUARTZ VEIN LODES
DEEP-DERIVED METAMORPHIC FLUID
0 2 4 6
Km
DEVONIAN

study area. Figure 5.3a portrays an obducted ophiolite slab undergoing erosion. Minor carbonate alteration is shown along obduction-related faults, but the dominant alteration is that of regional greenschist grade metamorphism. A result of ocean floor hydrothermal activity. Mineralization is present as ophiolite-type massive sulphide deposits. Ophiolitic and island-arc sequences are widespread at this stage occurring in deep structural stacks, from a considerable distance onto the continental margin, well out into the present-day Dunnage Zone.

Figure 5.3b shows the onset of formation of the Cape St. John Group and intrusion of the sub-volcanic Cape Brule Porphyry. Caldera development is initiated and an active fault scarp, along which clastic sediments are deposited, occurs at the south margin of the caldera. This scarp may begin to form a locus for dehydration-derived fluids causing silica-carbonate alteration. Elevated gold contents occur in the carbonate altered rocks.

Figure 5.3c is a plan view representation of the geologic development which has transpired to the time of Figure 5.3b.

Figure 5.3d illustrates the proposed relationship between Acadian orogenesis, deformation in the lithologic

groups present, intense silica-carbonate alteration, formation of shear zone controlled fracture systems and gold mineralization. This stage is considered the principle time of mineralization. Some brittle deformational adjustments proceed after the main stage of mineralization.

The greenschist altered ophiolitic rocks represent a large reservoir of fluid which can be mobilized at this stage when compressional forces cause crustal thickening and the formation of a prograde metamorphic regime. Dehydration reactions at depth liberate potentially ore-forming connate fluids which migrate upward along pre-existing structures. The connate fluids are comprised mostly of seawater which was trapped in ophiolitic rocks during a previous seafloor hydrothermal event(s).

## 5.4 Regional Significance:

Gold mineralization similar to that in the Betts Cove Complex occurs in ophiolitic rocks elsewhere on the Baie Verte Peninsula, throughout Newfoundland and around the world. The model proposed here for mineralization in the Betts Cove Complex is not intended to be rigidly applied elsewhere. There are, however, several points that can be taken from the model and used during exploration for similar mineralization, or as guidelines for studies

similar to this.

1) Economic quantities of gold mineralization can only occur where suitable structures exist to tap large fluid sources at depth, and focus the fluids during ascent.

2) The often observed relationship between ophiolitic rocks and gold mineralization can be explained by a combination of two factors: A) the emplacement of ophiolites onto a continent requires the formation of large, complex structural systems, which are in turn a requirement for gold mineralization, and B) ophiolitic crust, hydrated and commonly mineralized through seafloor hydrothermal processes, provides a source for fluids and gold which is proximal to the structures.

3) Structural systems with a complex deformational history should have the greatest potential to host significant gold mineralization. The metamorphism and plutonism that commonly accompany deformation are the principal heat sources available to drive fluid convection.

4) Silica-carbonate alteration is an indicator of the hydrothermal systems capable of generating lode gold deposits. These alteration zones are commonly not gold-bearing but, where gold occurs in ophiolitic terranes, silica-carbonate alteration is almost always closely associated.

## 5.5 Outstanding Problems:

1) The source of the $CO_2$ in the fluid that was responsible for the large areas of carbonate alteration is uncertain. It is acknowledged that large amounts of $CO_2$ could not be derived through dehydration of ultramafic rocks. It is possible, however, that the carbonate alteration could have resulted from interaction with very large volumes of fluid with a small fraction of $CO_2$. Fluid inclusion data would be useful to determine the respective fractions of $CO_2$ and $H_2O$ in the mineralizing fluid.

2) The model presented here is based mainly on evidence from rare earth elements as tracers of the source rock and fluid composition. More data on the REE composition of the cumulate ultramafic rocks, Cape Brule Porphyry and volcanic rocks of the Betts Cove Complex and Cape St. John Group would be useful to supplement the conclusions.

3) The age of the mineralization might be better constrained by $^{40}Ar/^{39}Ar$ dating of sericite and fuchsite in the veins and alteration envelopes.

4) Some clues about the mobility of the platinum group metals in hydrothermal systems were obtained from this study. It is apparent that Pt and Pd have been depleted in the ultramafic rocks during carbonate alteration. The mechanisms of depletion, and the destination of the Pt and Pd, are questions that should be pursued by further studies.

# REFERENCES

Barton, P.B., Bethke, P.M., Roedder, E., 1977, Environment of ore deposition in the Creede Mining district, San Juan Mountains, Colorado, Part III, Progrees toward interpretation of the chemistry of the ore-forming fluid of the OH vein, Economic Geology, v. 72, p. 1-24

Bohlke, J.K., Kistler, R.W., 1986, Rb-Sr, K-Ar, and stable isotope evidence for the ages and sources of fluid components of gold-bearing quartz veins in the northern Sierra Nevada foothills metamorphic belt, California, Economic Geology, v. 81, p. 296-322.

Blackwood, R.F., 1982, Geology of the Gander Lake (2D/15) and Gander River (2E/2) area. Mineral Development Division, Department of Mines and Energy, Government of Newfoundland and Labrador, report 82-4, 56 p..

Boyle, R.W., 1979, The geochemistry of gold and its deposits, Geological Survey of Canada, Bulletin 280, 584 p..

Brugmann, G.E., Arndt, N.T., Hofmann, A.W., Tobschall, H.J., 1987, Noble metal abundances in komatiite suites from Alexo, Ontario, and Gorgona Island, Columbia, Geochimica et. Cosmochimica Acta, v. 51, p. 2159-2169.

Buisson, G., LeBlanc, M., 1985, Gold in carbonatized ultramafic rocks from ophiolite complexes, Economic Geology, v. 80, p. 2028-2029.

\- 1986, Gold-bearing Listwaenites (carbonatized ultramafic rocks) from ophiolite complexes, in Metallogeny of Basic and Ultrabasic Rocks, Gallagher, M.J., Ixer, R.A., Neary, C.R., Prichard, H.M. eds., proceedings of the conference "Metallogeny of Basic and Ultrabasic Rocks", held in Edinburgh, Scotland, p.121-132.

\- 1987, Gold in mantle peridotites from upper Proterozoic ophiolites in Arabia, Mali and Morocco, source unknown, 17 p.

Bursnall, J.T., DeWit, M.J., 1975, Timing and development of the orthotectonic zone in the Appalachian Orogen of northwest Newfoundland, Canadian Journal of Earth Science, v. 12, p. 1712-1722.

Cawood, P.A., Williams, H., 1988, Acadian basement thrusting, crustal delamination, and structural styles in and around the Humber Arm Allochthon, Western Newfoundland, Geology, v. 16, p. 370-373.

Chandler, F.W., Sullivan, R.W., Currie, K.L., 1987, The age of the Springdale Group, western Newfoundland, and correlative rocks-evidence for a LLandovery overlap assemblage in the Canadian Appalachians, Transactions of the Royal Society of Edinburgh: Earth Sciences, v. 78, p. 41-49.

Church, W.R., 1969, Metamorphic rocks of the Burlington Peninsula and adjoining areas of Newfoundland and their bearing on continental drift in the north Atlantic, in North Atlantic Geology and Continental Drift, Kay, M. ed., American Association of Petroleum Geologists, Memoir 12, p. 212-233.

Coish, R. A., Church, W.R., 1979, Igneous geochemistry of mafic rocks in the Betts Cove Ophiolite, Newfoundland, Contributions to Mineralogy and Petrology, Vol. 70, pages 29-39.

Coleman, R.G., 1977, Ophiolites, ancient oceanic lithosphere?, Springer-Verlag, New York, 229 p..

Colman-Sadd, S.P., 1982, Two stage continental collision and plate driving forces, Tectonophysics, v. 90, p. 263-282.

Colvine, A.C., Andrews, A.J., Cherry, M.E., Durocher, M.E., Fyon, M.E., Lavigne, M.J., MacDonald, A.J., Marmont, S., Poulsen, K.H., Springer, J.S., Troop, D.G., 1984, An integrated model for the origin of Archean lode gold deposits: Ontario Geological Survey, Open file report 5524, 99 p..

Coyle, M., Strong, D.F., 1986, The Springdale Caldera, Geological Association of Canada, Newfoundland Branch, Field trip guide October 17-19, 21 p..

Coyle, M., Strong, D.F., 1987, Geology of the Springdale group: a newly recognized epicontinental-type caldera in Newfoundland, Canadian Journal of Earth Sciences, v. 24, p. 1135-1148.

Crawford, M.L., 1981, Fluid inclusions in metamorphic rocks-low and medium grade, in Short Course in Fluid Inclusions: Applications to Petrology, Hollister, L.S., Crawford, M.L., eds., Mineralogical Association of Canada, Held at the annual meeting, Calgary, Alta. p. 157-181.

Crocket, J.H., MacRae, W.E., 1986, Platinum-group element distribution in komatiitic and tholeiitic volcanic rocks from Munro Township, Ontario, Economic Geology, v. 81, p. 1242-1251.

Dean, P.L., 1977, A report on the geology and metallogeny of the Notre Dame Bay area to accompany metallogenic maps 12H/1,8,9 and 2E/3,4,5,6,7,9,10,11 and 12, Newfoundland department of Mines and Energy, Mineral Development Division, report 77-10, 17 p..

Dean, P.L., 1978, The volcanic stratigraphy and metallogeny of Notre Dame Bay, Memorial University of Newfoundland, Geology Report 7, 205 pgs.

DeGrace, J.R., Kean, B.F., Hsu, E., Green, T., 1976, Geology of the Nippers Harbour map area (2E/13), Newfoundland, Department of Mines and Energy, Mineral Development Division, report 76-3, 73 p..

Dunning, G.R., Krogh, T.E., 1985, Geochronology of ophiolites of the Newfoundland Appalachians, Canadian Journal of Earth Science, v. 22, p. 1659-1670.

Eckstrand, O.R., 1975: The Dumont Serpentinite: a model for control of nickeliferous opaque mineral assemblages by alteration reactions in ultramafic rocks. Economic Geology, vol.70, pgs 183-201.

Elias, P., Strong, D.F., Paleozoic granitoid plutonism of southern Newfoundland: contrasts in timing, tectonic setting and level of emplacement, Transactions of the Royal Society of Edinburgh: Earth Sciences, v. 73, p. 43-57.

Faure, G., 1986, Principles of isotope geology, 2nd ed., John Wiley and Sons, Inc., 589 p..

Fitzpatrick, D.S., 1981, Geology and mineral potential of upper ophiolitic rocks near Mings Bight, Burlington Peninsula, Newfoundland, Unpublished B.Sc. thesis, Memorial University of Newfoundland, 90 pgs.

Frew, A.M., 1971, Petrographic and geochemical comparison of two gold mineralized zones, Mings Bight area, White Bay, Newfoundland, Unpublished B.Sc. thesis, Memorial University of Newfoundland, 35 p.

Fryer, B.J., Taylor, R.P., 1987, Rare earth element distributions in uraninites: implications for ore genesis, Chemical Geology, v. 63, p. 101-108.

Grant, T.A., 1986, The isochon diagram-a simple solution to Gresens' equation for metasomatic alteration, Economic Geology, v. 81, p. 1976-1982.

Goncharenko, A.I., 1970, Auriferous listwanites as a new type of mineralization in the northern part of the Kuznetsk Ala-Tai: Tomsk Politekh. Inst. Izv., v. 239, p. 110-113.

Graf, J.L., 1977, Rare earth elements as hydrothermal tracers during the formation of massive sulphide deposits in volcanic rocks, Economic Geology, v. 72, p. 527-548.

Hamlyn, P.R., Keays, R.R., Warrington, E. C., Crawford, A.J., Waldron, H.M., 1985, Precious metals in magnesian low-Ti lavas: implications for metallogenesis and sulphur saturation in primary magmas, Geochimica et. Cosmochimica Acta, v. 49, p. 1797-1811.

Haskin, L.A., Paster, T.P., 1979: Geochemistry and mineralogy of the rare earths, in Handbook on the Physics and Chemistry of the Rare Earths, Gscheidner, K.A., Eyring, L., eds., North Holland Publishing Co., pgs. 1-79.

Heald, P., Foley, N.K., Hayba, D.O., 1987, Comparative anatomy of volcanic-hosted epithermal deposits: acid-sulphate and adularia-sericite types, Economic Geology, v. 82, p. 1-26.

Henley, R.W., 1973, Solubility of gold in hydrothermal chloride solutions, Chemical Geology, v. 11, p. 73-87.

Hibbard, J., 1983, Geology of the Baie Verte Peninsula, Newfoundland, Department of Mines and Energy, Mineral Development Division, Government of Newfoundland and Labrador, Memoir 2, 279 p..

Hodgson, C.J., in press, The structure of shear-related, vein-type deposits: a review.

Hodgson, C.J., MacGeehan, P.J., 1982, Geological characteristics of gold deposits in the Superior Province of the Canadian Shield, CIMM spec. v. 24, p. 211-232.

Howley, J.P., 1918, Report for 1902: Geological exploration in the district of White Bay, in Reports of the Geological Survey from 1881-1909, by A. Murray and J.P. Howley, Geological Survey of Newfoundland, p. 484-501.

Jenner, G.A., Fryer, B.J., 1980, Geochemistry of the upper Snooks Arm basalts, Burlington Peninsula, Newfoundland: evidence against formation in an island arc, Canadian Journal of Earth Sciences, v. 17, p. 888-900.

Kean, B.F., 1977, Geological compilation of the Newfoundland central volcanic belt, 1:250,000

Kerrich, R., 1983, Geochemistry of gold deposits in the Abitibi greenstone belt, CIMM spec. pap. 27, 75 p.

Kerrich, R., Fryer, B.J., 1979, Archean precious-metal hydrothermal systems, Dome Mine, Abitibi greenstone belt. II. REE and oxygen isotope relations, Canadian Journal of Earth Sciences, v. 16, p. 440-458.

Kerrich, R., Fryer, B.J., King, R.W., Willmore, L.M., van Hees, E., 1987, Crustal outgassing and LILE enrichment in major lithosphere structures, Archean Abitibi greenstone belt: evidence on the source resevoir from strontium and carbon isotopes, Contributions to Mineralogy and Petrology, v. 97, p. 156-168.

Kimball, K.L., Gerlach, D.C., 1986, Sr isotopic constraints on hydrothermal alteration of ultramafic rocks in two oceanic fracture zones from the South Atlantic Ocean, Earth and Planetary Science Letters, v. 78, p. 177-188.

Knopf, A., 1929, The Mother Lode system of California: U.S. Geol. Sur. prof. pap. 157, 88p..

Kusmirski, R., Norman R.E., 1982, Geology between Tilt Cove and East Pond, east Burlington Peninsula, Licence numbers 1810-1812, 12241-12242, 1807, 12261, Newmont Exploration of Canada Ltd., 2E/13 434.

Landefield, L.A., Silberman, M.L., 198?, Geology and geochemistry of the Mother Lode belt, California compared with Archean lode gold deposits, in Bulk Mineable Precious Metal Deposits of the Western United States, Johnson, J.L., ed., Geological Society of Nevada, 1987 symposium, p. 213-222.

Lobochnikov, V.N., 1936, Ilchirsk and other serpentines and serpentinites: Tsentralnogo Geologo Razvedochnogo Inst. Trudy, No. 38, p. 24-56.

Marten, B.E., 1971, Stratigraphy of volcanic rocks in the Western Arm area of the central Newfoundland Appalachians, Geological Association of Canada, proceedings, v. 24, p. 73-84.

Martin, W., 1983, Once upon a mine: story of pre-Confederation mines on the island of Newfoundland, CIMM spec. vol. 26, 98 p..

McLennan, S.M., Taylor, S.R., 1979, Rare earth element mobility associated with uranium mineralization, Nature, v. 282, p. 247-250.

Michard, A., Albarede, F., 1986, The REE content of some hydrothermal fluids, Chemical Geology, v. 55, p. 51-60.

Mottl, M.J., 1983, Metabasalts, axial hot springs, and the structure of hydrothermal systems at mid-ocean ridges, Geological Society of America Bulletin, v. 94, p. 161-180. p. 1-24.

Murphy, J.B., Hynes, A.J., 1986: Contrasting secondary mobility of Ti, P, Zr, Nb and Y in two metabasaltic suites in the Appalachians. Canadian Journal of Earth Sciences, vol. 23, no. 8, pgs 1138-1144.

Neale, E.R.W., 1957, Ambiguous intrusive relationship of the Betts Cove - Tilt Cove serpentinite belt, Newfoundland, Geological Association of Canada, Proceedings, v. 9, p. 95-107.

Neale, E.R.W., Kennedy, M.J., 1967, Relationship of the Fleur de Lys group to younger groups of the Burlington Peninsula, Newfoundland, in Geology of the Atlantic Region, Neale, E.R.W. and Williams, H. eds., Geological Association of Canada, spec. pap. 4, p. 139-169.

Neale, E.R.W., Kean, B.F., Upadhyay, H.D., 1975, Post-ophiolite unconformity, Tilt Cove - Betts Cove area, Newfoundland, Canadian Journal of Earth Sciences, v. 12, p. 880-886.

Norman, D.I., Landis, G.P., 1983, Source of mineralization components in hydrothermal ore fluids as evidenced by $^{87}Sr/^{86}Sr$ and stable isotope data from the Pasto Bueno Deposit, Peru, Economic Geology, v. 78, p. 451-465

O'Laughlin, J.P.S., 1981, Geology of the Deer Lake Ophiolite Complex, Newfoundland, unpublished M.Sc. thesis, Acadia University, 151 p..

Phillips, G.N., 1986, Geology and alteration in the golden mile, Kalgoorlie, Economic Geology, v. 81, p. 779-808.

Pringle, J., 1978, Rb-Sr ages of silicic igneous rocks and deformation, Burlington Peninsula, Newfoundland, Canadian Journal of Earth Science, v. 15, p. 293-300.

Riccio, L.M., 1972, The Betts Cove ophiolite, Newfoundland, Unpublished M.Sc. thesis, University of Western Ontario, London, Ontario, 91 p..

Roberts, R.G., 1987, Ore deposit models #11. Archean lode gold deposits, Geoscience Canada, v. 14, No. 1, p.37-52.

Seward, T.M., 1973, Thio complexes of gold and the transport of gold in hydrothermal ore solutions,Geochimica et Cosmochimica Acta, v. 37, p. 379-399.

- 1982, The transport and deposition of gold in hydrothermal systems, in Gold '82: the geology, geochemistry and genesis of gold deposits, Foster, R.P. ed., Geological Society of Zimbabwe spec. pub. No. 1, p. 165-181

Snelgrove, A.K., 1931, Geology and ore deposits of the Betts Cove - Tilt Cove area, Notre Dame Bay, Newfoundland, CIMM Bulletin, v. 24, No. 4, 43 p..

- 1935, Geology of gold deposits of Newfoundland, Newfoundland Department of Natural Resources, Geological Section, Bulletin No. 2, 46 p.

Stockmal, G.S.,Colman Sadd,S.P., Keen, C.E., O'Brien, S.J., Quinlan, G., 1987, Collision along an irregular margin: a regional plate tectonic interpretation of the Canadian Appalachians, Canadian Journal of Earth Sciences, v. 24, p. 1098-1107.

Strong, D.F., 1977, Volcanic regimes of the Newfoundland Appalachians, Geological association of Canada, spec. paper 16, p. 61-90.

- 1980, Geology of the Long Pond - Tilt Cove - Beaver Cove Pond area, western Notre Dame Bay, Newfoundland, Unpublished confidential report for Newmont Exploration, 75 p..

- 1984a, Geological relationships of alteration and mineralization at Tilt Cove, Newfoundland, in Mineral Deposits of Newfoundland-A 1984 Perspective, CIMM Field Trip Guide, compiled by H. S. Swinden, Department of Mines and Energy, Mineral Development Division, Government of Newfoundland and Labrador, report 84-3, 203 p..

- 1984b, Rare earth elements in volcanic rocks of the Buchans area, Newfoundland, Canadian Journal of Earth Science, v. 21, p. 775-780.

Strong, D.F., Fryer, B.J., Kerrich, R., 1984, Genesis of the St. Lawrence Fluorospar Deposits as indicated by fluid inclusion, rare earth element, and isotopic data, Economic Geology, v. 79, p. 1142-1158.

Stumpfl, E.F., 1986, Distribution, transport and concentration of platinum group elements, in Metallogeny of Basic and Ultrabasic Rocks, Gallagher, M.J., Ixer, R.A., Neary, C.R., Prichard, H.M. eds., proceeding of the conference "Metallogeny of Basic and Ultrabasic Rocks" held in Edinburgh, Scotland, p.379-394.

Taylor, R.P., Fryer, B.J., 1982, Rare earth element geochemistry as an aid to interpreting hydrothermal ore deposits, in Metallization Associated With Acid Magmatism, Evans, A.M. ed., John Wiley and Sons Ltd., p. 357-365.

Taylor, R.P., Fryer, B.J., 1983a, Rare earth element lithogeochemistry of granitoid mineral deposits, CIMM Bulletin, December issue, p. 1-11.

Taylor, R.P., Fryer, B.J., 1983b, Strontium isotope geochemistry of the Santa Rita porphyry copper deposit, New Mexico, Economic Geology, v. 78, No. 1, p. 170-174.

Taylor, R.S., McLennan, S.M., 1985; The continental crust: its composition and evolution, Blackwell Scientific Publications, pg. 298.

Tuach, J., Dean, P.L., Swinden, H.S., O'Driscoll, C.F., Kean, B.F., Evans, D.T.W., 1988, Gold mineralization in Newfoundland: a 1988 review, Current Research, Department of Mines, Mineral Development Division, Government of Newfoundland and Labrador, p. 279-306.

Upadhyay, H.D., 1973, The Betts Cove ophiolite and related rocks of the Snooks Arm Group, Newfoundland, Unpublished Ph. D. thesis, Memorial University of Newfoundland, 224 p..

Watson, K. de P., 1947, Geology and mineral deposits of the Baie Verte-Mings Bight area, Newfoundland, Geological Survey of Newfoundland, Bulletin 21, 48 p..

Weir, R.H., Kerrick, D.M., Mineralogic, fluid inclusion, and stable isotope studies of several gold mines in the Mother Lode, Toulumne and Mariposa counties, California, Economic Geology, v. 82, p. 328-344.

Williams, H., 1969, Pre-Carboniferous development of Newfoundland Appalachians, in North Atlantic Geology and Continental Drift, Kay, M. ed., American Association of Petroleum Geologists, Memoir 12, p. 32-58.

Williams, H., St. Julien, P., 1982, The Baie Verte-Brompton Line: continent-ocean interface in the northern Appalachians, in Major Structural Zones and Faults of the Northern Appalachians, St. Julien, P., Beland, J. eds., Geological Association of Canada, spec. pap. No. 24, p. 177-207.

Williams, H., Hatcher, R.D., 1983, Appalachian suspect terranes, Geological Society of America, Memoir 158, p. 33-53.

Williams, H., Colman Sadd, S.P., Swinden, H.S., 1987, Tectonic-stratigraphic subdivisions of central Newfoundland, Geological Survey of Canada, paper 88-1A.

Wilton, D.H.C., 1985, REE and background Au/Ag evidence concerning the origin of hydrothermal fluids in the Cape Ray electrum deposits, southwestern Newfoundland, CIMM Bulletin, v. 78, p. 48-59.

# APPENDIX I

# GEOCHEMICAL DATA

## MAJOR ELEMENT DATA

A) ULTRAMAFIC ROCKS:

| Wt% | SiO2 | TiO2 | Al2O3 | Fe2O3t | MnO | MgO | CaO | Na2O | K2O | P2O5 | LOI | TOTAL |
|---|---|---|---|---|---|---|---|---|---|---|---|---|
| BC-1 | 41.6 | 0 | 0.76 | 9.23 | 0.14 | 36.5 | 0.82 | 0.07 | 0.01 | 0.01 | 10.94 | 100.08 |
| BC-2 | 50.2 | 0 | 3.04 | 6.43 | 0.13 | 24.25 | 11.72 | 0.08 | 0.01 | 0 | 4.21 | 100.07 |
| BC-3 | 37.8 | 0 | 0.58 | 10.76 | 0.14 | 38.95 | 0 | 0.01 | 0 | 0 | 11.25 | 99.49 |
| BC-4 | 38.2 | 0 | 0.64 | 9.23 | 0.07 | 39.3 | 0 | 0.01 | 0.01 | 0 | 12.21 | 99.67 |
| BC-5 | 44.3 | 0 | 1.79 | 9.37 | 0.17 | 30.45 | 5.14 | 0.05 | 0.01 | 0 | 8.02 | 99.3 |
| BC-6 | 40.8 | 0 | 0.38 | 6.77 | 0.1 | 40.5 | 0 | 0.01 | 0 | 0 | 11.8 | 100.36 |
| SA-2 | 46.6 | 0 | 0.83 | 5.77 | 0.1 | 25.65 | 6.14 | 0 | 0 | 0.01 | 14.64 | 99.74 |
| SA-4 | 35.9 | 0 | 0.57 | 5.9 | 0.06 | 33.55 | 0.44 | 0 | 0 | 0.03 | 22.3 | 98.75 |
| SA-5 | 33.8 | 0 | 0.34 | 5.72 | 0.06 | 34.3 | 0.24 | 0 | 0 | 0.02 | 25.44 | 99.92 |
| SA-6 | 31.4 | 0 | 0.45 | 5.77 | 0.07 | 37 | 0.72 | 0 | 0 | 0 | 24.99 | 100.4 |
| RCP-10 | 62.1 | 0 | 0.8 | 3.6 | 0.02 | 23.85 | 0 | 0.02 | 0.01 | 0 | 9.55 | 99.95 |
| RCP-17 | 45.1 | 0 | 0.94 | 8.78 | 0.04 | 31.65 | 0.04 | 0.01 | 0.01 | 0 | 14.21 | 100.78 |
| RCP-18 | 48.4 | 0 | 0.42 | 11.14 | 0.07 | 31.65 | 0.52 | 0.09 | 0 | 0.05 | 10.23 | 100.57 |
| TC-5 | 45.1 | 0 | 0.4 | 7.26 | 0.06 | 33.25 | 0.48 | 0 | 0 | 0.03 | 13.88 | 100.46 |
| 615-1 | 29.2 | 0 | 0.45 | 6.03 | 0.07 | 38.5 | 0.56 | 0.01 | 0 | 0.01 | 25.73 | 100.56 |
| 615-2 | 33.8 | 0 | 0.42 | 8.7 | 0.06 | 33.96 | 0.38 | 0.02 | 0 | 0.01 | 21.54 | 98.89 |
| 626-2 | 28.4 | 0 | 0.36 | 6.73 | 0.05 | 32.85 | 0.24 | 0.01 | 0 | 0 | 32.14 | 100.78 |
| 626-3 | 31.3 | 0 | 0.64 | 8.6 | 0.05 | 35.9 | 0.14 | 0.01 | 0 | 0 | 25.59 | 100.23 |
| 626-4 | 29.2 | 0 | 0.73 | 7.29 | 0.1 | 31.8 | 0.14 | 0.01 | 0 | 0 | 31.62 | 100.89 |
| 626-5 | 38 | 0 | 0.95 | 6.25 | 0.03 | 28.2 | 0.12 | 0.01 | 0 | 0 | 27.05 | 100.61 |
| TC-6 | 38 | 0 | 0.36 | 6.59 | 0.08 | 37 | 0.1 | 0 | 0 | 0.08 | 15.97 | 98.18 |
| TC-7 | 38.5 | 0 | 0.53 | 6.62 | 0.04 | 40.1 | 0.04 | 0 | 0 | 0.04 | 12.84 | 98.71 |
| 615-3 | 39.3 | 0 | 0.22 | 6.38 | 0.06 | 38.64 | 0.54 | 0.01 | 0 | 0 | 14.48 | 99.63 |
| 615-4 | 39.1 | 0 | 0.45 | 7.56 | 0.07 | 38.61 | 0.16 | 0.01 | 0 | 0 | 13.42 | 99.38 |
| TC-8 | 45.6 | 0 | 1.06 | 7.76 | 0.55 | 0.68 | 22.8 | 0.01 | 0.04 | 0.01 | 22.14 | 100.65 |
| TC-9 | 37.4 | 0 | 2.43 | 9.46 | 0.17 | 17.9 | 13.46 | 0 | 0.01 | 0.01 | 19.07 | 94.91 |
| TC-10 | 35.2 | 0 | 5.18 | 8.79 | 0.14 | 14.9 | 12.7 | 0 | 0.01 | 0.04 | 22.48 | 99.44 |
| TC-11 | 47.3 | 0 | 0.44 | 4.67 | 0.46 | 9 | 15.16 | 0.01 | 0.14 | 0.01 | 21.72 | 98.93 |
| 628-3 | 38.3 | 0 | 0.27 | 8.62 | 0.21 | 11.2 | 16.4 | 0.01 | 0 | 0 | 25.71 | 98.72 |
| 628-4 | 51.2 | 0 | 0.36 | 3.61 | 0.18 | 9.6 | 13.7 | 0.01 | 0.1 | 0.01 | 21.2 | 99.97 |
| 628-5 | 17.9 | 0 | 0.42 | 6.32 | 0.17 | 17.75 | 21.8 | 0.01 | 0 | 0 | 34.92 | 99.29 |
| 628-6 | 11.4 | 0 | 0.52 | 6.54 | 0.46 | 15.9 | 26.1 | 0.03 | 0.06 | 0 | 37.96 | 98.97 |
| TC-12 | 17.1 | 0 | 0.63 | 5.58 | 0.49 | 16.24 | 22.74 | 0 | 0 | 0 | 36.05 | 98.83 |

B) JASPER CLAST IN CAPE ST.JOHN GROUP CONGLOMERATE:

| | | | | | | | | | | | | |
|---|---|---|---|---|---|---|---|---|---|---|---|---|
| 729-1 | 94.5 | 0 | 0.51 | 3.57 | 0 | 0.09 | 0.02 | 0 | 0.1 | 0 | 0.21 | 99 |

C) VEIN CHEMISTRY:

| | | | | | | | | | | | | |
|---|---|---|---|---|---|---|---|---|---|---|---|---|
| V-1 | 22.3 | 0 | 0.15 | 4.84 | 0.35 | 34.15 | 0.18 | 0 | 0 | 0.01 | 35.56 | 97.54 |
| V-2 | 73.3 | 0 | 0.25 | 2.1 | 0.04 | 8.57 | 0.18 | 0 | 0 | 0 | 12.29 | 94.73 |
| 628-1 | 66.1 | 0 | 1.35 | 4.48 | 0.38 | 4.66 | 8.6 | 0.02 | 0.5 | 0 | 12.92 | 99.01 |

MAJOR ELEMENT DATA cont...

| Wt% | SiO2 | TiO2 | Al2O3 | Fe2O3t | MnO | MgO | CaO | Na2O | K2O | P2O5 | LOI | TOTAL |
|---|---|---|---|---|---|---|---|---|---|---|---|---|
| D) CAPE ST.JOHN GROUP: | | | | | | | | | | | | |
| RCP-1 | 72.2 | 0.28 | 12.9 | 5.6 | 0.14 | 0.34 | 0.04 | 2.61 | 3.12 | 0.05 | 1.52 | 98.8 |
| RCP-2 | 60.7 | 0 | 10.9 | 3.96 | 0.09 | 11.35 | 2.74 | 0.05 | 1.27 | 0.01 | 8.31 | 99.38 |
| RCP-3 | 58.8 | 0 | 8.95 | 2.68 | 0.11 | 5.27 | 7.38 | 0.08 | 3.07 | 0.01 | 12.82 | 99.17 |
| RCP-4 | 97.3 | 0 | 0.2 | 0.04 | 0 | 0.02 | 0 | 0.07 | 0.02 | 0 | 0.12 | 97.77 |
| RCP-5 | 36.5 | 0 | 2.82 | 5.04 | 0.18 | 10.67 | 18.6 | 0.05 | 0.63 | 0.01 | 26.09 | 98.59 |
| RCP-6 | 60.7 | 0.24 | 13.4 | 7.85 | 0.09 | 3.77 | 2.26 | 2.26 | 2.19 | 0.18 | 5.45 | 98.39 |
| RCP-7 | 80 | 0.04 | 7.09 | 7.29 | 0.03 | 0.71 | 0 | 0.06 | 1.7 | 0 | 1.47 | 98.39 |
| RCP-8 | 83.6 | 0.16 | 8.09 | 2.25 | 0 | 0.12 | 0 | 0.3 | 2.52 | 0.09 | 1.4 | 98.53 |
| RCP-9 | 83.4 | 0 | 6.36 | 3.01 | 0.02 | 1.76 | 0.4 | 0.05 | 1.73 | 0.05 | 1.75 | 98.53 |
| RCP-11 | 69.9 | 0 | 4 | 2.25 | 0 | 0.01 | 0.08 | 0.14 | 0.17 | 0.02 | 1.92 | 78.49 |
| RCP-12 | 74.6 | 0.04 | 3.45 | 0.95 | 0.01 | 0.01 | 0 | 0.1 | 0.21 | 0.03 | 1.69 | 81.09 |
| RCP-13 | 83.8 | 0.24 | 9.6 | 2.14 | 0.01 | 0.06 | 0 | 0.17 | 1.94 | 0.03 | 1.33 | 99.32 |
| RCP-14 | 85.1 | 0.16 | 8.7 | 0.82 | 0.01 | 0.13 | 0.02 | 0.18 | 2.49 | 0.02 | 1.31 | 98.94 |

## TRACE ELEMENT DATA

A) ULTRAMAFIC ROCKS:

| PPM | Cs | Rb | Ba | Sr | Tl | Li | Th | U | *Zr | *Y | Bi | W | Mo |
|---|---|---|---|---|---|---|---|---|---|---|---|---|---|
| BC-1 | 0.4 | 0.5 | 3.7 | 5.4 | 0.1 | 4.9 | | 0.2 | 6.0 | | | | |
| BC-2 | 0.1 | 0.4 | 6.9 | 5.8 | | 20.9 | 0.1 | 0.2 | 6.0 | | | 4.6 | |
| BC-3 | 0.1 | 0.2 | 2.9 | 1.8 | 0.1 | 1.5 | | 0.4 | 6.0 | | | 2.9 | |
| BC-4 | | 0.2 | 3.2 | 2.0 | | | | 0.2 | 6.0 | | | 2.5 | |
| BC-5 | 0.9 | 1.2 | 10.7 | 5.9 | 0.1 | 18.8 | 0.1 | 0.2 | 7.0 | | 0.1 | 8.6 | |
| BC-6 | | 0.1 | 2.2 | | | | | 0.3 | 5.0 | | | | 4.9 |
| SA-2 | | 0.1 | 7.5 | 69.9 | 0.1 | 1.4 | 0.1 | 0.1 | 4.0 | | 0.3 | 39.8 | |
| SA-4 | | | | | | 2.3 | | | 3.0 | | | | |
| SA-5 | | 0.1 | 5.7 | 3.6 | | 1.8 | | 0.1 | 3.0 | | 0.1 | | |
| SA-6 | | 0.2 | 5.2 | 6.3 | | 2.2 | 0.1 | 0.1 | 5.0 | | 0.1 | 3.1 | |
| RCP-10 | | 0.2 | 3.1 | | 0.1 | 4.7 | 0.1 | 0.2 | 4.0 | | 0.1 | 3.5 | 51.1 |
| RCP-17 | | 0.2 | 4.8 | 2.7 | 0.1 | 28.1 | 0.1 | 0.3 | 6.0 | | 0.1 | | |
| RCP-18 | | 0.3 | 12.3 | 6.8 | 0.2 | 3.5 | 0.1 | 0.2 | 5.0 | | | 4.0 | 53.0 |
| TC-5 | NA | NA | NA | *12 | NA | NA | NA | NA | 4.0 | | NA | NA | NA |
| 615-1 | NA | NA | NA | | NA | NA | NA | NA | | | NA | NA | NA |
| 615-2 | NA | NA | NA | | NA | NA | NA | NA | 2.0 | | NA | NA | NA |
| 626-2 | NA | NA | NA | | NA | NA | NA | NA | | | NA | NA | NA |
| 626-3 | NA | NA | NA | | NA | NA | NA | NA | 2.0 | | NA | NA | NA |
| 626-4 | NA | NA | NA | | NA | NA | NA | NA | | | NA | NA | NA |
| 626-5 | NA | NA | NA | | NA | NA | NA | NA | 2.0 | | NA | NA | NA |
| TC-6 | NA | NA | NA | | NA | 2.0 | NA | NA | 3.0 | | NA | NA | |
| TC-7 | NA | NA | NA | | NA | 1.9 | NA | NA | 4.0 | | NA | NA | |
| 615-3 | NA | NA | NA | *19.0 | NA | NA | NA | NA | | | NA | NA | NA |
| 615-4 | NA | NA | NA | *7.0 | NA | NA | NA | NA | 2.0 | | NA | NA | NA |
| TC-8 | NA | NA | NA | *210.0 | NA | 6.4 | NA | NA | 7.0 | | NA | NA | |
| TC-9 | 0.1 | 0.4 | 28.2 | 348.6 | 0.1 | 5.9 | 0.1 | 1.8 | 6.0 | 0.5 | 0.2 | 18.1 | |
| TC-10 | NA | NA | NA | 150.0 | NA | 21.2 | NA | NA | 6.0 | | NA | NA | |
| TC-11 | 0.1 | 4.8 | 21.9 | 124.8 | | | 0.039 | 0.2 | 5.0 | 1.9 | 0.1 | | |
| 628-1 | NA | 17.0 | NA | 157.0 | NA | NA | NA | NA | 7.0 | | NA | NA | NA |
| 628-3 | NA | | NA | 108.0 | NA | NA | NA | NA | 7.0 | | NA | NA | NA |
| 628-4 | NA | 100.0 | NA | | NA | NA | NA | NA | 4.0 | | NA | NA | NA |
| 628-5 | NA | | NA | 382.0 | NA | NA | NA | NA | 13.0 | | NA | NA | NA |
| 628-6 | NA | NA | NA | 354.0 | NA | NA | NA | NA | 12.0 | | NA | NA | NA |
| TC-12 | | 0.2 | 2.9 | 208.5 | | 2.2 | | | 5.0 | 3.5 | | | |

B) JASPER CLAST IN CAPE ST.JOHN GROUP:

| | | | | | | | | | | | | | |
|---|---|---|---|---|---|---|---|---|---|---|---|---|---|
| 729-1 | | *4 | *12 | | | | | | | | | | |

C) VEIN CHEMISTRY:

| | | | | | | | | | | | | | |
|---|---|---|---|---|---|---|---|---|---|---|---|---|---|
| V-1 | | | 11.8 | 3.7 | | | | | 4.0 | 6.0 | 31.6 | 6.7 | 5.1 |
| V-2 | | | 5.3 | 3.6 | | | | | 4.0 | 5.0 | 24.1 | 4.3 | |
| 628-1 | | 19.8 | *47 | 149.5 | | | | 9.4 | 7.0 | 8.0 | | | |

No value is indicated where element was not detected or was below detection limit
NA - element not analysed
* denotes XRF analysis, all other samples analysed by ICP-MS

TRACE ELEMENT DATA cont...

D) CAPE ST.JOHN GROUP:

| PPM | Cs | *Rb | *Ba | *Sr | Tl | Li | Th | U | *Zr | *Y | Bi | W | Mo |
|---|---|---|---|---|---|---|---|---|---|---|---|---|---|
| RCP-1 | 1.8 | 106.0 | 629.0 | 21.9 | 0.7 | 7.4 | 12.8 | 2.9 | 598.0 | 92.0 | 0.2 | 2.0 | 47.8 |
| RCP-2 | 0.8 | 55.4 | 190.8 | 81.8 | 0.4 | 69.0 | 7.6 | 4.8 | 49.0 | 31.0 | 1.2 | 2.4 | 0.3 |
| RCP-3 | 1.9 | 130.7 | 384.0 | 176.1 | 0.8 | 8.0 | 7.4 | 8.7 | 41.0 | 25.0 | 0.2 | 2.4 | 0.4 |
| RCP-4 | | 0.6 | 3.1 | | | 2.5 | | 0.2 | | | | | 59.9 |
| RCP-5 | 0.4 | 23.9 | 34.6 | 229.4 | 0.2 | 10.6 | 1.7 | 1.2 | 77.0 | 12.0 | | 4.0 | 60.3 |
| RCP-6 | 1.5 | 95.4 | 265.3 | 85.9 | 0.7 | 7.3 | 6.8 | 2.9 | 273.0 | 40.0 | 0.1 | 5.3 | 0.1 |
| RCP-7 | 0.6 | 46.7 | 241.7 | 5.6 | 0.3 | 8.9 | 5.1 | 1.3 | 183.0 | 53.0 | 0.1 | 4.9 | 0.8 |
| RCP-8 | 0.7 | 61.3 | 272.6 | 6.2 | 0.3 | | 9.4 | 3.9 | 454.0 | 65.0 | | | 1.0 |
| RCP-9 | 0.9 | 55.2 | 430.3 | 7.0 | 0.3 | 12.2 | 4.1 | 1.4 | 172.0 | 17.0 | 0.1 | | 49.3 |
| RCP-11 | 0.1 | 6.7 | 109.9 | 47.6 | 0.1 | 2.9 | 10.7 | 2.9 | 523.0 | 66.0 | 0.1 | 3.0 | 3.7 |
| RCP-12 | 0.1 | 7.6 | 121.1 | 34.6 | | 5.1 | 8.9 | 6.9 | 524.0 | 63.0 | 0.1 | 13.8 | 46.4 |
| RCP-13 | 0.4 | 41.5 | 250.4 | 41.4 | 0.7 | | 13.0 | 4.1 | 481.0 | 57.0 | | 2.2 | |
| RCP-14 | 0.8 | 53.9 | 377.5 | 27.6 | 0.4 | 2.5 | 9.5 | 3.2 | 405.0 | 49.0 | 0.1 | 2.8 | 37.7 |

No value is indicated where element was not detected or was below detection limit
NA - element not analysed
* denotes XRF analysis, all other samples analysed by ICP-MS

## TRACE ELEMENT DATA

A) ULTRAMAFIC ROCKS:

| PPM | Cd | Sn | As | Sb | Te | *Zn | *Cu | *Ni | *V | *Cr | Pb | Sc | Co |
|---|---|---|---|---|---|---|---|---|---|---|---|---|---|
| BC-1 | | 27.3 | | | 0.6 | 27.0 | | 1207.0 | 71.0 | 3580.0 | 6.2 | 11.6 | 91.4 |
| BC-2 | | 9.2 | | | | 23.0 | 27.0 | 552.0 | 135.0 | 2784.0 | 2.8 | 36.7 | 57.4 |
| BC-3 | | 13.0 | | 0.6 | | 40.0 | | 1372.0 | 50.0 | 3516.0 | 5.1 | 9.2 | 111.8 |
| BC-4 | | 10.3 | | 1.6 | | 12.0 | | 1651.0 | 53.0 | 2885.0 | 5.4 | 8.4 | 117.1 |
| BC-5 | | 13.2 | | | 0.6 | 31.0 | 11.0 | 764.0 | 97.0 | 3088.0 | 2.3 | 20.2 | 85.8 |
| BC-6 | | 14.5 | | | | 39.0 | | 2041.0 | 35.0 | 2289.0 | 8.7 | 7.0 | 84.7 |
| SA-2 | | 18.1 | 7.4 | | 0.7 | 26.0 | 110.0 | 1970.0 | 35.0 | 1565.0 | 14.2 | 6.9 | 75.1 |
| SA-4 | | 32.4 | 73.6 | 1.1 | | 15.0 | | 1986.0 | 32.0 | 2152.0 | | 8.3 | 81.0 |
| SA-5 | | 42.0 | 2.8 | 1.1 | 0.7 | 7.0 | | 1820.0 | 23.0 | 1686.0 | 8.8 | 6.6 | 90.9 |
| SA-6 | | 72.1 | 2.9 | 1.2 | | 14.0 | | 2010.0 | 27.0 | 1923.0 | 9.3 | 6.7 | 78.1 |
| RCP-10 | | 50.5 | | 3.5 | | 20.0 | | 1777.0 | 25.0 | 1744.0 | 17.5 | 7.8 | 62.3 |
| RCP-17 | 3.2 | 100.8 | | 48.8 | 154.9 | 13.0 | | 2154.0 | 34.0 | 2076.0 | 8.7 | 6.7 | 106.8 |
| RCP-18 | | 50.0 | 121.5 | 7.0 | 24.4 | 34.0 | 9.0 | 1364.0 | 40.0 | 2849.0 | 10.9 | 7.2 | 74.4 |
| TC-5 | NA | NA | NA | NA | NA | 20.0 | | 2227.0 | 32.0 | 2084.0 | NA | NA | NA |
| 615-1 | NA | NA | NA | NA | NA | | | 1810.0 | 29.0 | 2010.0 | NA | NA | NA |
| 615-2 | NA | NA | NA | NA | NA | 22.0 | 256.0 | 2302.0 | 23.0 | 2692.0 | NA | NA | NA |
| 626-2 | NA | NA | NA | NA | NA | 14.0 | | 1910.0 | 68.0 | 2587.0 | NA | NA | NA |
| 626-3 | NA | NA | NA | NA | NA | 10.0 | | 2120.0 | 31.0 | 2285.0 | NA | NA | NA |
| 626-4 | NA | NA | NA | NA | NA | 10.0 | | 1815.0 | 30.0 | 2316.0 | NA | NA | NA |
| 626-5 | NA | NA | NA | NA | NA | 19.0 | | 1760.0 | 57.0 | 2765.0 | NA | NA | NA |
| TC-6 | | 14.9 | 106.5 | 3.6 | | 16.0 | | 2150.0 | 32.0 | 2302.0 | NA | 7.1 | 111.6 |
| TC-7 | | 12.2 | 97.0 | 4.3 | | 11.0 | | 2152.0 | 38.0 | 1551.0 | NA | 6.6 | 97.5 |
| 615-3 | NA | NA | NA | NA | NA | 15.0 | | 1898.0 | 20.0 | 2071.0 | NA | NA | NA |
| 615-4 | NA | NA | NA | NA | NA | 13.0 | | 2044.0 | 30.0 | 2653.0 | NA | NA | NA |
| TC-8 | | 7.5 | 61.5 | 3.0 | | 143.0 | 6.0 | 226.0 | 49.0 | 1578.0 | NA | 14.2 | 27.9 |
| TC-9 | | 27.9 | 5.6 | 9.6 | 1.6 | 166.0 | | 1731.0 | 47.0 | 6799.0 | 10.5 | 6.7 | 160.8 |
| TC-10 | | 7.0 | 74.8 | 0.8 | | 85.0 | | 1005.0 | 56.0 | 3844.0 | | 10.4 | 72.2 |
| TC-11 | | 32.5 | 3.3 | 2.5 | | 60.0 | | 480.0 | 34.0 | 1041.0 | 21.5 | 6.3 | 41.0 |
| 628-1 | NA | NA | NA | NA | NA | 49.0 | | 347.0 | 35.0 | 1662.0 | NA | NA | NA |
| 628-3 | NA | NA | NA | NA | NA | 16.0 | | 1171.0 | 72.0 | 1859.0 | NA | NA | NA |
| 628-4 | NA | NA | NA | NA | NA | 21.0 | | 431.0 | 33.0 | 1127.0 | NA | NA | NA |
| 628-5 | NA | NA | NA | NA | NA | 17.0 | | 1515.0 | 26.0 | 1974.0 | NA | NA | NA |
| 628-6 | NA | NA | NA | NA | NA | 76.0 | | 1348.0 | 36.0 | 2079.0 | NA | NA | NA |
| TC-12 | | 9.9 | 2.8 | | | 44.0 | | 756.0 | 30.0 | 1439.0 | | 6.1 | 41.0 |

B) JASPER CLAST IN CAPE ST.JOHN GROUP CONGLOMERATE:

| | | | | | | | | | | | | | |
|---|---|---|---|---|---|---|---|---|---|---|---|---|---|
| 729-1 | | | | | | 63.0 | | 101.0 | 48.0 | 1560.0 | | | |

C) VEIN CHEMISTRY:

| | | | | | | | | | | | | |
|---|---|---|---|---|---|---|---|---|---|---|---|---|
| V-1 | 242.4 | | 14.2 | | 3633.0 | 769.0 | 23.0 | 372.0 | 12.0 | 4.6 | 55.7 |
| V-2 | 64.8 | | 63.7 | | 3424.0 | 422.0 | 16.0 | 475.0 | 14.4 | 2.5 | 25.4 |
| 628-1 | | | | 49.0 | | 347.0 | 35.0 | 1662.0 | | | |

No value is indicated where element was not detected or was below detection limit
NA - element not analysed
* denotes XRF analysis, all other samples analysed by ICP-MS

TRACE ELEMENTS cont...

D) CAPE ST.JOHN GROUP:

| PPM | Cd | Sn | As | Sb | Te | *Zn | *Cu | *Ni | *V | *Cr | Pb | Sc | Co |
|---|---|---|---|---|---|---|---|---|---|---|---|---|---|
| RCP-1 | 2.4 | 35.5 | 3.2 | 4.0 | | 64.0 | 4.0 | | 4.0 | | 16.3 | 11.7 | 1.3 |
| RCP-2 | 1.0 | 79.4 | 3.2 | 0.8 | | 43.0 | 22.0 | 362.0 | 86.0 | 791.0 | 19.2 | 13.6 | 28.6 |
| RCP-3 | | 36.8 | 10.4 | 0.5 | | 24.0 | | 217.0 | 33.0 | 458.0 | 60.3 | 8.7 | 13.7 |
| RCP-4 | | 11.0 | | 3.5 | 1.7 | | | | | | | 0.2 | 0.3 |
| RCP-5 | 1.0 | 22.3 | | 3.6 | | 17.0 | | 758.0 | 48.0 | 1487.0 | 39.9 | 8.2 | 38.9 |
| RCP-6 | | 84.0 | 2.0 | | 0.7 | 99.0 | 17.0 | 502.0 | 130.0 | 1029.0 | 11.2 | 21.3 | 35.0 |
| RCP-7 | | 131.4 | 3.2 | | | 48.0 | 4.0 | 29.0 | 10.0 | | 4.7 | 2.7 | 0.9 |
| RCP-8 | 1.9 | 50.0 | 3.3 | 0.5 | | | 2.0 | | 19.0 | | 9.7 | 3.0 | 0.9 |
| RCP-9 | | 29.3 | | 3.3 | | 8.0 | 4.0 | 23.0 | 48.0 | 102.0 | 6.9 | 8.2 | 2.2 |
| RCP-11 | 1.9 | 71.9 | 4.0 | 3.1 | 1.5 | | 6.0 | | 5.0 | | 11.3 | 1.7 | 0.5 |
| RCP-12 | 2.5 | 41.2 | 4.0 | 7.6 | | | 3.0 | | 8.0 | | 13.0 | 5.6 | 1.0 |
| RCP-13 | 2.0 | 47.1 | 7.5 | 3.0 | 2.0 | | 3.0 | 7.0 | 10.0 | | 16.8 | 4.8 | 1.2 |
| RCP-14 | 2.1 | 50.8 | 2.2 | 4.8 | | | 2.0 | | 9.0 | | 18.0 | 7.1 | 1.1 |

No value is indicated where element was not detected or was below detection limit
NA - element not analysed
* denotes XRF analysis, all other samples analysed by ICP-MS

RARE EARTH ELEMENT DATA
ICP ANALYSIS

| PPM | La | Ce | Pr | Nd | Sm | Eu | Gd | Tb | Dy | Ho |
|---|---|---|---|---|---|---|---|---|---|---|
| A) ULTRAMAFIC ROCKS: | | | | | | | | | | |
| BC-1A | 0.082 | 0.158 | 0.022 | 0.096 | 0.031 | 0.012 | 0.047 | 0.011 | 0.075 | 0.019 |
| BC-2A | 0.203 | 0.344 | 0.046 | 0.177 | 0.051 | 0.014 | 0.071 | 0.019 | 0.157 | 0.042 |
| BC-2B | 0.0996 | 0.0396 | 0.0205 | 0.0818 | 0.0206 | 0.0061 | 0.0236 | 0.0057 | 0.0431 | 0.0113 |
| BC-3B | 0.0310 | 0.0572 | 0.0068 | 0.0277 | 0.0065 | 0.0017 | 0.0098 | 0.0019 | 0.0156 | 0.0037 |
| BC-4A | 0.077 | 0.166 | 0.019 | 0.073 | 0.021 | 0.007 | 0.026 | 0.005 | 0.050 | 0.014 |
| BC-5A | 0.091 | 0.175 | 0.025 | 0.103 | 0.037 | 0.012 | 0.059 | 0.016 | 0.138 | 0.035 |
| BC-5B | 0.0459 | 0.0740 | 0.0126 | 0.0576 | 0.0192 | 0.0065 | 0.0274 | 0.0057 | 0.0421 | 0.0100 |
| BC-6A | 0.056 | 0.103 | 0.014 | 0.058 | 0.014 | 0.005 | 0.022 | 0.005 | 0.039 | 0.009 |
| SA-2B | 0.1525 | 0.2366 | 0.0322 | 0.1245 | 0.0286 | 0.1054 | 0.0293 | 0.0062 | 0.0483 | 0.0119 |
| SA-4A | 0.118 | 0.206 | 0.023 | 0.074 | 0.011 | 0.004 | 0.013 | 0.003 | 0.015 | 0.003 |
| SA-5B | 0.0260 | 0.0494 | 0.0052 | 0.0180 | 0.0037 | 0.0015 | 0.0046 | 0.0006 | 0.0056 | 0.0012 |
| SA-6A | 0.089 | 0.170 | 0.021 | 0.075 | 0.013 | 0.001 | 0.015 | 0.003 | 0.016 | 0.004 |
| RCP-10A | 0.112 | 0.122 | 0.022 | 0.085 | 0.023 | 0.004 | 0.031 | 0.007 | 0.049 | 0.010 |
| RCP-17B | 0.1475 | 0.3018 | 0.0356 | 0.1257 | 0.0309 | 0.0035 | 0.0304 | 0.0063 | 0.0452 | 0.0101 |
| RCP-18A | 0.153 | 0.262 | 0.028 | 0.099 | 0.018 | 0.029 | 0.019 | 0.004 | 0.025 | 0.006 |
| 628-3A | 0.259 | 0.392 | 0.069 | 0.335 | 0.110 | 0.063 | 0.176 | 0.038 | 0.252 | 0.050 |
| 628-3B | 0.1799 | 0.2650 | 0.0494 | 0.2352 | 0.0800 | 0.0427 | 0.1173 | 0.0235 | 0.1369 | 0.0260 |
| 628-4B | 0.0855 | 0.1332 | 0.0206 | 0.1012 | 0.0336 | 0.0097 | 0.0548 | 0.0098 | 0.0570 | 0.0101 |
| 628-5B | 0.0855 | 0.1359 | 0.0214 | 0.0933 | 0.0265 | 0.0117 | 0.0378 | 0.0041 | 0.0243 | 0.0042 |
| 628-6B | 0.2532 | 0.3784 | 0.0435 | 0.1593 | 0.0371 | 0.0176 | 0.0506 | 0.0060 | 0.0379 | 0.0070 |
| B) JASPER CLAST IN CAPE ST.JOHN GROUP CONGLOMERATE: | | | | | | | | | | |
| 729-1B | 0.1796 | 0.3691 | 0.0493 | 0.2076 | 0.0720 | 0.0117 | 0.0578 | 0.0098 | 0.0500 | 0.0081 |
| C) VEIN CHEMISTRY: | | | | | | | | | | |
| V-1B | 0.0257 | 0.0490 | 0.0055 | 0.0225 | 0.0050 | 0.0018 | 0.0060 | 0.0012 | 0.0089 | 0.0024 |
| V-2A | 0.089 | 0.220 | 0.029 | 0.121 | 0.034 | 0.007 | 0.041 | 0.008 | 0.049 | 0.013 |
| V-2B | 0.0223 | 0.0550 | 0.0072 | 0.0268 | 0.0083 | 0.0024 | 0.0093 | 0.0015 | 0.0111 | 0.0026 |
| 628-1B | 0.3366 | 1.0101 | 0.1993 | 1.1795 | 0.5426 | 0.1385 | 0.7383 | 0.1267 | 0.8271 | 0.1123 |
| D) WHOLE ROCK STANDARDS: | | | | | | | | | | |
| SY-2A | 60.799 | 140.104 | 17.457 | 64.258 | 13.814 | 1.894 | 13.547 | 2.565 | 17.331 | 4.001 |
| SY-2B | 80.4826 | 183.3149 | 22.0355 | 83.3901 | 17.6148 | 2.4643 | 16.1810 | 3.0498 | 20.7097 | 4.8340 |
| PCC-1A | 0.351 | 0.107 | 0.020 | 0.077 | 0.018 | 0.003 | 0.019 | 0.002 | 0.021 | 0.007 |
| PCC-1A' | 0.253 | 0.081 | 0.009 | 0.032 | 0.006 | 0.001 | 0.007 | 0.001 | 0.012 | 0.002 |
| PCC-1B | 0.3879 | 0.0793 | 0.0107 | 0.0427 | 0.0080 | 0.0023 | 0.0102 | 0.0014 | 0.0200 | 0.0045 |
| E) CALCULATED DETECTION LIMITS - ULTRAMAFIC ROCK DETERMINATIONS: | | | | | | | | | | |
| PPM | 0.0005 | 0.0005 | 0.0004 | 0.0024 | 0.0022 | 0.0000 | 0.0000 | 0.0000 | 0.0000 | 0.0000 |

A and B after the sample numbers designate groups of samples analysed at different times
Ultramafic rocks and PCC-1 whole rock standard were stripped of 1 and 2 valency cations in ion exchange columns prior to ICP-MS analysis.

RARE EARTH ELEMENT DATA
ICP ANALYSIS

| PPM | Er | Tm | Yb | Lu |
|---|---|---|---|---|
| A) ULTRAMAFIC ROCKS: | | | | |
| BC-1A | 0.068 | 0.010 | 0.083 | 0.013 |
| BC-2A | 0.161 | 0.027 | 0.194 | 0.032 |
| BC-2B | 0.0376 | 0.0054 | 0.0391 | 0.0067 |
| BC-3B | 0.0141 | 0.0020 | 0.0151 | 0.0024 |
| BC-4A | 0.050 | 0.009 | 0.062 | 0.012 |
| BC-5A | 0.129 | 0.020 | 0.159 | 0.027 |
| BC-5B | 0.0325 | 0.0051 | 0.0386 | 0.0069 |
| BC-6A | 0.029 | 0.005 | 0.033 | 0.005 |
| SA-2B | 0.0416 | 0.0066 | 0.0513 | 0.0095 |
| SA-4A | 0.014 | 0.003 | 0.023 | 0.005 |
| SA-5B | 0.0046 | 0.0008 | 0.0078 | 0.0014 |
| SA-6A | 0.017 | 0.004 | 0.032 | 0.007 |
| RCP-10A | 0.045 | 0.007 | 0.054 | 0.011 |
| RCP-17B | 0.0366 | 0.0059 | 0.0389 | 0.0072 |
| RCP-18A | 0.022 | 0.003 | 0.025 | 0.004 |
| 628-3A | 0.142 | 0.017 | 0.106 | 0.015 |
| 628-3B | 0.0742 | 0.0087 | 0.0501 | 0.0068 |
| 628-4B | 0.0249 | 0.0028 | 0.0154 | 0.0022 |
| 628-5B | 0.0103 | 0.0013 | 0.0069 | 0.0012 |
| 628-6B | 0.0200 | 0.0029 | 0.0154 | 0.0029 |
| B) JASPER CLAST IN CAPE ST.JOHN GROUP CONGLOMERATE: | | | | |
| 729-1B | 0.0238 | 0.0034 | 0.0207 | 0.0029 |
| C) VEIN CHEMISTRY: | | | | |
| V-1B | 0.0096 | 0.0017 | 0.0125 | 0.0019 |
| V-2A | 0.046 | 0.009 | 0.069 | 0.012 |
| V-2B | 0.0096 | 0.0018 | 0.0129 | 0.0024 |
| 628-1B | 0.2763 | 0.0317 | 0.1739 | 0.0230 |
| D) WHOLE ROCK STANDARDS: | | | | |
| SY-2A | 13.540 | 2.186 | 15.965 | 2.680 |
| SY-2B | 17.2629 | 2.8619 | 20.2810 | 3.3820 |
| PCC-1A | 0.025 | 0.006 | 0.040 | 0.009 |
| PCC-1A' | 0.008 | 0.002 | 0.016 | 0.003 |
| PCC-1B | 0.0212 | 0.0032 | 0.0297 | 0.0058 |
| E) CALCULATED DETECTION LIMITS - ULTRAMAFIC ROCK DETER | | | | |
| PPM | 0.0009 | 0.0003 | 0.0014 | 0.0002 |

RARE EARTH ELEMENT DATA cont...

| PPM | La | Ce | Pr | Nd | Sm | Eu | Gd | Tb | Dy | Ho |
|---|---|---|---|---|---|---|---|---|---|---|
| F) CAPE ST.JOHN GROUP: | | | | | | | | | | |
| RCP-1 | 44.465 | 103.193 | 13.599 | 56.383 | 12.42 | 2.305 | 7.888 | 1.082 | 5.979 | 1.258 |
| RCP-2 | 6.533 | 15.137 | 1.928 | 7.144 | 1.933 | 0.076 | 1.468 | 0.246 | 1.549 | 0.327 |
| RCP-3 | 5.875 | 14.084 | 1.84 | 6.989 | 2.21 | 0.056 | 1.726 | 0.342 | 2.416 | 0.492 |
| RCP-4 | 0.143 | 0.297 | 0.031 | 0.146 | 0.042 | 0.0001 | 0.021 | 0.003 | 0.026 | 0.003 |
| RCP-5 | 7.849 | 15.187 | 2.027 | 8.065 | 1.779 | 0.429 | 1.399 | 0.25 | 1.488 | 0.3 |
| RCP-6 | 28.852 | 56.141 | 7.33 | 30.432 | 6.482 | 1.183 | 4.381 | 0.587 | 3.131 | 0.63 |
| RCP-7 | 32.032 | 70.485 | 8.698 | 34.601 | 7.876 | 1.565 | 5.892 | 0.705 | 2.93 | 0.484 |
| RCP-8 | 30.65 | 67.904 | 8.46 | 32.47 | 7.116 | 1.529 | 6.371 | 1.101 | 5.501 | 1.148 |
| RCP-9 | 20.359 | 40.56 | 5.303 | 20.654 | 4.448 | 1.684 | 2.991 | 0.374 | 1.463 | 0.238 |
| RCP-11 | 17.373 | 44.038 | 6.821 | 30.317 | 7.957 | 1.383 | 5.56 | 0.842 | 5.019 | 1.132 |
| RCP-12 | 22.138 | 45.867 | 6.219 | 25.152 | 6.054 | 1.28 | 4.942 | 0.898 | 4.988 | 1.176 |
| RCP-13 | 42.645 | 93.129 | 11.957 | 48.916 | 11.178 | 1.793 | 5.358 | 0.718 | 4.301 | 0.989 |
| RCP-14 | 38.606 | 84.77 | 11.115 | 42.818 | 8.62 | | | | 4.814 | 0.974 |
| G) CHONDRITE VALUES ( ): | | | | | | | | | | |
| | 0.367 | 0.957 | 0.137 | 0.711 | 0.231 | 0.087 | 0.306 | 0.058 | 0.381 | 0.0851 |

RARE EARTH ELEMENT DATA cont...

| PPM | Er | Tm | Yb | Lu |
|---|---|---|---|---|
| F) CAPE ST.JOHN GROUP: | | | | |
| RCP-1 | 3.952 | 0.652 | 4.231 | 0.683 |
| RCP-2 | 1.041 | 0.203 | 1.407 | 0.245 |
| RCP-3 | 1.608 | 0.299 | 1.971 | 0.307 |
| RCP-4 | 0.019 | 0.004 | 0 | 0 |
| RCP-5 | 0.929 | 0.133 | 0.837 | 0.128 |
| RCP-6 | 2.018 | 0.352 | 2.325 | 0.403 |
| RCP-7 | 1.358 | 0.221 | 1.511 | 0.253 |
| RCP-8 | 3.615 | 0.567 | 4.509 | 0.735 |
| RCP-9 | 0.71 | 0.119 | 0.849 | 0.141 |
| RCP-11 | 3.822 | 0.673 | 4.608 | 0.755 |
| RCP-12 | 3.917 | 0.67 | 5.511 | 0.884 |
| RCP-13 | 3.254 | 0.548 | 3.93 | 0.658 |
| RCP-14 | 3.226 | 0.554 | | |
| G) CHONDRITE VALUES ( ): | | | | |
| | 0.249 | 0.0356 | 0.248 | 0.0381 |

PRECIOUS METAL DATA

| PPB | Au | Pt | Pd | Ru | Rh | Ir |
|---|---|---|---|---|---|---|
| A) ULTRAMAFIC ROCKS: | | | | | | |
| BC-1 | 0.00 | 7.01 | 2.83 | 2.69 | 1.59 | 0.00 |
| BC-2 | 0.00 | 5.62 | 5.87 | 0.45 | 0.74 | 0.00 |
| BC-3 | 0.00 | 0.00 | 0.00 | 0.00 | 0.00 | 0.00 |
| BC-4 | 0.00 | 16.49 | 30.01 | 1.20 | 1.37 | 0.00 |
| BC-5 | 0.00 | 17.19 | 3.90 | 1.21 | 1.84 | 0.00 |
| BC-6 | 0.00 | 6.96 | 3.66 | 5.88 | 1.34 | 2.48 |
| SA-2 | 47.11 | 2.23 | 1.75 | 4.26 | 0.91 | 1.57 |
| SA-4 | 116.99 | 7.19 | 7.58 | 8.03 | 1.60 | 3.24 |
| SA-5 | 91.68 | 2.63 | 0.39 | 6.36 | 1.25 | 1.69 |
| SA-6 | 97.79 | 5.57 | 4.36 | 7.21 | 1.45 | 2.89 |
| RCP-10 | 0.77 | 4.53 | 15.70 | 4.75 | 1.22 | 2.65 |
| RCP-17 | 0.70 | 3.96 | 1.05 | 7.58 | 0.93 | 3.85 |
| RCP-18 | 1.34 | 4.68 | 1.34 | 7.69 | 1.67 | 4.34 |
| TC-5 | 6.00 | 7.72 | 4.31 | 7.94 | 1.86 | 3.66 |
| 615-1 | 3.90 | 3.77 | 0.94 | 2.96 | 0.81 | 2.02 |
| 615-2 | 19.25 | 4.72 | 1.02 | 5.10 | 0.89 | 3.57 |
| 626-2 | 12.82 | 4.72 | 1.33 | 5.31 | 0.74 | 2.95 |
| 626-3 | 1.48 | 9.14 | 0.94 | 5.78 | 1.21 | 3.76 |
| 626-4 | 146.53 | 3.36 | 0.88 | 3.22 | 0.44 | 2.05 |
| 626-5 | 300.07 | 7.13 | 5.35 | 6.85 | 1.51 | 3.56 |
| TC-6 | 0.00 | 8.44 | 10.94 | 8.27 | 2.71 | 3.26 |
| TC-7 | 4.29 | 9.45 | 10.06 | 8.17 | 2.29 | 3.99 |
| 615-3 | 1.17 | 5.03 | 5.73 | 4.44 | 1.05 | 2.34 |
| 615-4 | 16.52 | 8.24 | 2.54 | 4.62 | 0.92 | 2.54 |
| TC-8 | 4.98 | 16.08 | 1.86 | 2.40 | 0.92 | 1.31 |
| TC-10 | 126.57 | 2.09 | 2.81 | 1.86 | 0.48 | 0.57 |
| TC-11 | 125.78 | 8.98 | 4.50 | 4.56 | 2.21 | 1.80 |
| 628-1 | 1294.33 | 0.46 | 0.57 | 2.07 | 0.46 | 1.26 |
| 628-3 | 23.15 | 2.29 | 2.15 | 3.50 | 0.54 | 1.75 |
| 628-4 | 9.52 | 1.90 | 1.40 | 2.66 | 0.51 | 1.52 |
| 628-5 | 26.58 | 1.54 | 1.69 | 6.15 | 1.38 | 4.00 |
| 628-6 | 7.58 | 4.84 | 4.35 | 7.25 | 1.61 | 3.38 |
| B) LONG POND EAST SHOWING: | | | | | | |
| TC-16 | 408.49 | 20.04 | 26.33 | 10.60 | 8.83 | 7.95 |

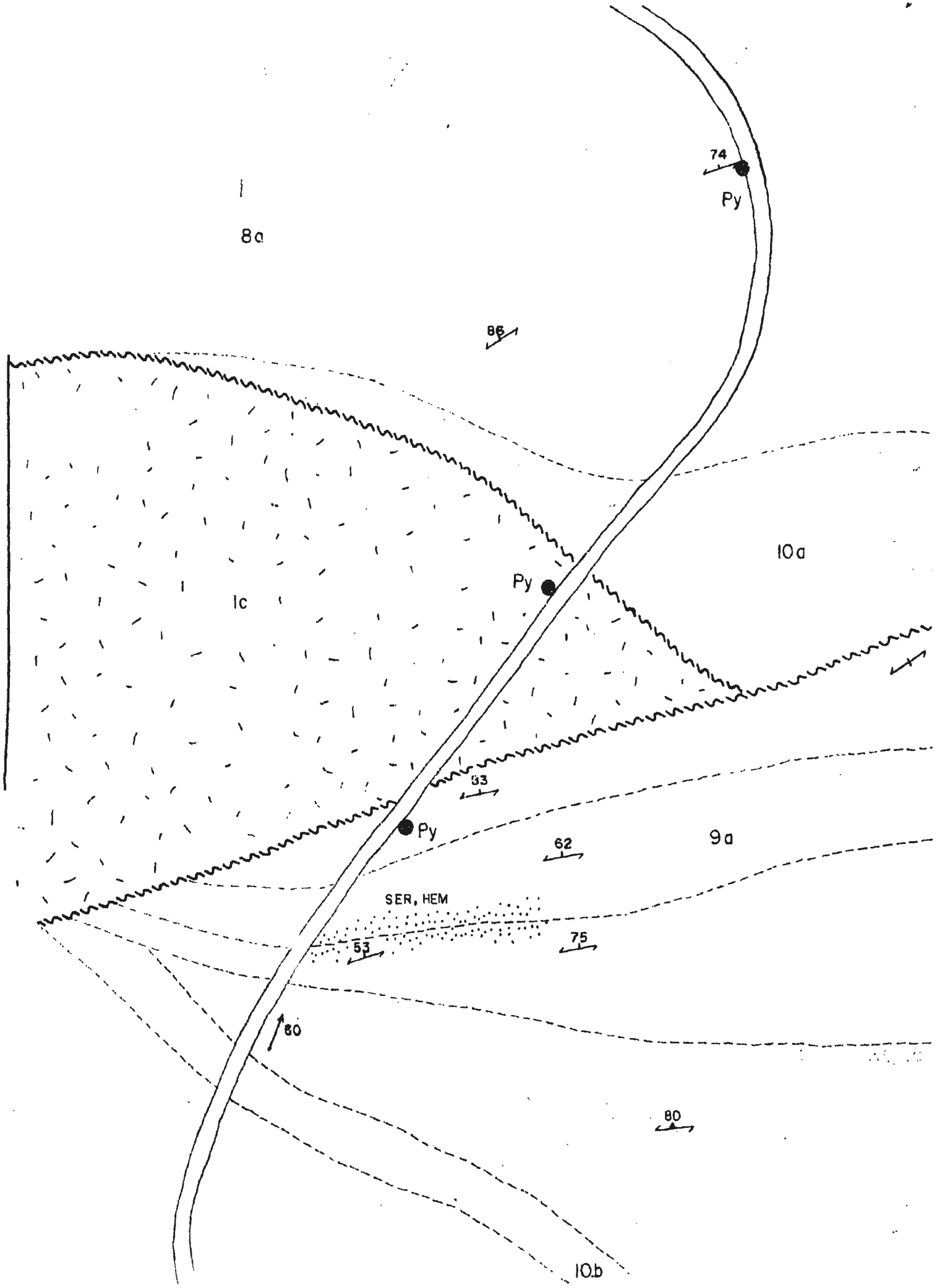
8a
74
Py
86
1c
Py
10a
33
Py
62
9a
SER, HEM
53
75
80
80
10b

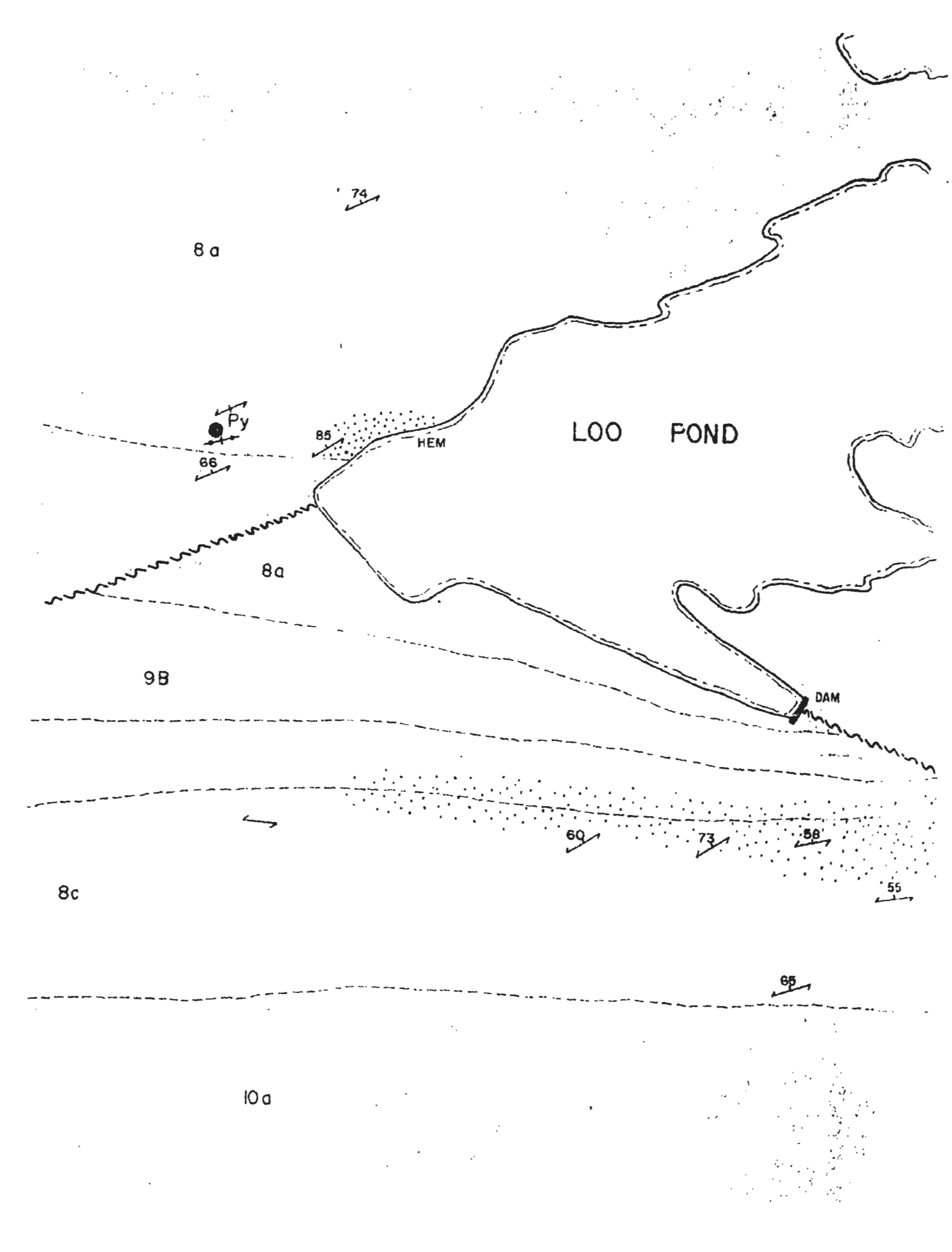
LOO POND
HEM
DAM
Py
74
85
66
60
73
58
55
65
8a
8a
9B
8c
10a

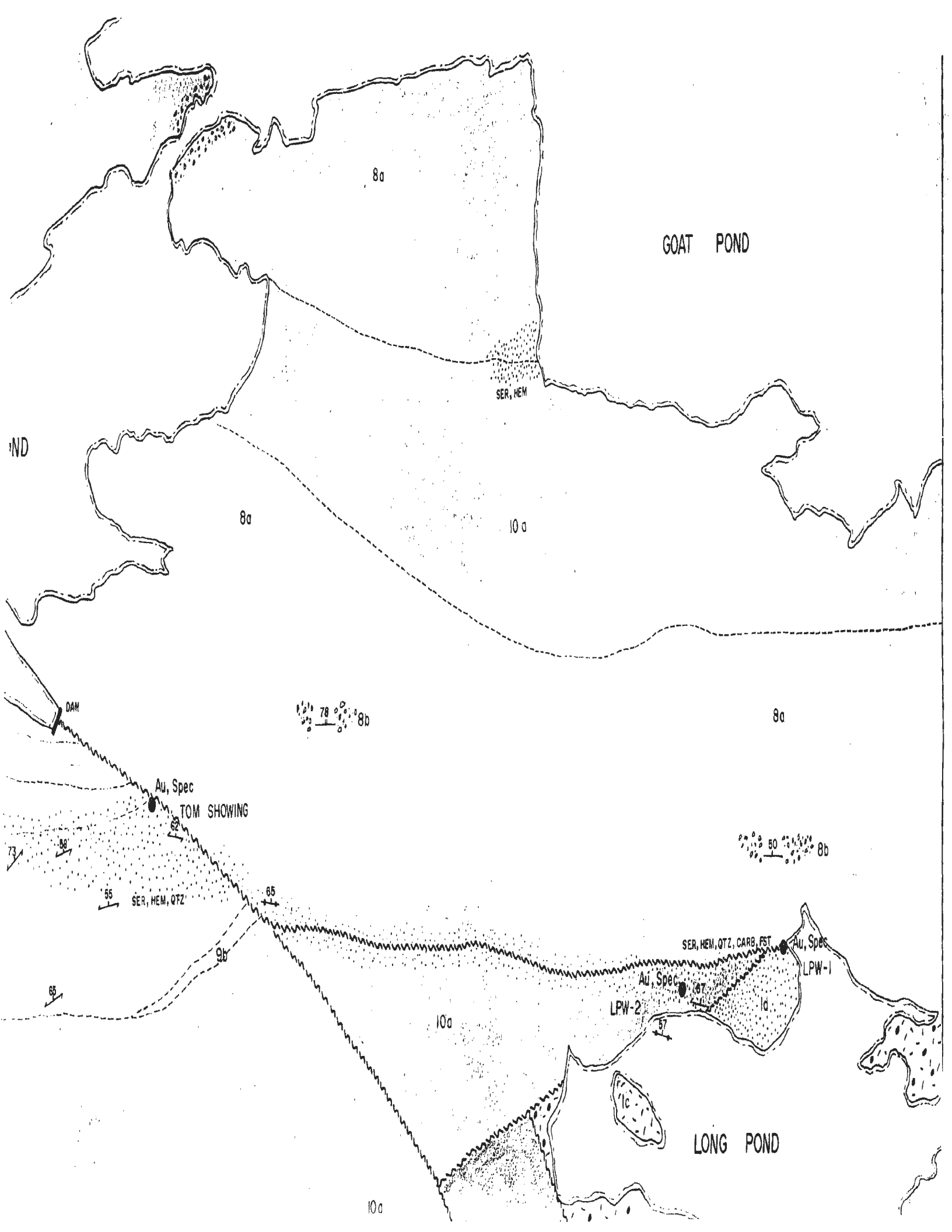
GOAT POND
8a
SER, HEM
ND
8a
10a
DAM
78
8b
8a
Au, Spec
TOM SHOWING
62
73
88
50
8b
55
SER, HEM, QTZ
65
9b
SER, HEM, QTZ, CARB, FST
Au, Spec
LPW-1
Au, Spec
67
LPW-2
1d
57
10a
1c
LONG POND
10a

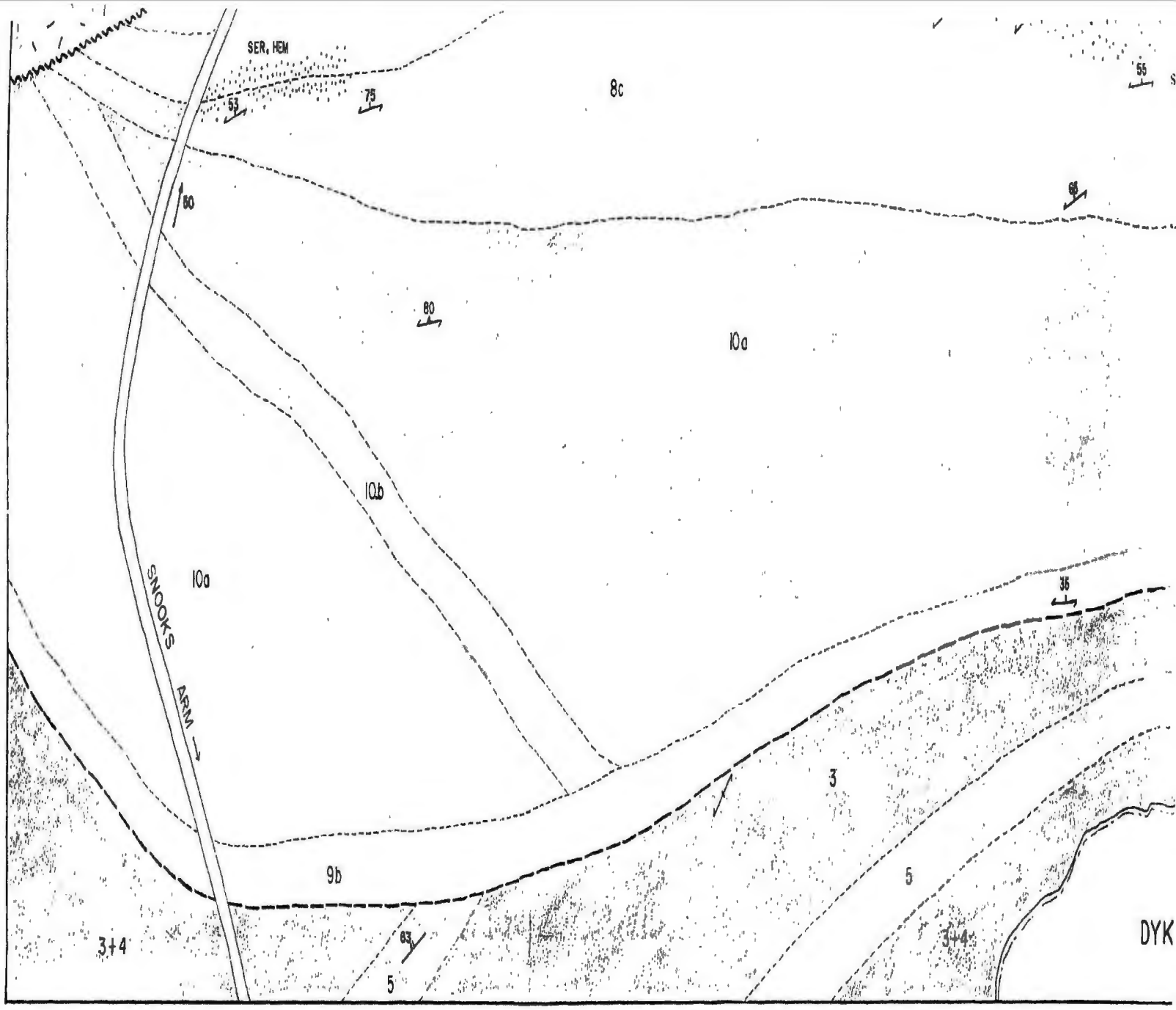


# LOO POND - LONG PON

MAP NO. 87-01-b

## LEGEND

| | |
|---|---|
| 10a | MAFIC, MASSIVE, AMYGDALOIDAL SHEET FLOWS |
| 10b | MAFIC - INTERMEDIATE FELDSPAR PHYRIC FLOWS |
| 9c | ARKOSE AND LITHIC WACKE - REWORKED CRYSTAL TUFF |

GROUP

SCALE

0 Meters

## SYMBOLS

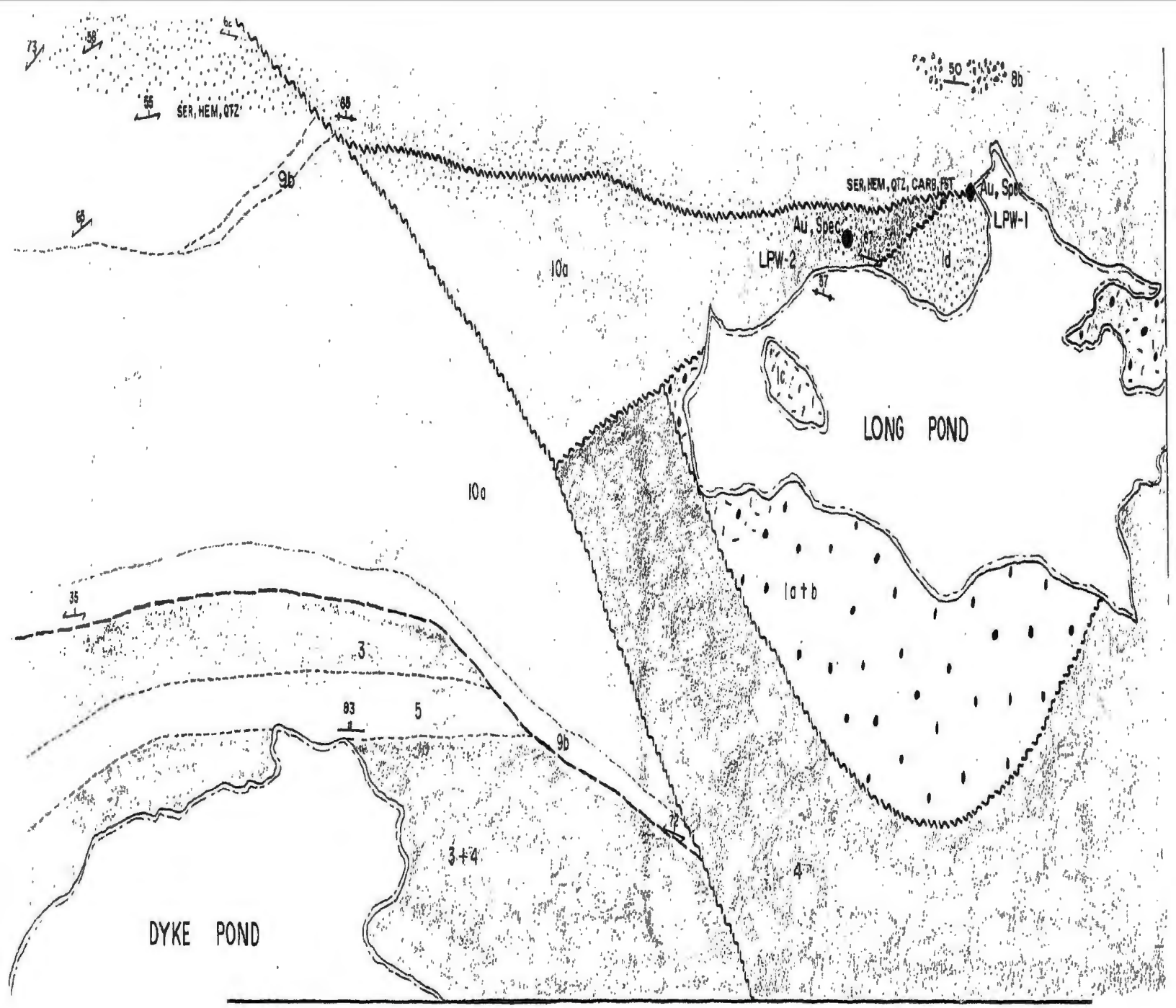


POND - LONG POND AREA

MAP NO. 87-01-b

SCALE

0 Meters 200

OND - LONG POND AREA

MAP NO. 87-01-b

SCALE

Meters 200

CAPE ST JOHN GROUP

9a — [illegible]

9a,b — POLYMICTIC CONGLOMERATE & JASPEROID, RHYOLITE AND BRIGHT GREEN ULTRAMAFICS, b ARGILLITE, MAFIC AND FELSIC VOLCANIC AND JASPEROID CLASTS

8a — QUARTZ - FELDSPAR CRYSTAL AND CRYSTAL - LITHIC TUFF

8b - b' — REWORKED PYROCLASTICS CONGLOMERATES AND SANDY BEDS WITH ABUNDANT JASPEROID

8c — FELSIC VOLCANIC TUFFS - FINE TO MEDIUM GRAINED

BETTS COVE COMPLEX

5 — INTERPILLOW RED AND GREEN ARGILLITE AND GREYWACKE

4 — PILLOW LAVAS AND MINOR DIABASE DYKES

3 — DIABASE AND SHEETED DIABASE DYKES

1a — ULTRAMAFIC SERPENTINITE

1b — SERPENTINE - CARBONATE

1c — TALC - CARBONATE

1d — SILICA - CARBONATE - HEMATITE +/- FUCHSITE

SEE MAP 87-0 FOR LOCATION

Au — MINERAL SHOWING

(520-1 — SAMPLE LOCATION

50 — SCHISTOSITY

50 50 — BEDDING TOPS KNOWN, UNKNOWN

50 — QUARTZ VEIN

50 — TREND AND PLUNGE OF FOLD AXIS

GEOLOGIC CONTACT

UNCONFORMITY

FAULT

SER — ALTERATION ZONE

## MINERAL ABBREVIATIONS

| | |
|---|---|
| Gn | GALENA |
| Py | PYRITE |
| Spec | SPECULARITE |
| SER | SERICITE |
| HEM | HEMATITE |
| QTZ | QUARTZ |
| FST | FUCHSITE |
| CARB | CARBONATE |


N